

Fluorescent Adolescence:
Shedding Light on Neural Encoding of Task Information
in the Adolescent vs. Adult Frontal Cortex

By

Madeline E. Klinger

A dissertation submitted in partial satisfaction of the
requirements for the degree of

Doctor of Philosophy

in

Neuroscience

in the

Graduate Division

of the

University of California, Berkeley

Committee in charge:

Professor Linda Wilbrecht, Co-chair

Professor Markita Landry, Co-chair

Professor Hillel Adesnik

Professor Na Ji

Spring 2024

Abstract

Fluorescent Adolescence: Shedding Light on Neural Encoding of Task Information in the Adolescent vs. Adult Frontal Cortex

by

Madeline E. Klinger

Doctor of Philosophy in Neuroscience

University of California, Berkeley

Professor Linda Wilbrecht, Co-chair

Professor Markita Landry, Co-chair

Adolescence is a developmental stage of life broadly viewed as a transitional period between juvenility and adulthood. This stage is characterized by sexual maturation and physical growth in addition to specific behavioral phenotypes, such as increased exploration, risk-taking, and impulsivity. Concurrent with these behavioral changes, the frontal cortex continues to develop throughout adolescence. Some of the physiological changes in the frontal cortex during adolescence mirror those that occur in sensory cortices at earlier ages, when certain sensory functions undergo a “critical period” of development. During a critical period, neurophysiological changes facilitate the emergence of specialized neural functioning, and developmental disruptions during a critical period can result in irreparable deficits in neural function. It has been postulated that there may be critical, or “sensitive”, periods for behavioral functions in addition to neural functions. However, it remains unclear how the concept of a critical or sensitive period may translate from the sensory cortices to the functions of and emergent behaviors involving the frontal cortex. In this dissertation, I explore the possibility of an adolescent sensitive period for encoding of task-related information in the dorsomedial region of the prefrontal cortex of mice.

In Chapter 1, I describe the developmental changes that occur over the course of adolescence. I focus on anatomical and neurophysiological remodeling in the dorsomedial prefrontal cortex at the cellular level and give a brief overview of a subset of the existing literature examining adolescent behavior. There are many classes of behavioral tasks employed in adolescent studies, but I describe only those related to response inhibition, a behavior of relevance to the research herein. In Chapter 2, I outline the mechanisms of critical period onset from previous work in sensory cortices and demonstrate how these mechanisms are reflected in the frontal cortex during adolescence. I construct the hypothesis that, if adolescence does indeed represent a sensitive period for frontal cortical function, we may expect to see greater encoding of environmentally relevant information in the adolescent frontal cortex compared to the adult. I then present my work examining learning of a go/no-go task and encoding of task information in the dorsomedial prefrontal cortex of adolescent and adult mice. I show that adolescent mice learn the task faster and run more during the task than adults. Moreover, adolescent frontal cortex encodes certain task

variables with greater specificity at the population level, but not at the single-cell level, than adult frontal cortex. I argue that this evidence, supported by previous literature documenting the development of the dorsomedial prefrontal cortex, lends credence to the concept of an adolescent sensitive period. This chapter contains material in preparation for publication with co-authors Hongli Wang, Lung-Hao Tai, Albert Qü, Mei Murphy, and Linda Wilbrecht.

In Chapter 3, I discuss methodologies for investigating catecholamine neuromodulation in the brain. I emphasize that while recent advances in fluorescent sensors have enabled unprecedented access to catecholamine dynamics in animal models, few studies have employed optical techniques in the adolescent brain, possibly due to limitations of existing tools. In this chapter, I present research that documents first steps toward expanding the repertoire of available imaging methods. This research leverages the fluorescent properties of single-walled carbon nanotubes to develop a functionalized optical fiber capable of detecting nanomolar concentrations of dopamine *in vitro* in small volumes of biological fluids and *ex vivo* in mouse brain tissue. This form factor bypasses the need for genetic integration of a fluorescent protein, potential permitting greater translatability. I also introduce the development of a dual-near-infrared mobile fiber photometry rig that permits flexible use of our tool. I discuss the utility of this tool in its current form and outline potential future applications. This chapter contains material in preparation for publication with co-authors Rigney Miller, Linda Wilbrecht, and Markita Landry.

Finally, in Chapter 4, I return to the discussion of the adolescent sensitive period. I reiterate some of the major changes developing in the adolescent frontal cortex and suggest potential mechanisms of action for their contributions to the onset of a sensitive period. I explore the possibility that mechanisms of sensitive period onset beyond those observed in sensory cortices are at play in the frontal cortex and suggest future directions of research. I conclude by stressing the importance of research on the adolescent brain from a public health perspective. Overall, this dissertation aims to communicate the possibility of an adolescent sensitive period for the development of the frontal cortex, introduce a new potential tool for investigation of catecholamine dynamics, and advocate for greater attention to the adolescent brain.

This dissertation is dedicated to my Ava & Aja,
Djanger & Jadmana Emgushov,
in return for their lifelong dedication to their family.

The blood, sweat, and tears embedded in this work
are incomparable to those which enabled me to get here.

May this work represent recognition of your hard work,
my endless, inexpressible love,
and just one piece of your American Dream.

...

This dissertation is also dedicated to my adolescent self,
half a lifetime ago.
I am proud of you. Don't you give up.
Look at us now!

Table of Contents

| | |
|---|----|
| Chapter 1: Cells Like Teen Spirit..... | 1 |
| Adolescent development of frontal cortices..... | 2 |
| Adolescent development of response inhibition..... | 7 |
| Adolescent development shapes adult outcomes..... | 9 |
| Chapter 2: Let’s Get Critical..... | 11 |
| Critical period regulation and motivation for studying dmPFC..... | 11 |
| Materials & Methods..... | 13 |
| Results..... | 18 |
| Discussion..... | 26 |
| Chapter 3: Shine On, You Crazy Hexagon..... | 32 |
| Current techniques for catecholamine research and background on the utility of single-walled carbon nanotubes..... | 32 |
| Materials & Methods..... | 35 |
| Results..... | 37 |
| Discussion..... | 43 |
| Chapter 4: Teenage Dream..... | 46 |
| Additional factors underlying dmPFC plasticity & areas of future research..... | 47 |
| Final remarks: the case for adolescence..... | 52 |
| References..... | 54 |

List of Figures & Tables

Figures

| | |
|---|----|
| Figure 1: Developmental timeline and associated events..... | 2 |
| Figure 2: Timeline of adolescence..... | 3 |
| Figure 3: Interacting systems in dmPFC during adolescence..... | 6 |
| Figure 4: Two-photon calcium imaging..... | 19 |
| Figure 5: Adolescents learn a go/no-go task more quickly than adults..... | 21 |
| Figure 6: Similar proportions of neurons encode task variables in adult and adolescent dmPFC... | 22 |
| Figure 7: Example stimulus-encoding neuron from an adolescent animal..... | 23 |
| Figure 8: Decoding task variables from adult and adolescent neural population data..... | 25 |
| Figure 9: Task information is better decoded from adolescent neural population data even after controlling for differences in running..... | 26 |
| Figure 10: Functionalized fiber manufacture and response to dopamine..... | 38 |
| Figure 11: Dopamine response from all prepared fibers..... | 38 |
| Figure 12: Fiber response to dopamine under different conditions..... | 40 |
| Figure 13: Fiber response to dopamine in biological fluids..... | 41 |
| Figure 14: <i>Ex vivo</i> fiber response to dopamine..... | 43 |
| Figure 15: Potential applications of the functionalized fiber..... | 45 |
| Figure 16: Schematic of information representation through dendritic spines..... | 49 |

Tables

| | |
|--|----|
| Table 1. Behavior in response inhibition tasks during adolescence..... | 7 |
| Table 2. Mice trained on the go/no-go task..... | 15 |
| Table 3. Summarized fiber responses to dopamine..... | 42 |

Acknowledgements

Many scientists contributed to the completion of this dissertation over the past six years. First, my advisors, Linda Wilbrecht and Markita Landry, were indispensable in guiding my scientific process. I want to thank Linda and Markita for championing my work even when I doubted myself, pushing me to expand my thinking, and demonstrating such powerful examples of multitalented women in science. These were hard projects, and I couldn't have completed them without your belief that they could be done. Additional members of my thesis committee, Hillel Adesnik and Na Ji, provided crucial feedback and technical advice that substantially expanded my scientific intuition. I benefitted from countless conversations with motivated and generous postdocs, including J. Travis Del Bonis-O'Donnell, Nuria Vendrell Llopis, Will Liberti, and Hongli Wang—thank you for sharing your time with me, and I hope to pay it forward with my own mentees. A huge thanks to my labmates: Albert Qü, for all your statistical and computational support and boundless energy, and Juliana Chase, for engaged feedback, late-night lab chats, and moral support. And to Lung-Hao Tai, the real MVP—thank you so much for always being there to help me build, fix, or troubleshoot any component of my research. Finally, I want to recognize the support and guidance of other professors and scientific mentors I've had the pleasure of working with over the years in Berkeley, Chicago, and Frankfurt, including Dan Feldman, Mark Sheffield, Danko Nikolić, Elliot Gershon, and Jason MacLean. You all have enabled me to become the scientist I am.

Next, to the friends who supported me throughout this trying process, who witnessed countless evolutions of myself as I navigated the trials of grad school, a global pandemic, and my 20s—you have no idea how much I relied on your support. In particular, thanks to Courtney, for your honest perspective and insightful observations; Kathy, for keeping me connected to what matters; Maité, for being there to receive all my emotions; Maddie, for teaching me so much about myself and sharing in the electrifying joy of our brains buzzing together; and Willa, for sticking out this crazy journey with me from start to finish, and for seeing the good, the bad, and the ugly, and still being there. There are so many others I've appreciated and loved, and I'm genuinely indebted to all of your generosity. I couldn't have done this without you.

Finally, none of this would be possible without my crazy family. Thank you to my grandparents, for all your hard work and your belief in me; to all my aunts and uncles, and in particular, Cathy and Lisa, my “vacation moms”, for sending care packages, checking in, and treating me throughout my entire academic career; to my brothers, Nash and Bodhi, for being giant loveable weirdos and making me so proud—it has been an inspiration to grow up alongside you; to my dad, the original Dr. Klinger, for your unconditional love, support, and advice for the last three decades; and to my mama, for being unabashedly true to yourself, for always wanting the best for me, and for still being willing to learn and grow. I see myself in all of you, and I am so proud to be your family.

Chapter 1

Cells Like Teen Spirit: An Introduction to the Adolescent Frontal Cortex

Across the developing brain, windows of heightened synaptic plasticity in the neural circuitry of specific brain regions underlie “critical” or “sensitive” periods for developmental milestones. First described at the cellular level in the development of ocular dominance in the visual system, impairment of a system during a critical period results in irreversible deficits later in life (Wiesel & Hubel, 1963). In the context of ocular dominance, this means that if one eye is covered during the critical period, most visual cortex neurons fail to develop sensitivity to inputs from that eye, even after it is uncovered. Over time, critical periods for other primary cortical sensory areas have been described, including somatosensory (Erzurumlu & Gaspar, 2012; Lo et al., 2017; O’Leary et al., 1994) and auditory (Barkat et al., 2011; Takesian et al., 2018). Onset of these periods has been shown to be regulated by similar mechanisms, especially changes in γ -Aminobutyric acid (GABA) -ergic inhibition (Espinosa & Stryker, 2012; Hensch, 2005; Levelt & Hübener, 2012). Inhibition may facilitate critical period onset by suppressing spontaneous activity relative to stimulus-evoked activity, thus sharpening the signal-to-noise ratio of stimulus encoding.

Critical periods for higher cognitive skills such as language acquisition (Penfield & Roberts, 1959), mastery of a second language (DeKeyser et al., 2010; DeKeyser, 2000; Hartshorne et al., 2018; J. S. Johnson & Newport, 1989; Newport, 1990), fear learning (Pattwell et al., 2011), sociocultural learning (Blakemore & Mills, 2014), and other social behaviors (Bicks et al., 2020; D. C. Li et al., 2024) have also been described, but their mechanistic regulation is not well understood. Notably, critical periods for sensory processing tend to occur in juvenility, while critical periods for higher-order cognitive skills, many of which rely on activity in the frontal cortex, are shifted towards adolescence (Fig. 1). While the mechanisms underlying potential frontal cortical critical periods are not fully known, it is worth investigating whether factors that regulate critical periods are conserved across cortical regions. Because it remains unclear precisely how a critical period in the frontal cortex might manifest or unfold, I use the term “sensitive” rather than “critical” to describe a period of heightened developmental sensitivity in the frontal cortex throughout this text.

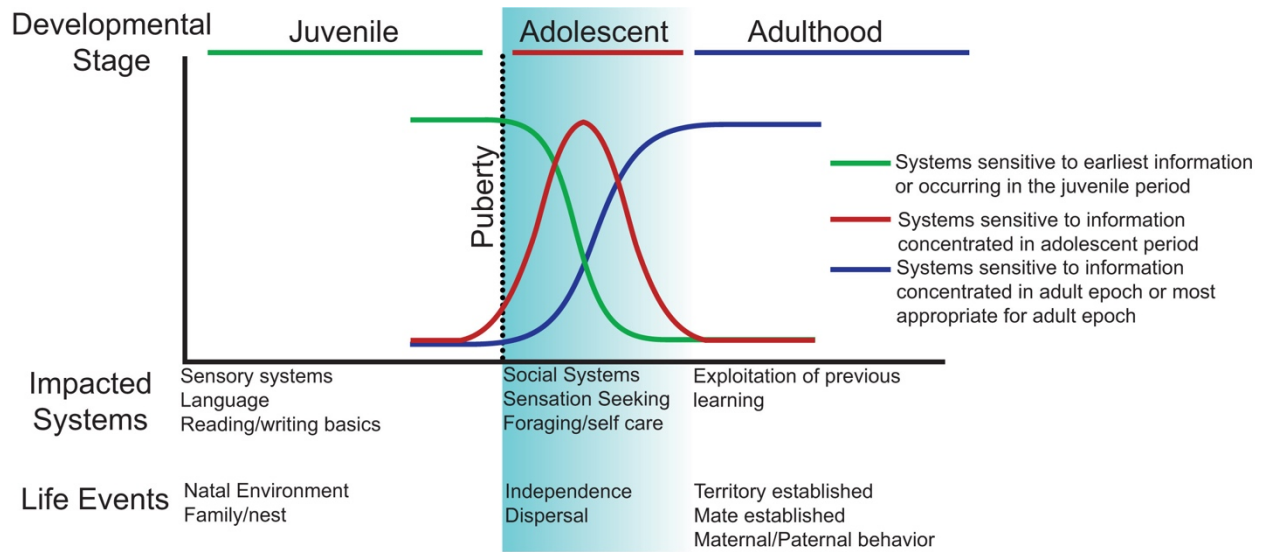


Figure 1: Developmental timeline and associated events. During the juvenile period (green line), animals undergo critical periods for sensory systems; humans also experience critical periods for language skills. Puberty (dotted line) indicates the onset of adolescence, when new behaviors that facilitate independence and exploration emerge. For certain systems (red line), there may exist an adolescent critical period. In adulthood (blue line), animals finesse previously gained skills. Figure reprinted from Piekarski, Johnson, et al., 2017.

In adolescence, the frontal cortex undergoes structural and functional remodeling, including pruning of synaptic connections, maturation of the dopaminergic system, and an increase in GABAergic inhibitory neurotransmission (Caballero et al., 2016; Delevich et al., 2019; Piekarski, Johnson, et al., 2017). Given the extensive literature demonstrating the role of inhibitory neurotransmission in the induction of critical periods, as well as more recent arguments supporting the role of dopamine in shaping adolescent skill development (Larsen & Luna, 2018; Luciana & Collins, 2022; Reynolds et al., 2019), my dissertation is centered on the question of an adolescent sensitive period in the frontal cortices. Here, in Chapter 1, I first review what is known about changes occurring in the frontal cortex during adolescence primarily in rodents, but also including humans and nonhuman primates. I then detail experiments in which we compared adolescent and adult learning in a go/no-go task and the capacity for the frontal cortices to encode task variables at different ages (Chapter 2), as well as the development of a fluorescent probe to detect dopamine in biological environments (Chapter 3). Through this work, I discuss the possibility that structural and functional development of the adolescent frontal cortex may support a putative sensitive period for learning.

Adolescent development of frontal cortices

Mice are weaned at postnatal day (P) 21, and the period referred to as adolescence spans P28-44 in mice. Pubertal onset generally occurs around P30, with vaginal opening driven by an increase in estradiol in females and preputial separation driven by an increase in testosterone in males; full sexual maturity is reached by P60. In humans, this timeline corresponds roughly to ages 7.5-11.5, marked by estradiol-mediated initiation of breast development in girls and an increase in testicular volume in boys (Piekarski, Johnson, et al., 2017) (Fig. 2). In rodents, for the purposes of this work,

we can further subdivide adolescence into early (P28-35) and late (P36-44) epochs. I use specific ages as appropriate throughout the text.

The frontal cortices in rodents, like in primates, have been divided into multiple subregions (Laubach et al., 2018). Here, I focus particularly on the dorsomedial prefrontal cortex (dmPFC), including the secondary motor and anterior cingulate cortices (the area is targeted for neuronal imaging in Chapter 2), and the medial prefrontal cortex (mPFC), including the anterior cingulate, prelimbic, and infralimbic cortices. The ventromedial prefrontal cortex (vmPFC) includes only prelimbic and infralimbic cortices. I aim to refer to each subregion specifically when applicable but refer broadly to mPFC or frontal cortex as a whole when necessary.

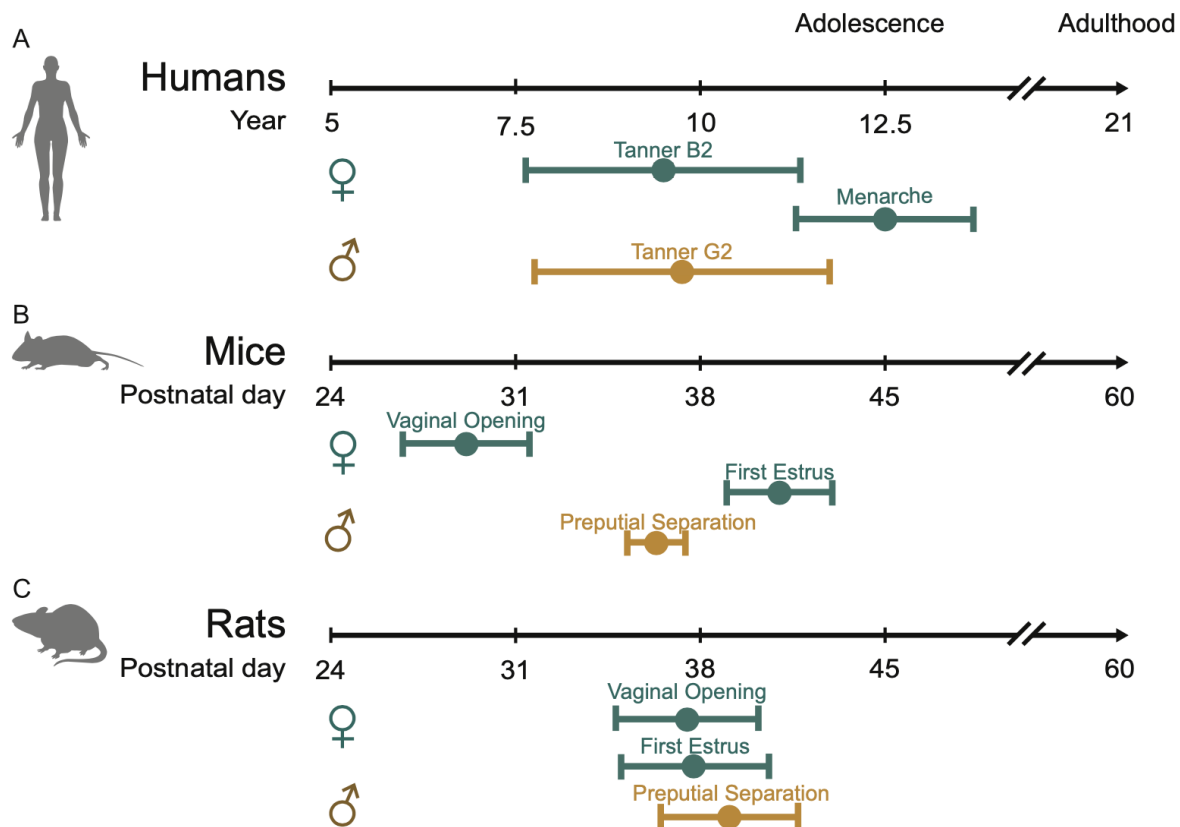


Figure 2. Timeline of adolescence in humans and rodents marked by pubertal events. Here, we define adolescence in mice to include ages postnatal day (P) 28-44. Figure reprinted from Piekarski, Johnson, et al., 2017.

Macroscale: gray and white matter development

In humans, gray matter, corresponding to cell bodies, peaks around puberty onset in the frontal and associative cortices and then declines to adult levels (Gogtay et al., 2004; Gogtay & Thompson, 2010). White matter, corresponding to myelinated axonal tracts, increases into adulthood (Asato et al., 2010; Barnea-Goraly et al., 2010; De Bellis et al., 2001; Lebel et al., 2008; Perrin et al., 2008, 2009). Studies in rats show that the number of neurons in rat vmPFC, but not dmPFC, decreases between adolescence and adulthood, while glial cells show an opposite pattern:

they increase in number in dmPFC, but not vmPFC (Markham et al., 2007). Sex differences have also been reported, with a decrease in vmPFC neurons specifically between P35-45 in female, but not male, rats, though white matter increased steadily in both sexes across development (Willing & Juraska, 2015). The functional implications reduced neuron count in vmPFC and increased glial count in dmPFC at puberty are not completely understood, though recent evidence suggests a role for microglia in synaptic pruning of cortical layer (L) 2/3 pyramidal neurons (PYR) in dmPFC during early adolescence (Pöppel et al., 2023).

Mesoscale: development of the dopaminergic system in frontal cortices

The frontal and associative cortices are known to be involved in multiple cognitive processes that are mediated by dopamine, including working memory, decision making, associative learning, action planning, behavioral flexibility, integration of rewarding and aversive stimuli, and response inhibition (Chau et al., 2018; Floresco & Magyar, 2006; Friedman & Robbins, 2022; Goldman-Rakic, 1998; Ott & Nieder, 2019; Pignatelli & Bonci, 2015; Puig et al., 2014; Sheynikhovich et al., 2022; Vander Weele et al., 2018; Winter et al., 2009). On the cellular and subcellular level, dopamine has also been shown to play a role in facilitating long-term potentiation and depression in pyramidal neurons in prefrontal cortex (Bai et al., 2014; Huang et al., 2004; Meunier et al., 2017; Otani et al., 2015) and modulating neuronal activity in prefrontal cortex (Di Domenico & Mapelli, 2023; Lohani et al., 2019). Importantly, the mesocortical dopamine pathway connecting the basal ganglia to the prefrontal cortex continues to develop throughout adolescence, implicating adolescence as a time of change and refinement in higher cognitive skills (Caballero et al., 2016; Hoops & Flores, 2017; Wahlstrom et al., 2010).

The development of this dopaminergic system is threefold, concerning dopaminergic axonal projections from the midbrain, dopamine receptor density, and dopaminergic neuron firing rate. Multiple teams have shown that dopaminergic innervation of rodent frontal cortex continues through adolescence until early adulthood (~P60) (Benes et al., 2000; Hoops et al., 2018; Kalsbeek et al., 1988; Manitt et al., 2011a; Naneix et al., 2012; Reynolds, Pokinko, Torres-Berrío, et al., 2018); this development is not strictly regulated by pubertal hormones, but is rather age dependent (Willing et al., 2017). Likewise, dopamine D1 and D2 receptor density increases until the same age (Andersen et al., 2000; Tarazi & Baldessarini, 2000; Weickert et al., 2007). Moreover, D1 receptor activation mediates depolarization of mPFC pyramidal neurons only in adult rats, suggesting dopamine enhances glutamatergic signaling through N-methyl-D-aspartate (NMDA) receptors only in adulthood (Flores-Barrera et al., 2014; Tseng & O'Donnell, 2005). Similarly, D2 receptor activation increases firing frequency in mPFC GABAergic interneurons only in adult rats (Tseng & O'Donnell, 2007), suggesting dopamine influence, through multiple receptor types on multiple cell types in mPFC, is still maturing over adolescence. Finally, data from anesthetized rats show midbrain dopaminergic neuron firing rates peak at mid-adolescence (McCutcheon & Marinelli, 2009). In mice, optogenetically stimulating these neurons increased synaptic bouton formation on their projections in dmPFC during adolescence, but not adulthood, indicating that adolescent mesocortical dopamine projections are more plastic (Mastwal et al., 2014).

Microscale: spine density, dendritic arborization, and inhibitory neurotransmission

Across the brain, synapses develop rapidly after birth, then are pruned and stabilized at some point from late childhood to early adulthood. Human studies have shown that synapse density in prefrontal cortex exhibits protracted pruning compared to other cortices, with connectivity continuing to develop through adolescence and dendritic spines stabilizing not until one's 20s (Gogtay et al., 2004; Huttenlocher & Dabholkar, 1997; Kolb et al., 2012; Petanjek et al., 2011; Sowell et al., 2003). Again, this pattern is mirrored in rodents as well, as multiple groups have shown that spine density and turnover—the fraction of new spines developed each day relative to the fraction pruned—both decrease between early adolescence (P27-29) and early adulthood (P60) in both L2/3 and L5 of anterior cingulate and prelimbic cortices (Boivin et al., 2018; Delevich et al., 2020; Drzewiecki et al., 2016; Johnson et al., 2016; Koss et al., 2014; Pöppelau et al., 2023; Zhang et al., 2021; Zuo et al., 2005). While each group examined rodents of varying age groups, from P14 to P90, spine density was reported to be highest at P28-35 (Pöppelau et al., 2023; Zhang et al., 2021). Moreover, dendritic arborization complexity increased between P20 and P35, peaking at P33-35 (Koss et al., 2014; Pöppelau et al., 2023).

Prior to and during adolescent changes in spine density and turnover, the frontal cortices also undergo remodeling of inhibitory neurotransmission onto the principal pyramidal neurons in both superficial (L2/3) and deep cortical layers (L5 and L6). While excitatory neurotransmission, measured in recordings of mini excitatory postsynaptic currents (mEPSCs), is similar between adolescent and adult mice in both L2/3 and L5 PYR of the dmPFC, inhibition increases with age. In macaque monkeys, inhibitory postsynaptic currents (IPSCs) increase in amplitude in L3 PYR of the dorsolateral PFC regions 9 and 46 until periadolescence (32.7-34.8 months) (Gonzalez-Burgos et al., 2015). mIPSCs also increase in both frequency and amplitude between P24-27 and P40-50 in L2/3 PYR, which are intratelencephalic projecting (IT-type), and in amplitude in IT-type, but not pyramidal tract projecting (PT-type), PYR neurons of L5 neurons in mice (Piekarski, Boivin, et al., 2017; Vandenberg et al., 2015). These data have been used to suggest that adolescent IT-type neurons, specifically, of L2/3 and L5 may be more likely to undergo a sensitive period of plasticity than PT-type neurons between P27-40 in mice (Delevich et al., 2018, 2021; Piekarski, Boivin, et al., 2017; Piekarski, Johnson, et al., 2017; Vandenberg et al., 2015). Increase in phasic inhibition in L2/3 pyramidal neurons is likely mediated through an increased release probability of presynaptic GABAergic vesicles, as evidenced by changes in paired-pulse ratio in experiments that used hormones to speed the maturation of phasic inhibition in adolescence (Piekarski, Boivin, et al., 2017a). However, tonic inhibition, measured in current through extrasynaptic GABA receptors expressing the δ subunit, decreases over adolescence in the L2/3 PYR of dmPFC, possibly to offset increases in phasic inhibition (Piekarski, Boivin, et al., 2017).

Several pieces of evidence suggest that this remodeling of GABAergic inhibition is facilitated by parvalbumin-expressing inhibitory interneurons (PV INs) in dmPFC. Expression of parvalbumin increases in fast-spiking inhibitory interneurons throughout multiple regions of mPFC, increasing to near-adult levels between P35 and P45 (Caballero et al., 2014). In adult mice, feed-forward inhibition from long-range projections onto L2/3 PYR in dmPFC is mediated specifically through PV INs, highlighting their importance in consolidating information from other brain areas (Delevich et al., 2015). In adolescent rats (P31-49), PV INs undergo a period of excitatory receptor remodeling exhibited in a markedly reduced NMDA:AMPA ratio due to an increase in α -amino-

3-hydroxy-5-methyl-4-isoxazolepropionic acid (AMPA) receptors (Wang & Gao, 2009). This NMDA:AMPA balance may help increase and stabilize PV IN activity, which may impact their increased downstream influence on L2/3 PYR in adolescence. For instance, one study showed that optogenetic activation of PV INs in mouse prelimbic cortex more strongly inhibited L2/3 PYR linearly with age from juvenility to adulthood (Pöpplau et al., 2023). This finding corroborates the increase in mIPSC frequency and amplitude observed in L2/3 PYR that occurs between the juvenile and early adulthood stages (Piekarski, Boivin, et al., 2017a). Together, multiple lines of evidence demonstrate maturation of inhibitory microcircuits within dmPFC during adolescence and support the idea that there is an increase in GABAergic inhibition, mediated by PV INs, onto IT-type neurons, occurring around P30 (Fig. 3). This could, in theory, initiate a putative sensitive period for plasticity in the frontal cortices.

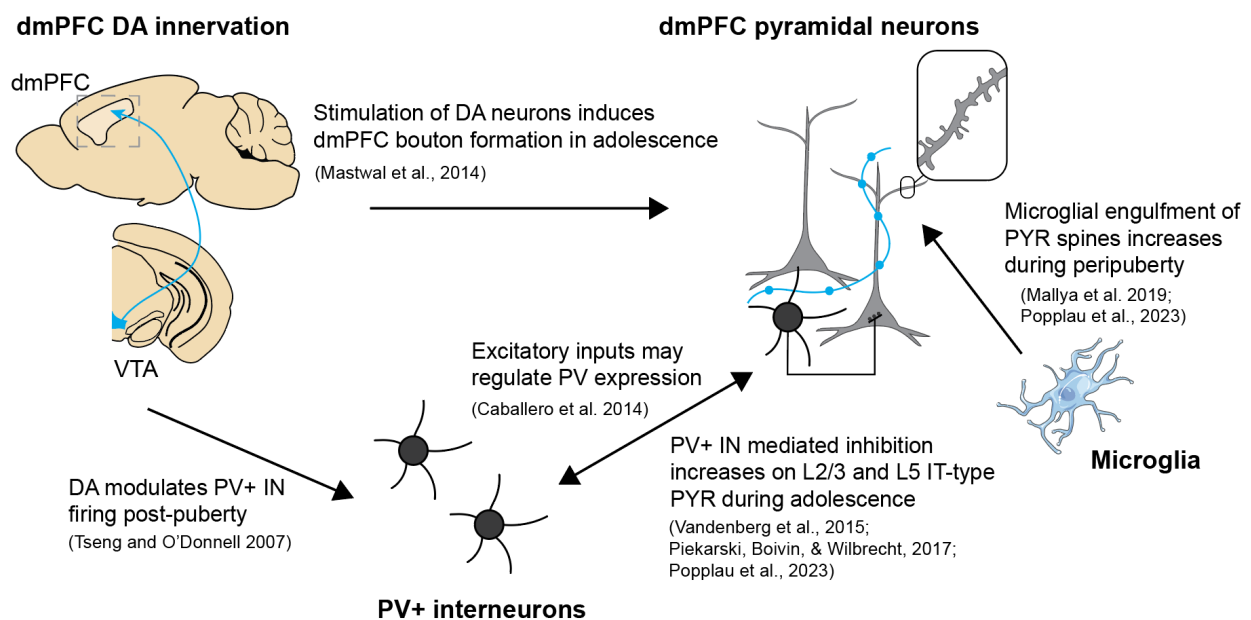


Figure 3. Interacting systems in dmPFC during adolescence. L2/3 and L5 PYR exhibit a higher spine density during adolescence. Dopamine (DA) induces synaptic plasticity in dmPFC in adolescence and modulates PV IN excitability in adulthood. PV IN inhibition onto L2/3 and L5 IT-type PYR increases during adolescence. Microglia contribute to spine pruning during adolescence. Figure revised and reprinted from Delevich et al., 2021.

The concept of an adolescent critical or sensitive period also applies to behavior. A growing body of literature has elucidated variations in adolescent performance on certain cognitive tasks, showcasing both strengths and weaknesses relative to other ages. In the sensory cortices, sensitive periods are associated with greater plasticity that more readily enables encoding of environmental stimuli. Following this line of reasoning, we might assume greater plasticity would support greater encoding of externally relevant information in the frontal and associative cortices. The role of these cortices, and dmPFC in particular, is largely to integrate information from other brain areas, including subcortical regions as well as sensory cortices, to enable appropriate decision making and action selection (Barthas & Kwan, 2017; Brecht, 2011; Ebbesen et al., 2018; J.-H. Yang & Kwan, 2021). Thus, greater plasticity in dmPFC could translate into greater ability to learn or perform executive functions. However, though adolescents have a demonstrated aptitude for

behavioral flexibility and learning under certain circumstances (Eckstein et al., 2022; C. Johnson & Wilbrecht, 2011; Simon et al., 2013; van der Schaaf et al., 2011; Westbrook et al., 2018), they are generally considered to exhibit underdeveloped executive functions (Delevich et al., 2021; Larsen & Luna, 2018; Piekarski, Johnson, et al., 2017b; Wilbrecht & Davidow, 2024). Next, I briefly consider studies of adolescent behavior in humans, nonhuman primates, and rodents. I call into question whether behavioral differences, particularly in tasks requiring response inhibition, may reflect changes in frontal cortical circuit organization and plasticity, and whether these changes might, indeed, mark a sensitive period in adolescence for learning or encoding of environmental information.

Adolescent development of response inhibition

Examination of response inhibition is commonly employed in laboratory tasks that aim to determine how well subjects can withhold from performing a learned action, often under time pressure, threat of punishment, or reward incentive. While they share the same descriptor, it does not necessarily follow that increased inhibitory neurotransmission in dmPFC drives improved response inhibition at the behavioral level, though this category of task is one of many shown to rely on frontal cortical activation (Adleman et al., 2002; Constantinidis & Luna, 2019; Huizinga et al., 2006; Liston et al., 2006; Luna et al., 2015; van de Laar et al., 2014). Response inhibition tasks take many forms, including antisaccade, flanker, go/no-go, stop signal, Stroop, contingency degradation, and delay discounting tasks, among others, and behavior varies across ages and species depending on the task (Table 1). For instance, performance in the antisaccade task, in which participants must look in the opposite direction of a visual stimulus, plateaus around the onset of puberty (Luna et al., 2004; Ordaz et al., 2013; Ravindranath et al., 2022). Other lines of evidence show unique advantages or disadvantages mid-adolescence. In a stop signal task, in which participants must inhibit an over-trained response to a visual stimulus only when accompanied by an infrequent auditory stimulus, adolescents have been reported to outperform younger and older ages (Williams et al., 1999), but adolescents also make more incorrect responses than both older and younger ages in a go/no-go task (Somerville et al., 2011).

Table 1. Behavior in response inhibition tasks during adolescence.

| Authors | Species | Ages | Task | Results |
|---------------------------|---------|----------------------------|-------------|---|
| Luna et al., 2004 | humans | 8-30 years old, continuous | Antisaccade | Gradual improvement with age that plateaus around age 14 |
| Ordaz et al., 2013 | humans | 9-26 years old, continuous | Antisaccade | Gradual improvement with age that plateaus around age 15 |
| Ravindranath et al., 2022 | humans | 8-19 years old, continuous | Antisaccade | Gradual improvement with age, even when controlling for pubertal stage |
| Williams et al., 1999 | humans | 6-81 years old, continuous | Stop signal | Stop signal response time follows an inverted U shape with trough at ages 13-17 |
| Bedard et al., 2002 | humans | 6-82 years old, continuous | Stop signal | Stop signal response time plateaus starting at ages 13-17 |

| | | | | |
|-------------------------------------|----------|---|------------------------------------|--|
| Somerville, Hare, & Casey, 2011 | humans | children (6-12), teens (13-17), adults (18-29) | go/no-go | Teens exhibit greater false alarm trials than children or adults |
| Lewis et al., 2017 | humans | 6, 8, 10 years old | go/no-go | False alarm trial rate decreases between ages 6-8; little improvement between ages 8-10 |
| Marsh et al., 2006 | humans | 7-57 years old, continuous | Stroop task | Gradual improvement with age that plateaus around age 20 |
| Hirst et al., 2019 | humans | children (6-11), young adults (18-25), older adults (60-84) | Stroop task | Error rate follows an inverted U shape with trough at young adulthood |
| Cragg, 2016 | humans | 7, 10, 20 years old | Flanker task | Improvement between ages 7-10; no further improvement between 10-20 |
| Zhou et al., 2016 | macaques | 4, 6 years old | Antisaccade | Adults perform better than adolescents |
| Sturman, Mandell, & Moghaddam, 2010 | rats | P28-42, >P60 | Contingency degradation | Adolescents continue to lever-press at a higher rate than adults after the action is no longer rewarded |
| Adrezejewski et al, 2011 | rats | P25-31; P80-86 | Contingency degradation | Adolescents continue to lever-press at a higher rate than adults after the action is no longer rewarded |
| Naneix et al., 2012 | rats | P25-40, P70-85 | Contingency degradation | Adolescents, but not adults, continued to lever-press after the action was no longer required to obtain reward |
| Adriani & Laviola, 2003 | mice | P30-49; >P60 | Delay discounting | Adolescents choose the small but immediate reward over the larger but delayed reward more often than adults |
| Pinkston & Lamb, 2011 | mice | P35-42, P77-84 | Delay discounting | Adolescents choose the small but immediate reward over the larger but delayed reward more often than adults |
| Burton & Fletcher, 2012 | rats | P25-26, >P70 | 2 choice serial reaction time task | Adolescents responded before the “go” signal more often than adults |
| Simon et al., 2013 | rats | P28-48, >P60 | Cued response inhibition task | No difference between adult and adolescent ability to inhibit in response to a “no-go” cue |

Adolescent rodent performance on response inhibition tasks is not as well documented, but two relevant paradigms include contingency degradation and delay discounting. In contingency degradation experiments, animals first learn the association between a specific action, such as a

lever press, and reward delivery. The association is then degraded such that rewards may be administered independently of the action, rendering it unnecessary, or rewards may no longer be administered at all, rendering the action futile. Adolescents exhibit a higher rate of lever-pressing after contingency degradation than adults (Andrzejewski et al., 2011; Naneix et al., 2012; Sturman et al., 2010), suggesting they are less able to inhibit a learned action. In delay discounting paradigms, animals must choose between a small but immediate reward or a larger but delayed reward by nose-poking in a corresponding reward slot. Similarly, while adults learn that the larger-but-delayed option is more advantageous and act accordingly, adolescents choose the small-but-immediate reward more often (Adriani & Laviola, 2003; Pinkston & Lamb, 2011), potentially demonstrating a lack of inhibitory control. In contrast, adolescent rats perform just as well as adults in a cued response inhibition task (Simon et al., 2013). In this task, an inhibitory cue—a continuous tone varying in length from 5-30 seconds—instructed animals to wait. After the tone ended, animals had a 10-second response period to retrieve a food pellet reward via nose poke into a food port. If animals nose-poked during the presentation of the inhibitory cue, no reward was administered, and the response was classified as “incorrect”; if animals did not retrieve the reward after the inhibitory cue ended, the response was classified as “omission”. No difference was found in either the proportion of incorrect trials or the proportion of omission trials between adolescents and adults. Thus, even from a relatively sparse sample of studies, our understanding of adolescent rodent inhibitory control is not fully clear.

Taken together, evidence from both humans and rodents paints a nuanced and incompletely understood picture of adolescent response inhibition that warrants further investigation. In particular, it is unclear why the improvement plateau in adolescence observed in multiple human studies is not reflected in rodent studies. Moreover, to our knowledge, neural activity in the rodent adolescent dmPFC has not been monitored concurrently with studies of response inhibition. Developing a better understanding of adolescent behaviors and the mechanisms that underlie them will be critical to our understanding of adolescent and adult behavioral disorders.

Adolescent development shapes adult outcomes

Adolescence is also a period of relevance from a public health perspective, as adolescent experience can impact adult brain function and behavior. Thus, adolescence is increasingly seen as a critical period for intervention to reduce vulnerability and enhance positive outcomes in adulthood (Dahl et al., 2018). Studies of adolescent animals have been used to demonstrate how adolescent experience can contribute to illnesses and disorders in humans. Importantly, many psychiatric disorders that manifest in perturbations in higher-order cognition, such as depression, anxiety, bipolar disorder, schizophrenia, and addiction, have documented peak onsets in adolescence (Paus et al., 2008). Moreover, early life adversity is a known trigger for many of these disorders (Juwariah et al., 2022; Kessler et al., 2010; Waters & Gould, 2022). While adolescents share many common forms of adversity with younger children, they may also be uniquely susceptible to educational, social, and romantic adversities that have been shown to contribute to depression in early adulthood (Pollmann et al., 2023). Though this topic has been reviewed extensively elsewhere (Crone & Dahl, 2012; Dahl et al., 2018; Larsen & Luna, 2018; Lipner et al., 2023; Malave et al., 2022; Paus et al., 2008; Piekarski, Johnson, et al., 2017), I briefly discuss a

few examples that illustrate how interference in the adolescent dmPFC changes described above may impact behavior and health outcomes in adulthood.

Not unexpectedly, early life adversity negatively impacts physical and mental health, but the cellular-level implications of adversity are only beginning to be understood. In rodents, one type of adversity can be modeled in males using a social defeat paradigm, in which one animal is placed in another's cage; the cage resident typically attacks the intruder ("social defeat"). Social defeat in adolescence has been shown to increase social avoidance and decrease performance on both set-shifting and go/no-go tasks in adulthood (Vassilev et al., 2021; Zhang et al., 2016). Moreover, social defeat dysregulated expression of mesocortical dopamine axon guiding cues in the basal ganglia, leading to increased dopamine fiber varicosities in the prelimbic cortex in adulthood (Vassilev et al., 2021). A similar paradigm, social isolation, was employed to investigate changes in prefrontal PYR structure during adolescence. Chronic social isolation in adolescence in mice caused reduced dendritic length, reduced dendritic complexity, and reduced density of stubby-shaped spines, but increased long/thin and filopodia-shaped spines (Li et al., 2022). Reversing the order of these manipulations revealed similar effects, as preventing pruning of L5 PYR during adolescence by GABA receptor knockdown increased anxiety behaviors in an elevated plus maze in adult female mice (Evrard et al., 2021).

Importantly, disruption of inhibitory maturation during adolescence also seems to play a role in adult mental health. An fMRI study in humans administered GABA agonist benzodiazepine to examine the effects of acute inhibition on functional connectivity throughout the adolescent brain, from ages 8 to 22. From these data, researchers generated a model of expected change in the excitatory to inhibitory (E:I) neurotransmission ratio with age. They found, specifically in association cortex, a predicted reduction in the E:I ratio over adolescence. Critically, adolescents with mood disorders exhibited a stable E:I ratio with age, rather than showing the expected decrease (Larsen et al., 2022). This finding is echoed in a rodent study that demonstrated that early life stress causes an increase in excitatory synapses on L2/3 PYR in prefrontal cortex and increased activity of dopaminergic neurons projecting to PFC from the ventral tegmental area, perpetuating an elevated E:I ratio over adolescence (Oh et al., 2021). Taken together, these data illustrate how adversity during adolescence can alter expected changes in adolescent PFC structure and function with potentially lasting effects. These findings further motivate our interest in better understanding adolescence as a putative sensitive period.

Conclusion

In conclusion, adolescence can be described as an epoch marked by change, both in terms of frontal cortical remodeling as well as in cognitive development and behavior. A growing body of research on adolescent development is beginning to give rise to the concept of an adolescent sensitive period for learning and frontal cortical encoding. Here, I outline our approach to testing this idea, through implementation of a go/no-go task with simultaneous imaging of calcium transients in L2/3 of the dmPFC (Chapter 2). I also present the development of a novel probe for detection of catecholamines in biological environments as a step toward expanding our toolbox of imaging methods (Chapter 3). Finally, I conclude by offering thoughts on future directions in the investigation of adolescent brain development.

Chapter 2

Let's Get Critical: Adolescent Frontal Cortex and the Possibility of a Critical Period for Encoding of Task Variables

In the previous chapter, I outlined changes in the developing adolescent brain and introduced the lines of reasoning to propose a sensitive period for frontal cortex development and function. In this chapter, I examine the ability of the dmPFC to encode go/no-go task information during adolescence (P30-44) and early adulthood (P60-74) and compare learning and performance of adolescent and adult mice on this task. This work is designed to assess whether the dmPFC during this adolescent period is endowed with greater, equal, or lesser ability to encode information than the dmPFC of the adult brain.

Critical period regulation and motivation for studying dmPFC

We can learn from sensory cortical areas how physiological changes drive critical period onset and investigate whether similar changes may implicate a putative sensitive period in the frontal cortices. Evidence from an extensive body of literature in the primary sensory cortices, particularly ocular dominance plasticity in the visual cortex, demonstrates that critical period plasticity in the upper layers of the neocortex is regulated by an increase in GABAergic inhibitory neurotransmission (Espinosa & Stryker, 2012; Hensch, 2005; Levelt & Hübener, 2012). In one classic study, Gad65-knockout mice, which exhibit reduced GABA synthesis, were found to lack a critical period for ocular dominance plasticity in the visual cortex (Hensch et al., 1998). This phenotype was rescued by administration of a GABA_A receptor agonist, specifically through activation of the $\alpha 1$ subunit (Fagiolini et al., 2004; Fagiolini & Hensch, 2000). More recently, transplant studies suggest GABAergic neurons themselves convey critical factors. Transplant of embryonic inhibitory neurons into the visual cortex of young mice was shown to induce a later critical period, once the implanted neurons matured to the age of typical critical period onset (Southwell et al., 2010; Tang et al., 2014).

These classic experiments highlighting the importance of GABAergic inhibition in the onset of sensory cortical critical periods motivated us to examine whether similar factors might be at play in other cortices, particularly the frontal cortex. We posited that PYR neurons, which experience a developmental increase in GABAergic inhibition during the 4th week of life in mice, might also be entering a period of enhanced plasticity, similar to ocular dominance plasticity in visual cortex. This hypothesis is supported by extensive work in frontal cortical PYR of adolescent mice. As discussed in Chapter 1, our lab found an increase in phasic inhibitory neurotransmission on to L2/3 and L5 IT-type PYR in *ex vivo* brain slices of the dmPFC from ~P25 to P40, with a marked change in the mEPSC/mIPSC ratio occurring between P27-28 and P31-33 (Delevich et al., 2015, 2019; Piekarski, Boivin, et al., 2017; Vandenberg et al., 2015). More recent data suggest this increase may come from parvalbumin-expressing interneurons (PV INs). Another group reported that the capacity of PV INs neurons to silence L2/3 PYR increased linearly across age groups, from juvenility (P16-23) to adulthood (P53-60). This group also found that PV IN-mediated

gamma frequency oscillations peak in early adolescence (P28–P35), then decrease during late adolescence (P36–P43), before stabilizing in adulthood (Pöpplau et al., 2023). In sum, these data demonstrate how frontal cortex changes in GABAergic inhibition are similar to those observed at the onset of the visual cortex critical period. As such, we hypothesized that a putative sensitive period may begin around P30 in L2/3 of dmPFC.

Other developmental changes may also contribute to enhanced plasticity and a putative sensitive period during adolescence. For example, spine density on L2/3 and L5 PYR and spine turnover both decrease throughout mPFC between P29-P60 (Boivin et al., 2018; Delevich et al., 2020; Johnson et al., 2016; Koss et al., 2014; Pöpplau et al., 2023; Zhang et al., 2021; Zuo et al., 2005). Spine pruning is thought to be mediated by microglia, as evidenced by an increase in glial cells in dmPFC (Willing et al., 2017) plus increased phagocytic activity of microglia in the same area (Pöpplau et al., 2023). Additionally, dopamine innervation and dopamine receptor density mature in dmPFC. Dopamine also increases firing frequency in PV INs specifically through the D2 receptor (Tseng & O'Donnell, 2007), which may be another mechanism by which inhibitory neurotransmission increases. Additionally, dopamine neuron firing rates peak and then decrease (McCutcheon & Marinelli, 2009), which may facilitate dmPFC dopamine neuromodulation, as evidenced by increased bouton formation following optogenetic activation of dopamine neurons in adolescence (Mastwal et al., 2014). Changes in dmPFC dopamine and spine density, in addition to changes in GABAergic neurotransmission, are thus poised to interactively shape dmPFC function (Delevich et al., 2021).

Additional studies have demonstrated the importance of frontal cortex development for cognitive skill by disrupting it during adolescence. For instance, chemogenetic inactivation of anterior cingulate cortex projections to visual cortex during early adolescence (P25-34), but not late adolescence/early adulthood (P45-54), increases adult error rate in a visual five choice serial reaction time task, indicating that neuronal activity in anterior cingulate during adolescence is critical for development of action selection and attention (Nabel et al., 2020). Similarly, mice treated with amphetamine during late juvenility/early adolescence (P22-31), but not late adolescence (P35-44), accrue more “false alarm” trials in a go/no-go task in adulthood (Reynolds et al., 2019). Histology performed on these amphetamine-treated mice in early adolescence reveals a reduced density of dopamine axon varicosities throughout mPFC and reduced dopamine metabolization, suggesting dopaminergic innervation during adolescence is critical for development of behavioral inhibition. These studies elegantly link the effects of perturbation of the frontal cortex during adolescence to deficits in behavioral outcomes later in life, thus demonstrating that adolescence experience can impact adult cognitive development.

These lines of evidence, particularly the extensive documentation of GABAergic inhibitory development specifically in L2/3 of dmPFC during adolescence, suggest that adolescence may represent a sensitive period for frontal cortical development and encoding of information in frontal cortices. If our hypothesis is correct, and dmPFC experiences a sensitive period during early adolescence (~P30-35), then we predict that dmPFC may show greater efficiency in encoding of task-related information in the P30s than in the P60s. A sensitive period at this time might also position adolescents to learn more efficiently than adults or reach a higher level of performance. If, on the other hand, adolescence is not a sensitive period and the mature development of adult brain is a more optimal state for encoding, we might instead expect that the adult dmPFC will

exhibit more robust encoding of task information, which may translate to more efficient learning or more effective performance in a behavioral task. We also consider a null hypothesis that despite differences in connectivity and plasticity, the adolescent and adult dmPFC will encode information about the task comparably; and/or learning and performance will be comparable.

Our investigation leverages the literature documenting these changes as a framework from which to investigate adolescent capability and dmPFC encoding in a go/no-go task. This task has been shown by others to depend on frontal cortical function (Liu et al., 2023; Reynolds et al., 2019; Salkoff et al., 2020). We trained groups of adolescent (P30-44) and adult (P60-74) mice on task for 14 consecutive days and examined neuronal dynamics while imaging calcium activity in L2/3 through a cranial window. We found that when behavior was expert and comparable between age groups, encoding of task relevant information was enhanced in population-level neural activity of the adolescent dmPFC, but encoding at the single-cell level was comparable between age groups. Adolescent mice were also faster than adults at learning the go/no-go task, but both age groups eventually reached comparable expert performance. In sum, our population level neural data and learning data support the hypothesis that a window in the ~P30s may be a putative sensitive period for dmPFC function.

Materials & Methods

Animals

We bred transgenic mice in-house, crossing tetO-GCaMP6 (<https://www.jax.org/strain/024742>) and CaMKIIa-tTA (<https://www.jax.org/strain/007004>) mice. For experiments, we used male and female mice heterozygous for the CaMKIIa-tTA transgene and homozygous for the tetO-GCaMP6s transgene. All mice were weaned on postnatal day (P)21 and housed in groups of 3-4 same-sex siblings on a 12:12 h reversed light:dark cycle (lights on at 22:00 h). Experimental mice belonged to two age cohorts: adolescent (P30-44) and adult (P60-74). Mice were socially housed alongside nonexperimental littermates during the time of experimentation. All animals were given access to food and water *ad libitum* prior to experiment start. During pre-training, training, and imaging of the experimental period, they had *ad libitum* access to food but access to water was restricted to 1 mL water per day. All procedures were approved by the Animal Care and Use Committee of the University of California, Berkeley and conformed to principles outlined by the NIH Guide for the Care and Use of Laboratory Animals.

Surgeries

Male and female mice (P28 or P58) were deeply anesthetized with 5% isoflurane (vol/vol) in oxygen and placed in a stereotaxic frame with ear bars (Kopf Instruments) on a heating pad for the duration of surgery. Anesthesia was maintained at 1%–2% isoflurane during surgery. An incision was made along the midline of the scalp and a 3 mm diameter circular craniotomy performed over the anterior cingulate area of the left hemisphere medial prefrontal cortex (coordinates relative to Bregma: A/P: -0.5 to 2.5 mm, M/L: -2.0 to 1.0 mm). Stacked glass coverslips of 3 mm and 5 mm diameter bonded with UV optical adhesive (Norland) were implanted over the craniotomy and sealed with dental cement (C&B Metabond® Quick Adhesive Cement, Parkell, Inc.). A stainless steel off-centered circular head bar (custom design, eMachineShop) was affixed above the cranial

window. Mice were given subcutaneous injections of meloxicam (10 mg/kg) during surgery and 24 and 48 h after surgery.

Pre-training, Handling, and Habituation

Four nights before surgery, access to water was restricted. The following morning, mice were placed in an arena with food and *ad libitum* water available from mounted lick spouts in order to pre-train mice to water-seeking behavior in a novel environment. After 4-6 hours, mice were removed from the arena and handled for at least 5 minutes before undergoing habituation to a running wheel placed in their home cage for 15 minutes. Mice underwent pre-training, handling, and running wheel habituation for a total of 3 days, receiving at least 1 mL water each day. Water was returned to the home cage after the third day of pre-training, and surgery was performed the following day. Due to rapid bone regrowth over the cranial window in adolescent animals, imaging began as soon as possible after surgery, following approval from the Animal Care and Use Committee. Thus, 24 hours after surgery, mice were administered analgesic, handled for 5 minutes, then habituated to the experimental arena for 15 minutes. Mice were placed on an acrylic running wheel rotating about the Y-axis and head-mounted to a custom steel bracket mounted above the wheel. Mice received access to water during this time through a lick spout. After habituation, mice were returned to the home cage. Water was removed from the home cage that evening. The next morning, approximately 48 hours after surgery, the experiment began. Weight was monitored daily.

Head-fixed go/no-go auditory discrimination task

In the go/no-go task, mice were trained to discriminate between 4 “go” and 4 “no-go” auditory cues (500 ms each) by licking to go cues and inhibiting licking to no-go cues. Water restricted mice began training on this task 48 hours after surgery, at P30 or P60. Mice trained one session per day for at most one hour. Mice were head-fixed atop a running wheel with access to a lick spout, which was connected to a capacitance sensor. Water rewards (2 μ L) were delivered by gravity drip regulated through a solenoid valve controlled by TTL pulses. On “direct delivery” trials mice received one reward, and on “hit” trials, two water rewards separated by 100 ms were administered for a total of 4 μ L. Auditory stimuli were delivered through speakers (Bohlender & Graebener, Neo3-PDR Planar Tweeter) placed on either side of the wheel. The task was administered through custom scripts written in MATLAB.

On the first day of training, all mice began the experiment with at least 50 “direct delivery” trials. In these trials, a 500ms go cue (7 kHz pure tone, “cue 2”) indicated the availability of a water reward, and mice had 3 s to respond by licking. Mice were immediately given a double reward (4 μ L water) upon licking; if they did not lick, a single reward (2 μ L water) was given at the end of the lick interval. Water delivery initiated an inter-trial interval (1-2 s, drawn from a Gaussian distribution) in which mice must not lick for the last full second before subsequent cue onset. Direct delivery trials continued until mice regularly began to lick in response to the auditory cue, receiving a double reward. After 20 consecutive double-rewarded trials, direct delivery ended; from that point on, mice had 3s after cue onset to lick, and water (double reward) was delivered only if mice licked (“hit” trial). If mice did not lick after 3s, no reward was given, and the trial was labeled a “miss”. After a further 20 hit trials, a 500ms no-go cue (14 kHz pure tone, “cue 7”) was introduced at a 1:9 ratio of no-go:go cues. In response to a no-go cue, mice must refrain from

licking for 3s in order to complete a “correct reject” trial and progress to the inter-trial interval. If mice licked (“false alarm” trial), incorrect action was signaled by a 500ms white noise burst and punished with a 10s timeout before progressing to the inter-trial interval. We noted during pilot sessions that introducing the first no-go cue at a 1:1 ratio with the go cue dissuaded most animals from participating in the task at all; thus, we employed a progressive strategy to introduce the first no-go cue first at a 10% frequency, increasing the frequency as tolerated by each animal to 20%, 30%, and finally 50%. By presenting the no-go cue with increasing frequency, animals gained positive reinforcement from the more-frequent go cue, and thus maintained motivation to continue engaging with the task. If mice disengaged with the task upon increasing the occurrence of no-go cues, the proportion of no-go cues was reduced with the goal to encourage consistent licking to go cues.

Once mice achieved tolerance of 1:1 no-go:go cues, we began tracking their performance using the metric d' . A rolling d' value was calculated over the past 50 trials as $d' = z(\text{hit rate}) - z(\text{false alarm rate})$. We used the MATLAB function `norminv()`, which calculates the inverse of the standard normal cumulative distribution function, to approximate a z-score. Because the `norminv(x)` function approaches infinity and negative infinity as x approaches 1 and 0, respectively, the upper bound of the hit rate and false alarm rate was set to 0.99 and the lower bound was set to 0.01. We determined a threshold of $d' = 1.8$, corresponding to a 100% hit rate and 70% false alarm rate (i.e., 30% correct no-go trials and 100% correct go trials). If mice sustained performance of $d' > 1.8$ for 20 consecutive trials, we introduced an additional cue set (go: 6.5 kHz, “cue 1”; no-go: 15 kHz, “cue 8”) alongside the first go and no-go cues for a total of 4 different tones at a 1:1:1:1 ratio. Similarly, after sustaining $d' > 1.8$ for 20 consecutive trials after at least 50 trials of these 4 cues, the next cue set was introduced (go: 8.5 kHz, “cue 3”; no-go: 12 kHz, “cue 6”) in equal proportion to existing cues; after sustaining $d' > 1.8$ for 20 consecutive trials after at least 50 trials of these 6 cues, the final cue set was introduced (go: 9 kHz, “cue 4”; no-go: 11.5 kHz, “cue 5”) in equal proportion to existing cues. Finally, after sustaining $d' > 1.8$ for 20 consecutive trials after at least 50 trials of all 8 cues, 8 probe cues were introduced at a 1% frequency each. These cues approximated go and no-go cues in that they preceded a 3s response window prior to the 1-2s inter-trial interval, but they did not yield reward or trigger a timeout, regardless of the mouse’s response. These trials were omitted from analysis. In order to learn the complete task, mice must maintain an average $d' > 1.8$ over at least one session with all cues and probes present. Mice trained for 14 consecutive days; experiments were ended earlier if mice either completed 3 consecutive sessions with all cues and probes or completely disengaged from the task for 3 consecutive sessions. Mice achieved various levels of completion (see summary in Table 2).

Table 2. Mice trained on the go/no-go task.

| Animal | Cohort | Sex | # sessions trained | # sessions with usable imaging data | Behavioral performance achieved |
|--------|-------------|-----|--------------------|-------------------------------------|---------------------------------|
| JUV010 | Adol-Dec21 | M | 14 | 0 | Learned complete task |
| JUV011 | Adol-Dec21 | M | 14 | 0 | Learned complete task |
| JUV012 | Adol-Dec21 | F | 14 | 0 | Learned complete task |
| JUV013 | Adol-Dec21 | F | 14 | 0 | Reached cue set #3 |
| ADT001 | Adult-Dec21 | F | 11 | 0 | Reached cue set #3 |
| ADT004 | Adult-Feb22 | M | 14 | 0 | Learned complete task |

| | | | | | |
|--------|-------------|---|----|----|-----------------------|
| ADT005 | Adult-Feb22 | M | 14 | 0 | Reached cue set #4 |
| ADT006 | Adult-Feb22 | M | 11 | 0 | Learned complete task |
| ADT007 | Adult-Feb22 | M | 14 | 0 | Reached cue set #1 |
| JUV014 | Adol-Apr22 | M | 14 | 13 | Learned complete task |
| JUV015 | Adol-Apr22 | M | 14 | 14 | Learned complete task |
| JUV016 | Adol-Apr22 | M | 14 | 14 | Learned complete task |
| ADT008 | Adult-Apr22 | M | 14 | 13 | Learned complete task |
| ADT009 | Adult-Apr22 | M | 10 | 9 | Learned complete task |
| ADT010 | Adult-Apr22 | M | 9 | 8 | Learned complete task |
| TRA001 | Adult-Sep22 | F | 13 | 0 | Learned complete task |
| TRA002 | Adult-Sep22 | F | 13 | 13 | Reached cue set #2 |
| TRA003 | Adult-Sep22 | M | 13 | 0 | Learned complete task |
| JUV017 | Adol-Nov22 | F | 13 | 12 | Learned complete task |
| JUV019 | Adol-Nov22 | F | 14 | 5 | Reached cue set #1 |
| JUV020 | Adol-Jan23 | M | 11 | 7 | Reached cue set #1 |
| JUV021 | Adol-Jan23 | M | 10 | 10 | Reached cue set #2 |
| JUV022 | Adol-Jan23 | F | 10 | 8 | Learned complete task |
| ADT012 | Adult-Feb23 | M | 13 | 3 | Reached cue set #1 |
| ADT013 | Adult-Feb23 | M | 12 | 0 | Learned complete task |
| ADT014 | Adult-Feb23 | F | 13 | 3 | Reached 30% no-go |
| ADT015 | Adult-Feb23 | F | 14 | 13 | Reached 30% no-go |
| JUV024 | Adol-Feb23 | F | 14 | 3 | Learned complete task |
| JUV025 | Adol-Feb23 | M | 13 | 12 | Learned complete task |
| ADT016 | Adult-Mar23 | F | 11 | 0 | Reached 30% no-go |
| ADT017 | Adult-Mar23 | F | 14 | 0 | Learned complete task |
| ADT018 | Adult-Mar23 | F | 14 | 0 | Learned complete task |
| ADT019 | Adult-Mar23 | M | 14 | 0 | Learned complete task |
| ADT020 | Adult-Mar23 | M | 14 | 0 | Learned complete task |
| ADT027 | Adult-Dec23 | F | 9 | 6 | Learned complete task |
| ADT028 | Adult-Dec23 | F | 10 | 10 | Learned complete task |
| ADT029 | Adult-Dec23 | M | 13 | 6 | Learned complete task |
| ADT030 | Adult-Dec23 | M | 14 | 3 | Reached cue set #1 |

Two-photon imaging

We performed calcium imaging of the dorsomedial prefrontal cortex, targeting layer 2/3 of the anterior cingulate area of the cortex and the medial 1 mm of the supplementary motor cortex (M2) (coordinates relative to Bregma: A/P: +0.8 to 1.8 mm, M/L: 0 to 1 mm, D/V: -0.2 to -0.35 mm; Fig. 4B). Animals were imaged through a cranial window while head-fixed and performing the task using a commercial two-photon microscope (Bruker) controlled by PrairieView software. Excitation light was provided by a Ti:Sapphire laser (Mai Tai, Newport Spectra-Physics) tuned to 910 nm; the beam was focused on layer 2/3 through a 20x water-immersion objective (NA 1.0, Olympus). Images were acquired through spiral scanning at 8 Hz, with a resolution of 256 x 256 pixels and frame diameter of 650 μm (0.39 pixels/ μm). Animals were scanned prior to training each day and were only imaged during that session if cells were clearly visible (see summary in Table 2).

Cell detection & preprocessing

Registration of imaging data was completed either in Suite2P (Pachitariu et al., 2017) or NoRMCorre (Pnevmatikakis & Giovannucci, 2017). Images were aligned with one round of non-rigid registration (in 64 x 64 pixel chunks) and up to five rounds of rigid registration. Images were manually evaluated for sufficient motion correction and quality prior to cell detection and were discarded if motion was still present or cells were insufficiently visible. All cell detection was completed in Suite2P, where each ROI was manually validated to be classified as a cell. Sessions with fewer than 50 cells were omitted from imaging analyses. Validated sessions were neuropil subtracted, and baseline fluorescence (F_0) was determined for each cell as follows: we calculated the mean and standard deviation for fluorescence values in a rolling 200-frame window, then set a threshold = mean + 1.5 standard deviations and calculated the mean of all frames in that window under the threshold. $\Delta F/F_0$ was calculated for each cell for each frame and used as the basis for all imaging analyses.

Behavioral & Statistical Analysis

Statistical analysis was performed either through custom MATLAB scripts (MathWorks Inc.), custom Python scripts using the SciPy package, or in GraphPad Prism (GraphPad Software Inc.). Our decoder was implemented through the Scikit-learn package for Python, using sklearn.svm.SVC. Data are reported as mean +/- standard error of the mean, unless otherwise noted.

Multiple Linear Regression

To determine how fluorescent signals may relate to choices and outcomes, we used multiple linear regression adopted from previous literature (Siniscalchi et al., 2019; Wang et al., 2022):

$$\begin{aligned} \frac{\Delta F}{F}(t) = & b_0 + b_1 c_{n+1} + b_2 r_{n+1} + b_3 s_{n+1} \\ & + b_4 c_n + b_5 r_n + b_6 s_n \\ & + b_7 c_{n-1} + b_8 r_{n-1} + b_9 s_{n-1} \\ & + b_{10} c_n r_n + b_{11} c_n s_n + b_{12} r_n s_n \\ & + b_{13} V_{run}(t) + b_{14} lick(t) + \varepsilon(t) \end{aligned}$$

where $\Delta F/F(t)$ is the fractional changes in fluorescence at time t in trial n ; c represents the animal's action choice (lick vs. no lick), r represents trial outcome (reward vs. no reward), and s represents stimulus identity (go vs. no-go); subscripts $(n+1)$, n , and $(n-1)$ represent the next trial, the current trial, and the previous trial, respectively; b_0, \dots, b_{14} are the regression coefficients; $V_{run}(t)$ is the running speed of the animal at time t ; $lick(t)$ takes the value of 1 if the animal licked at time t and is otherwise 0; and $\varepsilon(t)$ is the error term. For each session, the regression coefficients were determined by fitting the equations to data using python package statsmodels. Equations were fit in 100 ms time bins spanning from -2 to 2 s relative to cue onset, using mean $\Delta F/F_0$ within the time bins. For a given predictor and region of interest (ROI), if the regression coefficients were significant ($P < 0.01$) for at least 3 consecutive or 10 total time points, the ROI was considered significantly modulated by the predictor. To summarize the results, for each predictor, we calculated the proportion of ROIs in which the regression coefficient was significantly different from zero ($P < 0.01$). To determine if the proportion was significantly different from chance, we

performed a chi-square test against the null hypothesis that there was a 1% probability that a given predictor was mischaracterized as significant by chance in a single session. To determine if the proportion of different age groups were significantly different from each other, we performed a chi-square two sample test against the null hypothesis that the two groups were drawn from the same binomial distribution.

Decoding trial information from neural population data

To decode trial information from our calcium imaging neuronal data, we implemented a support vector machine using the Scikit-learn package for Python, `sklearn.svm.SVC`. Each trial was classified by stimulus type (go or no-go), animal choice (lick or no lick), or trial outcome (hit, false alarm, correct reject, or miss). 50% of trials from each session were used as a training dataset, and the remaining 50% of trials comprised the test dataset. This support vector machine projects our data into an n -dimensional space, where n = number of neurons in the recorded session, and aims to optimize a hyperplane between data points of different categories. The hyperplane was optimized through maximization of the margin between points of different categories. Decoder performance on the test dataset was compared to a null dataset, in which category labels are shuffled across trials. Fluorescence data was interpolated every 50 ms, and decoder performance was analyzed on every point of this interpolated data within the [-2, 2] window centered at cue onset (80 comparisons). Multiple t-tests are performed between age groups or between one age group and its null dataset with false discovery rate set to 0.05 through Benjamini-Hochberg correction.

Results

Adolescent mice learn an auditory discrimination task faster than adults

Here, we sought to investigate whether adolescent mice could learn a headfixed go/no-go task and how this task might be represented in dmPFC. We trained adolescent (P30-44) and young adult (P60-74) mice of both sexes that transgenically expressed calcium indicator GCaMP6s in cortical pyramidal neurons (CamKII-tTa^{+/+}/tetO-GCaMP6s^{+/+}). Prior to training, all mice underwent surgery for implantation of a cranial window centered over the left dmPFC, encompassing the medial secondary motor area and most dorsal aspect of the anterior cingulate. We recorded calcium transients in L2/3 PYR during each training session in all animals and obtained high-quality imaging data in 9/14 adolescent (7/10 expert) and 11/24 adult (6/15 expert) mice (Fig. 4; Table 2).

We designed a go/no-go auditory discrimination task specifically to be learned within a 14-day period spanning adolescence (Fig 5A). Training began with habituation to a 7 kHz pure tone go cue (“cue 2”), which signaled the availability of a 4 μ l water reward. Once mice consistently licked the waterspout in response to the go cue (typically 1-2 sessions), we introduced a 14 kHz no-go cue (“cue 7”), which required inhibition of licking for the 3 s response window; licking to a no-go

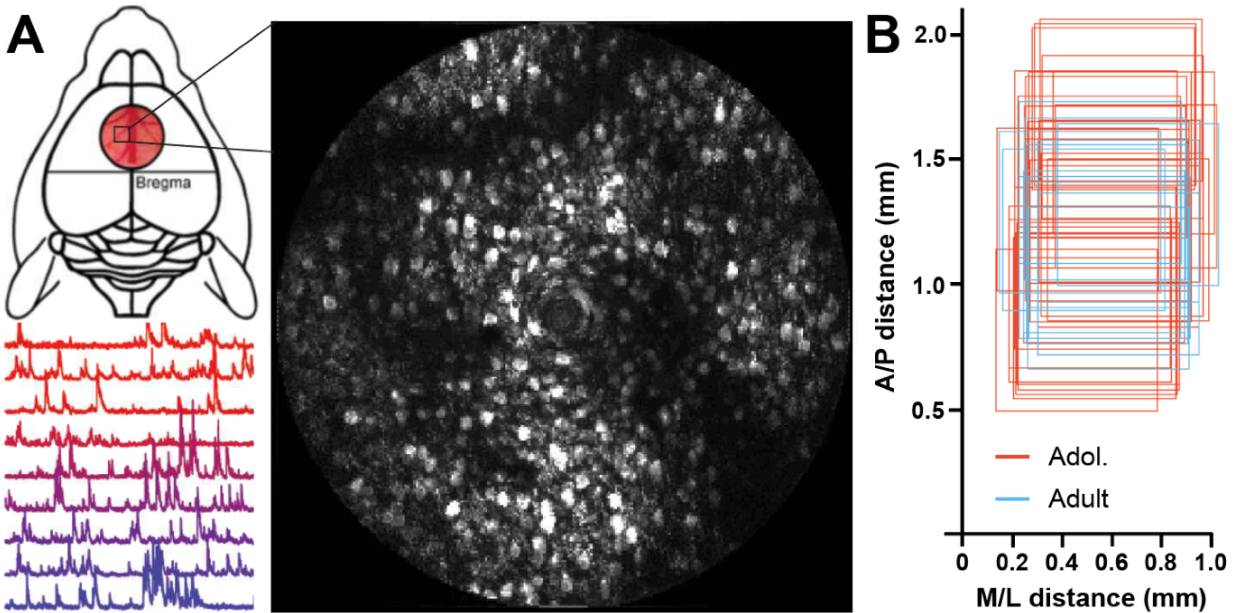


Figure 4: Two-photon calcium imaging. A) Left, top: schematic of imaging area relative to bregma on the mouse skull. Left, bottom: example calcium traces from individual ROIs. Right: example field of view (FOV). B) All imaging FOV locations from analyzed expert sessions relative to bregma.

cue triggered a 10 s time-out. Discrimination between the go and no-go cues was measured by d' , the ratio of z-scored hit rate to z-scored false alarm rate. Through pilot studies, we set a criterion for “task mastery” at $d' = 1.8$, corresponding to a false alarm rate of 0.7 given perfect go cue responses. If an animal sustained performance at $d' > 1.8$ for 50 trials on the initial 2 cues, additional go and no-go cues were introduced in pairs. The complete task consisted of 8 pure tone cues that tiled the mouse auditory spectrum (go cues: 6.5, 7, 8.5, 9 kHz; no-go cues: 11.5, 12, 14, 15.5 kHz; cues are numbered 1-8 from 6.5-15.5 kHz for convenience in Figs. 5-8). Mice trained for one hour each day for 14 consecutive days, or until mice had performed above criterion on all 8 cues for 3 consecutive days.

At the end of the 14-day training period, a similar fraction of mice from both age groups had learned the task to completion (9/14 adolescent and 15/24 adult mice; $\chi^2 = 0.012$, $df=1$, $p = 0.9128$). We first examined basic learning of the task in terms of d' scores over the first half of the sessions, before performance plateaued, by performing a linear regression to determine the slope of improvement in the task. In the first seven sessions, adolescent learning increased at a faster rate than adult learning (linear regression: adolescent slope = 0.34, $r^2 = 0.71$, $p \ll 0.001$; adult slope = 0.20, $r^2 = 0.29$, $p \ll 0.001$; one-way ANOVA between slopes: $F_{(1,163)} = 9.52$, $p = 0.002$). We then confirmed that adolescent mice learn faster than adults by performing a two-way ANOVA. We found a significant effect of age and an age \times session interaction (mixed-effects ANOVA, effect of age: $F_{(1,22)} = 4.47$, $p = 0.046$; interaction of age \times session: $F_{(7,153)} = 2.82$, $p = 0.009$; Fig. 5B). As a metric of learning efficiency, we next analyzed the number of training sessions required for adolescents and adults to reach our $d' = 1.8$ criterion. Of the animals trained, 10/14 adolescent and 15/24 adult mice reached criterion on at least one session within 14 days (one adolescent reached criterion but was unable to learn the complete task). Notably, adolescents reached criterion sooner than adults (adolescent median = day 6, adult median = day 11.5; $p = 0.017$, Gehan-Breslow-Wilcoxon test; Fig 5C). Adolescents that reached criterion all did so

between sessions 5-7, whereas adults reached criterion at various points between sessions 3-14; this represents a significant difference in variance in time to criterion between age groups (F-statistic = 13.19, $p < 0.001$).

We next compared performance of the two age groups after they both reached criterion on the complete task, becoming “experts”, which we defined as achieving $d' > 1.8$ on all 8 cues on session 6 and beyond. To this end, we compared licking rates to each of the 4 “go” and 4 “no-go” cues, combining sessions across 9 expert adolescents and 15 expert adults ($n = 42$ expert adolescent sessions, $n = 33$ expert adult sessions). We found that, when expert, both groups showed comparable licking to go cues (adult mean lick rate = 0.96 ± 0.01 , adolescent mean lick rate = 0.97 ± 0.01) and inhibition of licking to no-go cues (adult mean lick rate = 0.31 ± 0.03 , adolescent mean lick rate = 0.30 ± 0.02), as determined by two-way ANOVA (main effect of age: $F_{(1,73)} = 0.034$, $p = 0.855$; main effect of cue: $F_{(4, 248)} = 945.3$, $p \ll 0.001$; age \times cue interaction effect: $F_{(7,511)} = 0.757$, $p = 0.624$, Fig. 5D). Thus, although adolescents learned the task faster than adults, when experts of both groups were studied, their behavior was comparable.

We next asked whether the trial-by-trial licking of expert adolescents and adults during later sessions revealed any other differences in behavior. We first examined how past trial outcomes impacted licking behavior in the next trial. We first categorized trials by outcome: hit, false alarm (FA), correct reject (CR), or miss, where hit = licking to go cues, FA = licking to no-go cues, CR = inhibiting to no-go cues, and miss = inhibiting to go cues. We analyzed a total of 14,370 adult trials from 33 sessions and 18,070 adolescent trials from 42 sessions from expert mice. In adult sessions, hits made up $47.5 \pm 0.7\%$ of trials, FAs made up $18.1 \pm 1.4\%$ of trials, CRs made up $28.9 \pm 1.6\%$ of trials, and misses made up $1.9 \pm 0.4\%$ of trials; in adolescents, these fractions are comparable, at $45.0 \pm 0.6\%$, $15.7 \pm 0.9\%$, $29.6 \pm 1.0\%$, and $2.8 \pm 0.6\%$ for hits, FAs, CRs, and misses, respectively. We then calculated the likelihood of licking on a given trial given the previous trial’s outcome. We found that likelihood of licking was significantly modified by age in addition to the previous trial’s outcome (two-way ANOVA, effect of age: $F_{(1,73)} = 9.15$, $p = 0.003$; effect of previous trial: $F_{(3,210)} = 43.37$, $p \ll 0.001$; interaction: $F_{(3,210)} = 4.92$, $p = 0.003$; Fig. 5E). Post-hoc t-tests revealed that the effect of age was driven by previous miss trials; adults licked more frequently after miss trials than did adolescents ($p = 0.012$). Thus, even at the expert stage, adolescents and adults behaved differently, particularly after miss trials.

Similar proportions of adult and adolescent dmPFC neurons encode task information across learning

Given that inhibitory neurotransmission has been shown to increase over adolescence (Piekarski, Boivin, et al., 2017; Vandenberg et al., 2015), and that stimulus-evoked activity declines with stimulus familiarity (Pancholi et al., 2023), we first analyzed trends in neural activity levels over the imaging period in expert animals. For each session, we calculated the mean area under the curve from the $\Delta F/F_0$ traces of all cells imaged on each day, as a proxy measure of neural activity. Linear regressions revealed a negative slope indicating a decrease in activity in both adolescent (slope = -117.8 , $r^2 = 0.245$, $p \ll 0.001$; Fig. 6A) and adult groups (slope = -68.53 , $r^2 = 0.153$, $p = 0.005$; Fig 6B). Mixed-effects ANOVA showed a main effect of age ($F_{(1,11)} = 16.18$, $p = 0.002$; Fig. 6C) and session ($F_{(3,4,24.1)} = 3.26$, $p = 0.034$).

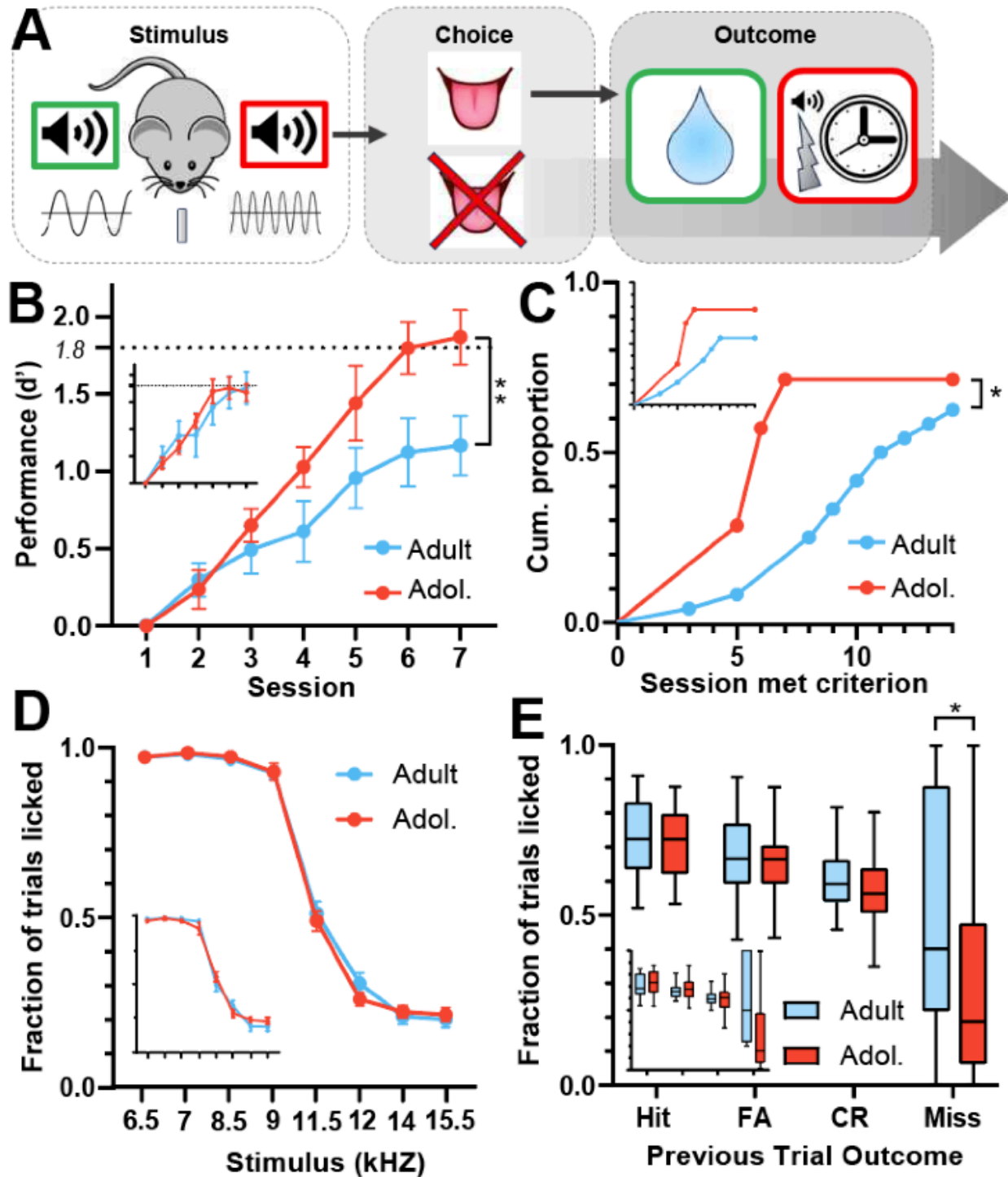


Figure 5: Adolescents learn a go/no-go task more quickly than adults. A) Schematic of task. B) Performance of animals that learned the task to completion by session; dotted line = criterion; inset = animals included for imaging data analysis (not all expert animals had high enough quality imaging data for inclusion). C) Cumulative proportion of animals that have reached criterion by session. Inset = animals included for imaging data analysis. D) Fraction of trials licked by stimulus during expert sessions; inset = sessions included for imaging data analysis. E) Fraction of trials licked by previous trial outcome from sessions in D; inset = sessions included for imaging data analysis.

We next sought to investigate the extent to which dmPFC encoded task-related variables, and whether expert adolescent dmPFC represented task variables differently from expert adult dmPFC when behavioral performance was comparable. We constructed a mixed linear regression model with coefficients representing task variables: stimulus (go vs. no-go), animal choice (lick vs. no lick), and trial outcome (hit, FA, CR, vs. miss). Because animal motion is distributively encoded throughout the cortex (Salkoff et al., 2020; Zatka-Haas et al., 2021), we also included terms to capture neural representation of animal licking and running. We applied the regression model to imaged expert sessions (adult $n = 13$ sessions, 92.8 ± 12.4 cells per session; adolescent $n = 28$ sessions, 127.7 ± 9.4 cells per session) and evaluated the proportion of neurons with significant coefficients for each variable. In concordance with previous work identifying task variable responsive neurons in frontal cortex (Peters et al., 2022; Reinert et al., 2021; Wool et al., 2023), our analysis revealed that a small fraction of neurons encoded task variables. We found $2.9\% \pm 0.6\%$ of imaged neurons encoded stimulus, $4.2\% \pm 1.5\%$ encoded outcome, and $6.6\% \pm 1.4\%$

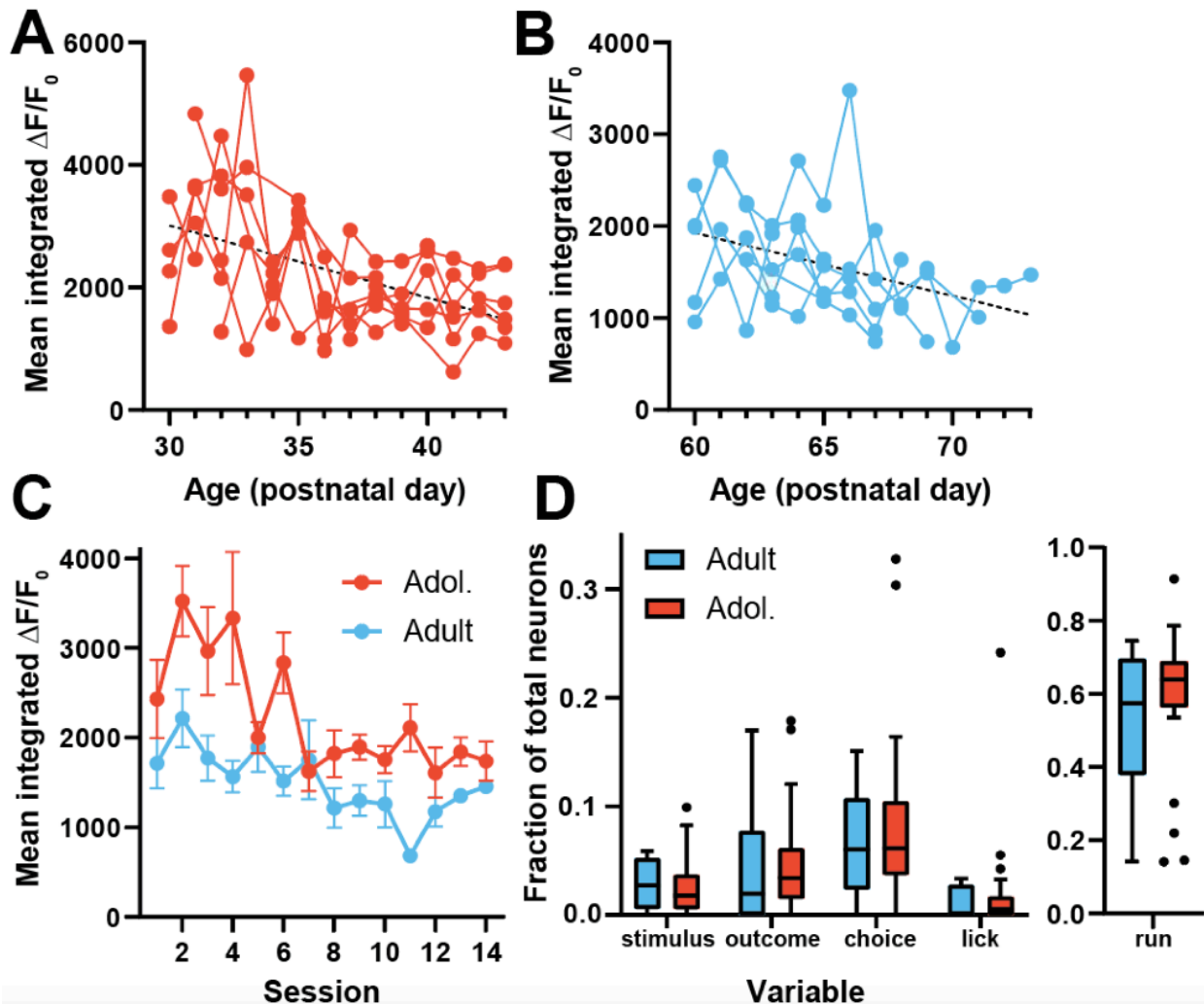


Figure 6: Similar proportions of neurons encode task variables in adult and adolescent dmPFC. A) Mean integrated fluorescence from all cells from all adolescent animals across sessions; individual lines = individual animals; dotted line = linear regression. B) Mean integrated fluorescence from all cells from all adult animals across sessions; individual lines = individual animals; dotted line = linear regression. C) Mean of A) and B). D) Fraction of total neurons imaged that encode task variables.

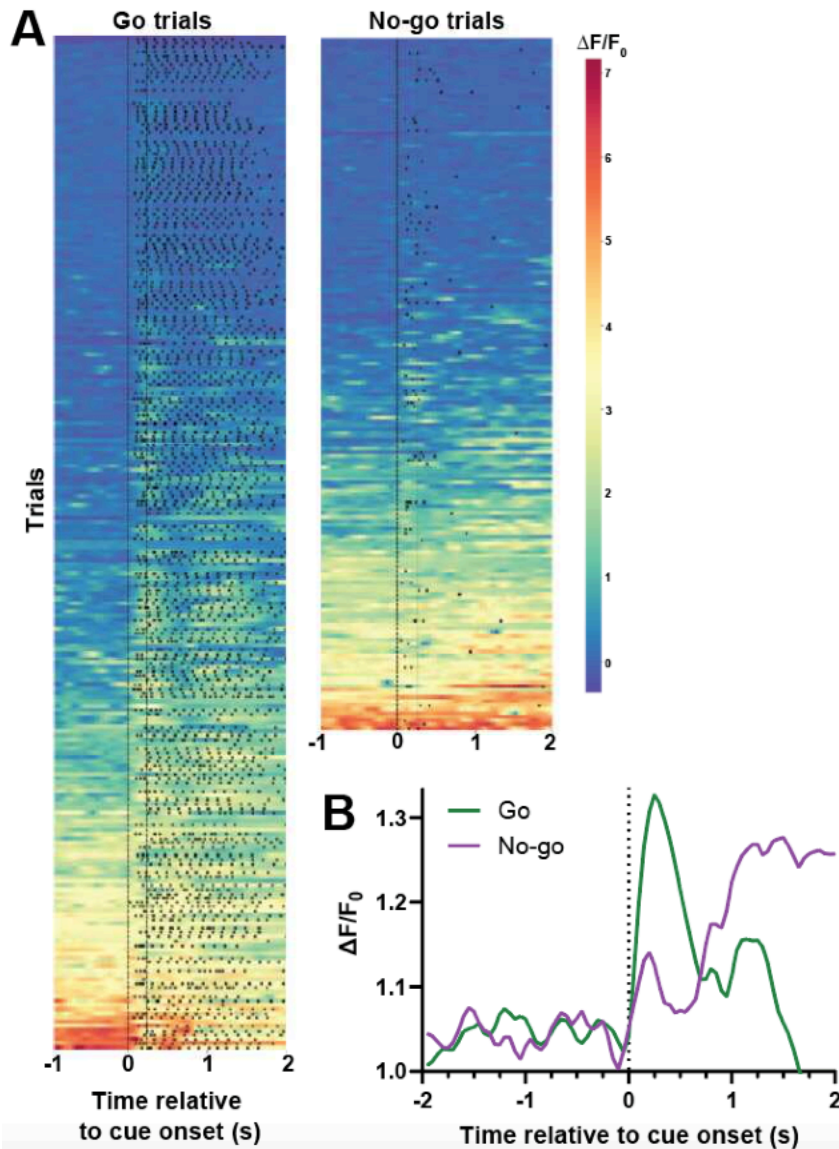


Figure 7: Example stimulus-encoding neuron from an adolescent animal. A) Neuronal activity on individual trials, separated by stimulus type (go vs. no-go), sorted by mean trial fluorescence. Dotted lines = cue onset and offset; black ticks = recorded licks. B) Mean fluorescent response from neuron shown in A) across all go and all no-go trials.

encoded choice in adults, and $2.6\% \pm 0.5\%$ encoded stimulus, $4.9\% \pm 0.9\%$ encoded outcome, and $8.6\% \pm 1.5\%$ encoded choice in adolescents (Fig. 6D; example stimulus-encoding neuron shown in Fig. 7). Close inspection of neurons identified as encoding task variables revealed a variety of response signatures closely aligned to stimulus onset. We found a significant difference in encoding between task variables, but despite the variability in neural response across animals and the relative immaturity of the adolescent dmPFC, our model found no significant difference in task variable encoding between expert adult and expert adolescent groups (two-way ANOVA, effect of variable: $F_{(1.5,60.4)} = 7.33$, $p = 0.003$; effect of age: $F_{(1,39)} = 0.718$, $p = 0.402$; interaction: $F_{(2,78)} = 0.397$, $p = 0.674$; Fig. 2F). Surprisingly, given the documented extent of encoded licking motion throughout the cortex (Zatka-Haas et al., 2021), only a very small percentage ($1.2\% \pm 0.4\%$ in adults; $1.8\% \pm 0.9\%$ in adolescents) encoded licking, though over half of all recorded neurons encoded running ($53.4\% \pm 5.4\%$ in adults, $59.7\% \pm 3.5\%$ in adolescents). Together, these data suggest that the fraction of cells encoding task information is not significantly larger in either adolescents or adults when performance is expert and comparable.

Trial information is better decoded from adolescent neural population activity than adults'

A growing body of research suggests that information represented by the prefrontal cortex may not be linearly encoded in single neurons, but instead emergent from neural activity at the population level, with individual cells exhibiting mixed selectivity for internal and external variables (Bernardi et al., 2020; Dang et al., 2021; Grant et al., 2021; Muller et al., 2024; Parthasarathy et al., 2017; Reinert et al., 2021; Rigotti et al., 2013; Wójcik et al., 2023; Wool et al., 2023). To compare population encoding between age groups, we trained a support vector machine on calcium imaging data from expert sessions to linearly decode stimulus type (go vs. no-go), choice (lick vs. no lick), and trial outcome (hit, miss, false alarm, or correct reject) (Fig. 8A). Though our adolescent sessions contained more cells than adult sessions (adult: 92.8 ± 12.4 cells per session; adolescent 127.7 ± 9.4 cells per session; $p = 0.034$, Mann-Whitney test), we found our decoder performance did not substantially improve with more than 50 neurons per session (Fig. 8B). We thus trained our model to classify individual trials using 50% of the trials in each session as training data and the remaining 50% of trials as test data. We found that, while decoders trained on data from both age cohorts performed above chance level at the late learning stage, decoders trained on adolescent data classified remaining trials with greater accuracy than decoders trained on adult data (Fig. 8C).

Given that over half the imaged neurons encoded animal running, differences in running could be a major influence on decoder results. We examined running speeds in the $[-2s, 2s]$ window around cue onset during both go and no-go trials from adolescent and adult expert sessions and found that running speed was significantly modulated by stimulus type and age, with adolescents running faster than adults and both ages pausing after cue onset on go trials (two-way ANOVA, effect of stimulus type: $F_{(1,38)} = 34.45$, $p < 0.001$; effect of age: $F_{(1,38)} = 15.23$, $p < 0.001$, interaction: $F_{(1,38)} = 15.92$, $p < 0.001$; Fig. 9A). We next evaluated running speeds to different cues within each stimulus category from the decoded sessions. While adults ran comparably to all cues within a stimulus category, adolescent no-go speeds differed between the cue closest to and the cue farthest from the category boundary, with greater modulation of running observed to cue 5 than cue 8 (paired t-test, $p < 0.001$; Fig. 9B).

To test how well the decoder performed when running speed was held constant, we trained our decoder to discriminate between pairs of cues from the same stimulus type within each age group. While this decoder failed to accurately discern between go cues for either adolescent or adult imaging data, it did successfully discriminate between no-go cues using adolescent, but not adult, data, performing significantly above chance level at multiple time points in the 2 seconds after cue onset. In particular, we detected above-chance discrimination between cues 5 and 6, cues 6 and 7, and cues 6 and 8 (Fig. 9C), where importantly, running modulation did not differ significantly between any of these pairs of cues (Fig. 9B). Though the observed effect is notably smaller than our initial decoding results, the fact that our decoder could discriminate between cues of the same stimulus type in the adolescent but not adult brain suggests that greater task information is encoded in the adolescent brain compared to the adult brain, even when running differences are held constant.

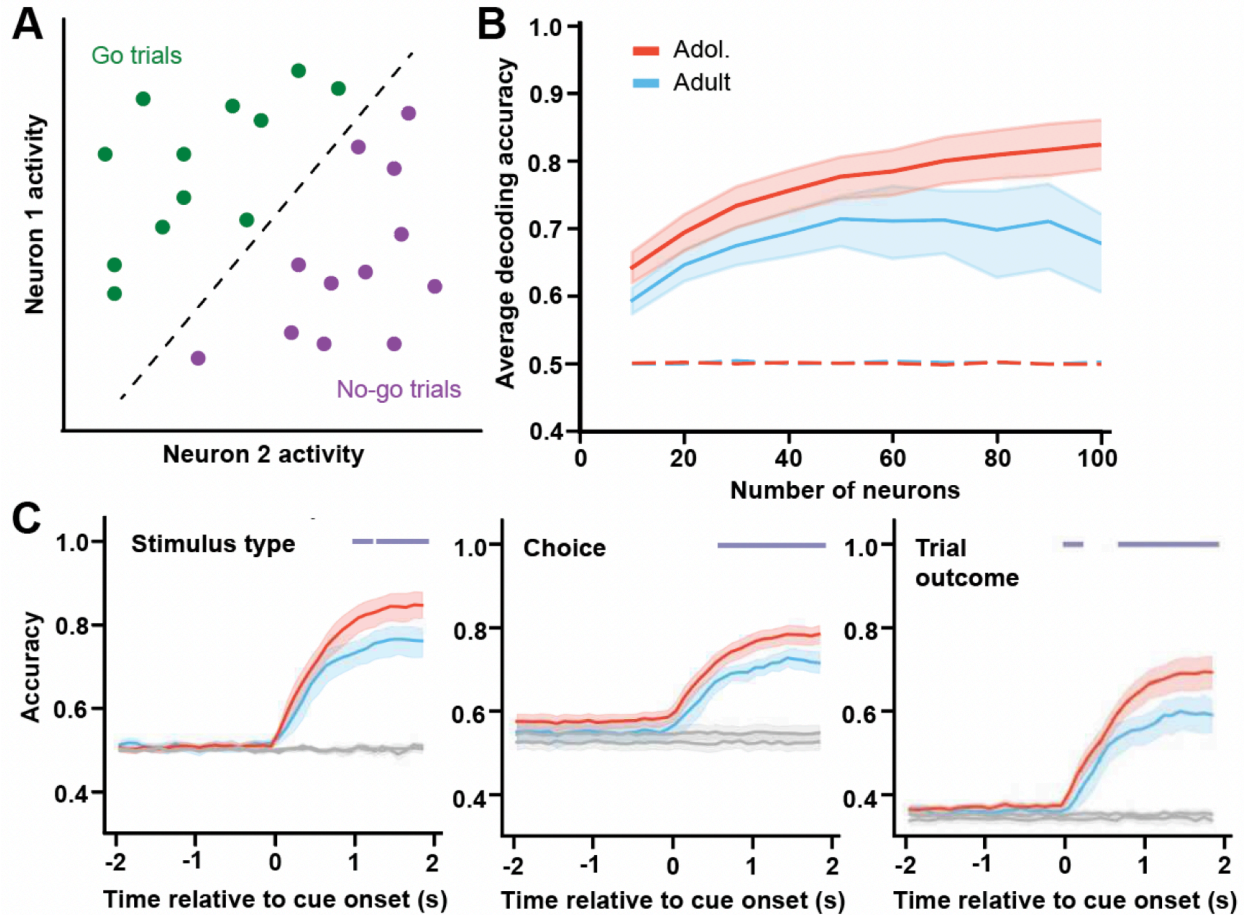


Figure 8: Decoding task variables from adult and adolescent neural population data. A) Schematic of support vector decoder, in which a hyperplane is fit between data points representing neural activity at each time point of each trial. B) Decoding accuracy as a function of the number of neurons included. Shaded region = bootstrapped 95% confidence interval. C) Decoding of stimulus type, animal choice, and trial outcome was more robust from adolescent group data than adult data. Gray bars above the plot indicate significant group difference at that time point ($p < 0.05$; multiple t-tests with false discovery rate = 0.05). Adult $n = 13$ sessions, 92.8 ± 12.4 cells per session; adolescent $n = 28$ sessions, 127.7 ± 9.4 cells per session. Shaded region = bootstrapped 95% confidence interval.

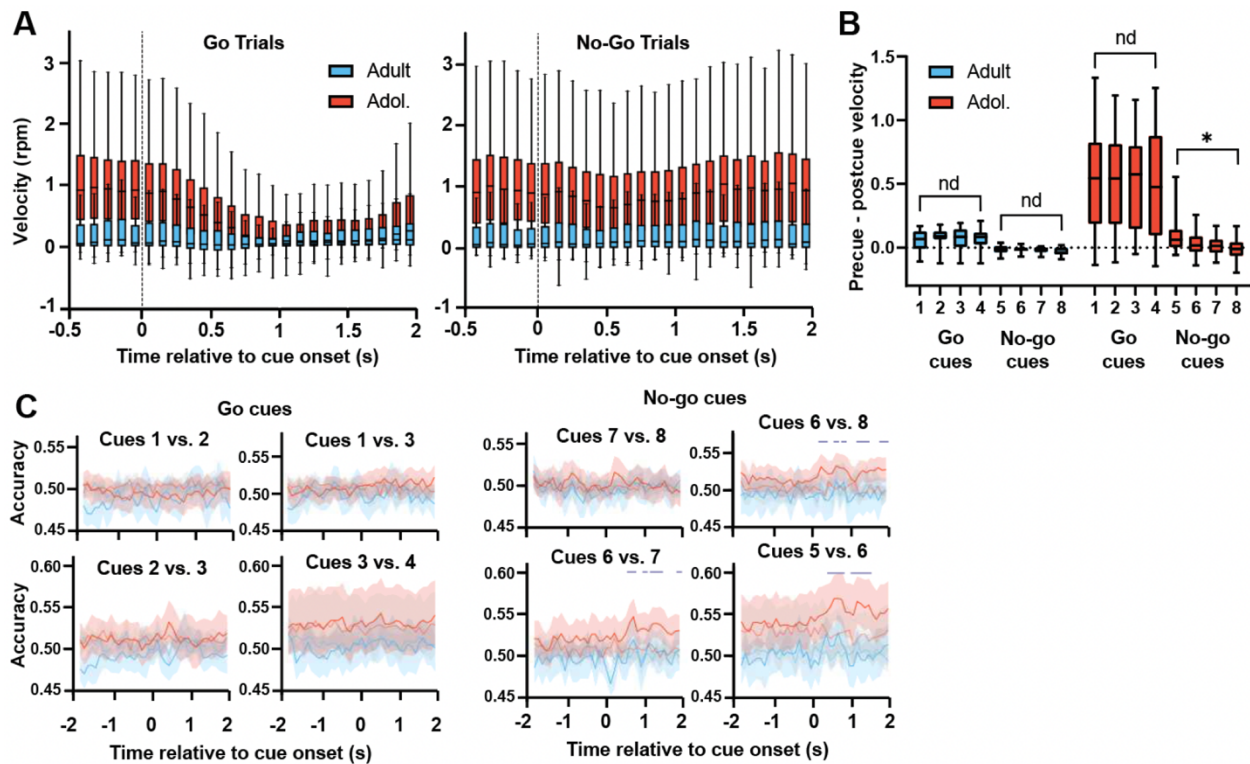


Figure 9: Task information is better decoded from adolescent neural population data, even after controlling for differences in running. A) Distribution of running velocities for expert animals segregated by stimulus type. B) Difference in running velocity (mean [-2,0] – mean [0,2]) by cue. Both age groups modulated running in response to the go cues. Within stimulus categories, running was consistent, with the exception of adolescent no-go cues; adolescents modulated their running more to the no-go clue closest to the stimulus boundary. C) Decoding of cues within stimulus type. Go cues could not be decoded from other go cues at any point in the [-2,2]s around cue onset in either adult or adolescent data. Some no-go cues could be decoded from other no-go cues during the [0,2]s window after cue onset (cue 6 v. cue 5, cue 6 v. cue 7, cue 6 v. cue 8) using adolescent, but not adult, dmPFC imaging data. Gray bars above signal indicate time points at which adolescent cues were decoded accurately significantly above chance level ($p < 0.05$). Shaded region = bootstrapped 95% confidence interval.

Discussion

The growing interest in the concept of a frontal cortex sensitive period motivated us to study go/no-go learning and encoding of task variables in dmPFC. Our study arose from three alternative hypotheses: first, that an adolescent sensitive period could support faster learning and stronger task encoding in the adolescent brain; second, that the immature developmental state of the adolescent brain could hinder learning and task encoding; and finally, that despite differences in neural network connectivity and plasticity, adolescents and adults might perform equally and encode task information comparably (Marder, 2011). Our results support our first hypothesis, as well as portions of the last (null) hypothesis.

Overall, our study shows that adolescent mice can learn a head-fixed go/no-go task more quickly than adult mice but that a comparable proportion of both groups achieve expert-level performance. We also found that expert mice in both groups reached a comparable level of performance. Examination of neural data from expert mice reveals that the fraction of individual neurons that

encode task variables in L2/3 dmPFC is comparable between adolescent and adult groups, but more information about task variables can be decoded from adolescent neural population activity.

Behavioral performance

Our results showing that adolescents learn faster than adults support our first hypothesis, which posits an adolescent sensitive period in learning. In contrast, our second hypothesis predicted a deficit in “no-go” learning based on the assumption that adolescents are generally worse at response inhibition. Indeed, there is evidence that adolescent mice do not show the same ability as adults in contingency degradation and delay discounting tasks (Adriani & Laviola, 2003; Andrzejewski et al., 2011; Burton & Fletcher, 2012; Naneix et al., 2012; Pinkston & Lamb, 2011; Sturman et al., 2010). These studies aim to gauge response inhibition by requiring animals to make value-based decisions. However, a different group reported that adolescent rats perform equally well as adults in a cued response inhibition task (described in Chapter 1), which is in line with our null hypothesis that both age groups perform comparably. This study, in contrast to the above studies on which adults outperformed adolescents, trained animals to perform using an explicit “no-go” cue, as in our task (Simon et al., 2013). To our knowledge, go/no-go learning, especially in a head-fixed context, has not previously been compared between adolescent and adult mice. Thus, it is possible that different mechanisms may be at play in this particular type of response inhibition, or that an adolescent sensitive period extends to only some tasks.

In addition to analyzing the rate of learning, we also examined behavior at the expert stage. In analyzing the behavior of expert animals, we found that adolescents and adults exhibited similar licking (Fig. 5D,E) but differences in running (Fig. 9C,D). Adolescents displayed comparable lick rates to adults on all cues and differed from adults only in lick rate after miss trials, when they were less likely to lick. As miss trials were very rare at the expert level ($1.9 \pm 0.4\%$ of adult trials; $2.8 \pm 0.6\%$ of adolescent trials), we interpret these results as showing adolescents losing interest in engaging with the task, whereas adults were potentially more willing to engage after a lapse in performance. In contrast to licking behavior, adolescent mice ran substantially more in the task than adult mice (Fig. 9C). Additionally, while both groups exhibited modulation of running speeds in response to go cues by stopping to lick, the change in velocity between pre-cue and post-cue periods was greater for adolescents (Fig. 9D), causing a marked behavioral difference between go and no-go cues for adolescents only. While we cannot directly test the effects of locomotion on task performance, it is interesting to note that previous studies have shown that voluntary wheel running for 4, 8, or 16 weeks can increase performance on the Morris water maze in adult mice (Huang et al., 2018; Liu et al., 2009; Wang et al., 2021). Moreover, regular periods of running may impact the dopamine system. One study of 6-week voluntary wheel running in adult mice found increased mRNA levels of tyrosine hydroxylase, an enzyme that facilitates synthesis of dopamine, in the VTA and reduced mRNA levels of the dopamine D2 receptor in the nucleus accumbens core (Greenwood et al., 2011), while another reported increased dopamine release in the dorsal striatum and nucleus accumbens core and shell after 30 days of voluntary running (Bastioli et al., 2022). As discussed, the mesocortical dopamine pathway continues to develop in adolescence, and it is yet unclear how locomotion-related alterations in dopaminergic activity might play out in adolescence. While the time scales of these locomotion studies are longer than our 14-day paradigm, it may be worth further investigating whether locomotion influences go/no-go task learning, whether increased locomotion may be a sign of learning, and whether there are particular

benefits of increased locomotion in adolescence for learning. Together, our behavioral study reveals both a faster rate of learning and greater incidence of running in a go/no-go task in adolescent mice compared to adults, though more work is needed to determine whether these findings are related.

Information represented in dmPFC

Our main goal of this study was to compare how the adolescent dmPFC represented information compared to adult dmPFC. We predicted that the adolescent brain should represent information differently due to ongoing changes in GABAergic inhibition, spine density and turnover, and dopamine innervation, in addition to other variables outside the scope of this work. Our multiple linear regression analysis revealed that a similar fraction of neurons encoded task-related variables in adolescents and adults (in adults: $2.9\% \pm 0.6\%$ for stimulus, $4.2\% \pm 1.5\%$ for outcome, and $6.6\% \pm 1.4\%$ for choice; in adolescents: $2.6\% \pm 0.5\%$ for stimulus, $4.9\% \pm 0.9\%$ for outcome, and $8.6\% \pm 1.5\%$ for choice; Fig. 2E). These numbers are comparable to previous reports that 5-10% of L2/3 dmPFC neurons are stimulus encoding and 2-5% encode choice (Reinert et al., 2021; Salkoff et al., 2020; Wool et al., 2023; Zatka-Haas et al., 2021), though one group reported 25% of neurons encoded choice (Salkoff et al., 2020), another reported 16% of neurons encoded stimulus (Peters et al., 2022), and another reported 24.2% encoded outcome (Wool et al., 2023). In concordance with existing reports of widespread cortical activity encoding animal licking and walking actions (Peters et al., 2022; Salkoff et al., 2020; Zatka-Haas et al., 2021), over 50% of our neurons were identified as encoding animal motion by multiple linear regression. It has been suggested that encoding of non-motor task variables in frontal cortices may be prescribed by the demands of the task (Siniscalchi et al., 2016, 2019; Wool et al., 2023). From our current data, we cannot rule out that execution of the task was carried out by other brain areas (i.e., other frontal area, auditory cortex, or basal ganglia), without need for engagement of dmPFC. However, recent work demonstrated that auditory go/no-go performance in adult mice was sensitive to optogenetic inhibition of the dmPFC (M2 area) projections to the dorsal striatum (Liu et al., 2023), suggesting that this area does play a verified role in go/no-go tasks in adult mice.

We also took into consideration that there may be a distributed representation of task variables in populations of neurons (Chelaru et al., 2021; Chiang et al., 2022; Grant et al., 2021; Lohani et al., 2019; Maggi et al., 2018; Ottenheimer et al., 2023; Rigotti et al., 2013; Wang et al., 2023) by employing a second approach to evaluation of functional neural activity. This method assumes task information may not be solely represented by major changes in activity in a few individual neurons, but rather by changes both obvious and subtle across the population of neurons. To compare how much task information was encoded by the population of neurons recorded in the dmPFC of adolescent and adult mice, we implemented a support vector machine decoder, which was trained on the entirety of session imaging data and thus may be able to discern differences between trials that are not discriminable through our multiple linear regression model. We found that our decoder was well able to discriminate between stimulus types, action choice, and trial outcome at above chance levels (Fig. 8C). Moreover, at several time points in the [0,2] second window after cue onset, task information was more readily decoded from adolescent dmPFC data than from adults.

While these data fit our prediction that the adolescent brain may be in a sensitive period that supports more robust encoding of information, we also considered that this result could come about simply due to differences in motor behavior between the two groups (Fig. 9A,B). To avoid this confound, we next employed a within-group analysis and trained our decoder to discriminate between cues of the same go or no-go category for which running was comparable (Fig. 9C). Though decoder performance in this application is less successful than discrimination between go and no-go cues, we can still decode no-go cue identity statistically above chance from adolescent data at multiple time points in the [0,2] second window after cue onset. Adult data did not support decoding above chance, suggesting that the adolescent neural population represented cue information with higher fidelity or specificity than the adult dmPFC.

Interestingly, the ability to discriminate between cues of the same type in the adolescent brain was observed only between no-go cues, not any of the go cues. Our cues spanned a continuous auditory range with go and no-go categories on either side of an inferred boundary. Mice showed no differences in lick rates between all go cues but a higher lick rate for no-go cue 5, closest to the boundary, than no-go cue 8 (Fig. 5D). Previous work in mice has shown that optogenetic or muscimol inactivation of dmPFC enhances false alarm rate in a go/no-go task (Liu et al., 2023; Salkoff et al., 2020), and human fMRI studies of go/no-go tasks have demonstrated greater frontal cortical activation during no-go trials (Aron, 2007; Chikazoe, 2010; Simmonds et al., 2008). We thus speculate that decoding between no-go cues may be attributed to greater dmPFC engagement when mice are required to inhibit an action, which also may be modulated by the difficulty of inhibition. In particular, it is possible that the difficulty of inhibiting to no-go cues closer to the decision boundary may drive differential engagement of frontal areas and thus greater discriminability between no-go cues.

Evidence for a putative adolescent sensitive period

Our study was motivated by a body of literature showing that at P30, the adolescent dmPFC exhibits high spine density and turnover, increasing dopaminergic innervation, and increasing inhibitory neurotransmission (Delevich et al., 2021). Based on past studies of the sensory cortices, we hypothesized that these dmPFC changes could support a sensitive period in this region. Because the dmPFC exhibits mixed selectivity rather than receptive fields, we set out to study population encoding of task variables as potential evidence of this sensitive period. We examined L2/3 of the dmPFC, a site where we have documented a substantial increase in mIPSCs on PYR neurons between P27 to P31, which continues through P36. We posited that this adolescent increase in GABA might enable a greater capacity for this region to encode task information in the P30s compared to the P60s. We also considered the alternate hypothesis that the adolescent brain is in an underdeveloped state that would be less efficient at encoding task information, which might manifest in a decreased ability to learn or perform reliably on the task. Finally, we considered a null hypothesis that despite different network configurations and levels of plasticity in the dmPFC of the two ages, the circuit may still function comparably and/or the behavioral performance may be comparable.

Our data support the sensitive period hypothesis and aspects of the null hypothesis. We found that at the level of individual cells, adolescents and adults encoded task information comparably, but at the population level, the capacity to encode information was greater in adolescents. One might

speculate that the greater capacity for encoding task information could possibly have enhanced the efficiency of learning in the adolescent mice, but the encoding advantage in adolescents was not seen in early learning, only after behavior was expert. Further experiments may be needed to sample the period of rapid learning in adolescents to test this relationship.

Manipulations of age and inhibitory mechanisms may also be used in future experiments to test the idea of a putative sensitive period in the frontal cortices. As phasic GABAergic inhibition increases in dmPFC, we posit it may uniquely poise L2/3 PYR to encode task relevant information that can be more quickly integrated to implement meaningful behavior. If, as in sensory cortices (Espinosa & Stryker, 2012; Hensch, 2005; Levelt & Hübener, 2012), this sensitivity is time restricted to the early adolescent ~P28-35 period after GABAergic inhibition increases, then studies that start training adolescent mice later may no longer see efficient learning or stronger encoding of task information. This could explain results from one study that reported poor performance of adolescents in a delay discounting task, which started training after P35, possibly too late to benefit from this putative sensitive period (Pinkston & Lamb, 2011).

The multifaceted roles of the frontal and association cortices are arguably more difficult to quantify and more amorphous than the stimulus tuning properties of sensory cortical neurons, so the delineations between the onset and offset of a dmPFC sensitive period may be somewhat ambiguous. We also do not intend to argue that dmPFC becomes incapable of learning after the offset of the sensitive period, but instead that it may operate via different cellular mechanisms, at a different rate, and/or through different strategies. We point to evidence from humans demonstrating that acquisition of a second language comes most readily prior to adulthood (DeKeyser et al., 2010; DeKeyser, 2000; Hartshorne et al., 2018; J. S. Johnson & Newport, 1989; Newport, 1990) – by no means is second-language learning impossible in adulthood, but it is arguably less efficient. Further study on the neural representation of higher cognitive skill will help hone hypotheses about and methods to measure putative frontal cortical sensitive periods.

It is also worth considering that there may be other factors at play in addition to maturation of inhibition. As noted, L2/3 PYR in the adolescent dmPFC exhibit a higher density of dendritic spines, as well as a higher rate of spine turnover, both of which are lower in adult mice. Synaptic pruning contributes to long term depression (LTD), which in turn is a key element of critical period plasticity in both visual and somatosensory cortex critical periods (Allen et al., 2003; Yoon et al., 2009). It has thus been suggested that a similar mechanism contributes to a critical period for frontal cortical function (Selemon, 2013), and theoretical work suggests that a lower density of spines may enable adult brains to learn more accurately, but more slowly, than adolescent brains (Averbeck, 2022). Similarly, increased innervation of dopaminergic fibers in dmPFC during adolescence may be a mechanism facilitating plasticity, and increasing interest is turning to the role of dopamine in adolescent development (Larsen & Luna, 2018; K. Z. Peters & Naneix, 2022; Reynolds & Flores, 2021). Previous work has shown that the experience of wheel running alone is sufficient to increase bouton formation on dopaminergic axons in the dmPFC of adolescent, but not adult, mice (Mastwal et al., 2014), and disruption of dopaminergic innervation of dmPFC during late juvenility/early adolescence (P22-31) by administration of amphetamines prevents successful learning of a similar go/no-go task in adulthood (Reynolds et al., 2019). Taken with evidence that dopaminergic activation of inhibitory interneurons increases in adulthood in rats (Tseng & O'Donnell, 2007), there may also be a role for dopamine in shaping the dmPFC sensitive

period by facilitating inhibitory maturation in this area or regulating spine pruning. Likely, all three of these developmental changes are intertwined to support plasticity, as the interactions between dopaminergic modulation, excitatory/inhibitory balance, and synaptic pruning in the cortex are increasingly being highlighted (Delevich et al., 2021; Lamanna et al., 2022; Lubec et al., 2021; Meunier et al., 2017).

Taken together, we have presented evidence that adolescents learn an auditory go/no-go task faster than adults, and that task information is better decoded from neural population activity in L2/3 dmPFC of the adolescent brain compared to the adult's. Given these data and substantial background literature demonstrating GABAergic inhibition mediating the onset of critical period plasticity across sensory cortices, combined with documentation of similar changes in inhibitory neurotransmission occurring in dmPFC during the early adolescent period in mice (P28-35), we propose that this age window is a putative sensitive period for the dmPFC. While further work is required to more clearly delineate the bounds of this putative sensitive period, as well as what particular behavioral functions are encoded by L2/3 of the dmPFC as opposed to other areas, these data show functional evidence that there may be coding advantage in the adolescent brain at a time when there is a unique transition in synaptic and circuit organization, thus lending new cellular basis for the concept of an adolescent sensitive period.

Chapter 3

Shine On, You Crazy Hexagon: Optical Fibers Functionalized with Single-Walled Carbon Nanotubes for Flexible Fluorescent Catecholamine Detection

In the previous chapter, I showed that adolescents exhibit an advantage in learning a go/no-go task and in encoding of task variables in dmPFC. This advantage may arise from the developing neural architecture of the adolescent brain. One changing aspect of the adolescent brain, as previously discussed, is the increasing innervation of dopaminergic fibers in dmPFC. Few studies have been able to directly examine dopamine release *in vivo* in adolescent animals, in part due to methodological limitations. One of those limitations is that the industry standard for fluorescent imaging of neural activity or biomolecules relies on genetically expressed fluorophores, which can take weeks to express following viral injection, a time scale that may not be compatible with adolescent studies. Moreover, genetic encoding of fluorophores limits their translatability to other model organisms or human patients. We thus sought to bridge this gap in available methodologies by developing an implantable probe for fluorescent dopamine detection. Here, I present the first steps in the development of this probe and examine the utility of its current form factor.

Current Techniques for Catecholamine Research and Background on the Utility of Single-Walled Carbon Nanotubes

The catecholamines dopamine and norepinephrine play a variety of important roles in the central and peripheral nervous systems. Dopamine in the central nervous system has been shown to play a key role in a variety of basic processes such as movement and reward prediction (Berke, 2018; Schultz, 1998; Ungerstedt, 1971), as well as in neurodegenerative diseases such as Parkinson's and Alzheimer's Diseases (Ehringer & Hornykiewicz, 1960; Goetz, 2011; Martorana & Koch, 2014; Murray et al., 1995), neuropsychiatric disorders such as schizophrenia and depression (Grace, 2016; Matthysse, 1973; Randrup et al., 1975), and, more recently, other behavioral conditions like autism spectrum disorder (Pavál, 2017). In addition, dopamine regulates immune and other physiological functions in the peripheral nervous system (Basu & Dasgupta, 2000; Bove et al., 2019; Harris & Zhang, 2012; Jose et al., 2003; Mignini et al., 2003; Rubí & Maechler, 2010). Dopamine is hydroxylated to norepinephrine (noradrenaline), which is similarly implicated in neurological and psychiatric illness (Henjum et al., 2022; Lambert et al., 2000; Rommelfanger & Weinshenker, 2007), as well as central and peripheral stress and arousal (Berridge, 2008; Berridge et al., 2012; España et al., 2016; Koob, 1999), memory (Ferry & McGaugh, 2000; Grella et al., 2021; Unsworth & Robison, 2017), and other functions (Tank & Lee Wong, 2015). While new technologies in the last few decades of research have honed hypotheses of catecholamine function, demonstrating corelease of and cooperative functions between dopamine and norepinephrine in health and disease (Del Campo et al., 2011; Devoto et al., 2001; Gaskill & Khoshbouei, 2022; Harley, 2004; Lambert et al., 2000; Moreno-Castilla et al., 2017; Ranjbar-Slamloo & Fazlali, 2019; Rommelfanger & Weinshenker, 2007; Sánchez-Soto et al., 2016; Xing et al., 2016), our understanding is far from complete, and physicians have limited tools to monitor catecholamine levels in human patients (Post & Sulzer, 2021). To accelerate this field of study, we need

technologies that are versatile enough to examine catecholamine dynamics in both preclinical settings in animal models and clinical settings in human patients.

Currently, the use of fluorescent indicators of neural activity and biomolecules is widespread in animal models. Genetically encoded calcium indicators (GECIs) enable specific targeting of dopaminergic or noradrenergic neurons in animal models, and recently developed genetically encoded dopamine indicators (GEDIs), based on modified DA receptors, enable direct optical readout of extracellular dopamine (Patriarchi et al., 2018; Sun et al., 2018). While these technologies have facilitated innumerable advances in our understanding of dopamine and norepinephrine in animal behavior, both GECIs and GEDIs are by nature subject to photo-bleaching, degradation, and optical interference. Similarly, though genetic encoding of fluorophores is an industry standard, this method commonly requires viral delivery and a wait time of at least two weeks for fluorescent protein expression, which incurs additional surgeries and stress on experimental animals and can hinder the progress of time-sensitive studies. Moreover, because GEDIs are modified dopamine receptors, they do not reliably signal dopamine concurrently with pharmacological agents that act on dopamine receptors. Finally, this strategy is inapplicable to genetically intractable systems and irreversible, making it unfit for human studies.

A number of methods currently exist to measure catecholamine levels in human subjects, but each have caveats. Magnetic resonance imaging (MRI) can detect tissue iron, a proxy measurement of dopamine receptor density used to infer the development of catecholamine-releasing terminals, but cannot report real-time release dynamics or short-term plasticity (Larsen & Luna, 2015; Price et al., 2021; Reneman et al., 2021). Positron emission tomography (PET) imaging can quantify catecholamine transmission but requires injection of a radioactive receptor-binding ligand into a patient's vein, and the detected ligand signal cannot be separated from its metabolite (Post & Sulzer, 2021). Probe implantation for microdialysis (Arbuthnott et al., 1990; Kilpatrick et al., 2010), or fast-scan cyclic voltammetry (FSCV) (Bang et al., 2020; Kishida et al., 2016) permits direct analysis of catecholamine release, but it is highly invasive, and FSCV, while more precise, has not yet been implemented for regular clinical use due to safety and standardization concerns (Jaquins-Gerstl & Michael, 2015; Lucio Boschen et al., 2021; Siegenthaler et al., 2020).

A less invasive strategy is to monitor catecholamine levels in bodily fluids, such as patient cerebrospinal fluid, blood serum, saliva, or urine samples. Altered catecholamine levels in biofluids can be an early marker of disease, including neuroblastoma (Grouzmann & Lamine, 2013; Matser et al., 2023; Verly et al., 2019), Parkinson's Disease (Goldstein et al., 2012; Kang et al., 2014; Paslawski et al., 2023; Vermeiren et al., 2020), Alzheimer's Disease (Elrod et al., 1997; Henjum et al., 2022; Liu et al., 2011), and psychosis (Elrod et al., 1997; Henjum et al., 2022; Liu et al., 2011). Conventionally, catecholamines are quantified using high-performance liquid chromatography with tandem mass spectrometry or electrochemical detection (Hubbard et al., 2010; Scheinin et al., 1984). In such assays, aliquots of sample are added to reagents, then run through a multi-step process, which is irreversible, expensive, and time-consuming. In combination with concurrent laboratory tests, dozens of milliliters of fluid may need to be collected from venous or lumbar puncture, which can contribute to patient suffering. Thus, a growing body of research has explored fluorescent detection of catecholamines in biofluids (Ray & Steckl, 2019; Santonocito et al., 2022; Wang et al., 2019).

In recent years, non-genetically encoded fluorescent molecules have emerged as viable tools for bioimaging both *ex vivo* and *in vivo*, most notably nanomaterials. In particular, single-walled carbon nanotubes (SWNTs) have demonstrated remarkable flexibility as biocompatible biosensors, capable of detecting DNA polymorphisms, ATP, nitric oxide, proteins, and other biomarkers (Hendler-Neumark & Bisker, 2019; Jain et al., 2015; Kruss et al., 2013). These sensors rely on the intrinsic near-infrared (nIR) fluorescence of SWNTs, which can be modulated by adsorbed polymers to emit only in the presence of select analytes. Functionalized SWNTs emit at 1000-1300nm, well within the nIR-II “second window” of optimal biological imaging, in which tissue absorbance and scattering of photons is minimal (Smith et al., 2009). Functionalized SWNTs employed in drug delivery investigations have demonstrated low toxicity *in vivo* (Li et al., 2017). Examination of blood serum biomarkers after intravenous injection of DNA-functionalized SWNTs suggests long-term (~5 months) biocompatibility in rodent models (Galassi et al., 2020), and SWNT-based chemical sensors have previously been used in a tissue-implant form factor to reliably measure nitric oxide in mice for over 400 days (Iverson et al., 2013). These features position SWNT-based biosensors as a promising candidate for long-term biological *ex vivo* and *in vivo* imaging, where their synthetic nature facilitates easy adoption for use across animal species.

Here, we leverage the functional properties of SWNTs to develop optical fibers surface-functionalized with near-infrared catecholamine nanosensors (nIRCats) to enable rapid detection of catecholamines in small volumes of biofluids without contamination of samples. nIRCats are SWNTs functionalized with (GT)₆ single-stranded DNA that emit up to a 24-fold and 35-fold increase in fluorescence ($\Delta F/F_0$) in response to dopamine and norepinephrine, respectively, *in vitro*, with ~3-fold higher affinity for dopamine (Beyene et al., 2019). To date, we have validated the use of nIRCats in solution for measuring evoked dopamine release in *ex vivo* striatal brain tissue with micron-level spatial resolution and millisecond-level temporal resolution, in the presence of pharmacological agents, and in the context of evaluating Huntington’s Disease progression (Beyene et al., 2019; Yang et al., 2022). nIRCats have also been used on immobilized glass surfaces to measure neuronal dopamine signaling on a sub-cellular scale (Bulumulla et al., 2022; Elizarova et al., 2022). Immobilizing nIRCats on optical fibers couples our catecholamine-sensing technology with fiber photometry, a commonly employed method in systems and behavioral neuroscience, thus expanding the available imaging toolkit to permit a more adaptable experimental paradigm for a wider variety of applications. Using these functionalized fibers, we demonstrate a fluorescent response to 10 nM dopamine in as little as 10 μ L biofluid *in vitro* and record endogenous dopamine transients evoked by electrical stimulation in *ex vivo* mouse brain tissue. We show that these fibers are shelf-stable for 24 weeks post-synthesis, reusable, non-biofouling in human plasma, and do not exhibit nanosensor desorption from the fiber. Together, these results suggest translatable potential to clinical applications for real-time readout of catecholamine release in biological environments. Here, we detail the development of a robust protocol for preparation of nIRCats-functionalized optical (nIRF) fibers and discuss their potential experimental utility.

Materials & Methods

Fiber preparation (standard):

Aminosilanes are a class of compounds commonly used as coupling agents for silica-based materials such as glass. In solution, the amine groups interact with negatively charged molecules, such as DNA. We leveraged this interaction to develop an aminosilane-based protocol, loosely based on previous demonstrations of silica silanization (Zhu, Lerum, & Chen, 2012), to immobilize nIRCats on glass optical fibers for photometric measurement of dopamine. We used a 400 μ m-diameter core multimode silica optical fiber (Thorlabs FP400URT, 0.5 NA) glued with epoxy into a 1.25mm diameter iron ferrule (Thorlabs SFLC440). The exposed length of fiber was trimmed to 4.5mm, the approximate depth of the rodent nucleus accumbens from the brain surface. Fibers were first cleaned by immersion for at least five minutes each in acetone, isopropyl alcohol, and molecular grade water, in that order.

Hydroxylation of silica surface: This procedure was incorporated only for data represented in Figure 13. Fibers were soaked in potassium permanganate solution for 30 minutes, washed repeatedly with water, soaked in a solution of potassium hydroxide in ethanol for 30 minutes, again washed with water, then placed in a glass vial which had been pre-treated with piranha solution (1:1 (v/v) concentrated sulfuric acid and 30% hydrogen peroxide). 300 μ L fresh piranha solution was added to the vial and fibers were incubated for 30 minutes. Fibers were then washed with water to remove ionic debris, ethanol to remove water and less polar contaminants, and toluene to remove ethanol.

Silanization: Prepared fibers were placed in an oven-dried 3-necked round-bottom flask containing 19ml anhydrous toluene. The flask was connected to a condenser and continuously flushed with nitrogen gas. Exposed flask necks were secured with septa, and 1ml (3-Aminopropyl)triethoxysilane (APTES, 99%, Sigma-Aldrich) was injected through one neck to create a 5% APTES solution in toluene. To increase APTES-silica hydrolyses and minimize APTES polymerization, we aimed to attenuate atmospheric humidity. The flask was then lowered into an 80°C heated oil bath and the condenser was flushed with cold tap water to reduce evaporate throughout the one-hour silanization reaction.

Functionalization with nIRCats: Post-silanization, tips were immersed for at least five minutes each in toluene, ethanol, and molecular grade water, in that order, to displace any residual weakly bonded silanes. Fibers were then dried overnight in a 110°C oven to promote formation of siloxane bonds. Afterwards, fibers were incubated in 50-200 mg/L nIRCats solution (manufactured in-house as in Beyene et al., 2019) for 30-60 minutes. Fibers were passively incubated or incubated with bath sonication for 30 minutes followed by a rest of at least 30 minutes. Immediately after nIRCats incubation, fibers were transferred to 1x phosphate buffered saline (PBS, Gibco) for at least ten minutes before spectra were assessed. Functionalized fibers can be stored long-term in clean plastic or glassware.

Laser/spectrometer data collection:

A 721-nm laser (Opto Engine LLC) was fiber-coupled to an inverted Zeiss microscope (Axio Observer D1). A 60 cm-long sheathed fiber with a plastic ferrule at one end was coupled directly to the light source in place of an objective and provided a conduit for excitation light. Each individual nIRF fiber was then plugged into the plastic ferrule at the end of the conduit fiber; laser power exiting the fiber was measured to be 4-8 mW. Each nIRF fiber was suspended in 40 ml 1x PBS. Fluorescence spectra were collected from 850-1300 nm by a Princeton Instruments spectrograph (SCT 320) and a liquid nitrogen-cooled Princeton Instruments InGaAs linear array detector (PyLoN-IR). Each fiber was equilibrated to the solution and laser light for ten minutes in 1x PBS with the microscope shutter open before baseline spectrum collection. Thereafter, a 1 mM DA solution was added directly into the PBS in increments of 0.4 μ l, 4 μ l, 40 μ l, and 400 μ l to produce 10 nM, 100 nM, 1 μ M, and 10 μ M DA solutions, respectively, unless otherwise noted. Spectra were collected one minute after each subsequent addition of DA. When assessing spectra in small volumes, fibers were suspended in individual 10 μ l aliquots of 10 nM, 100 nM, and 1 μ M DA. Fibers were equilibrated for 10 minutes in each solution before data was acquired.

Solutions:

Artificial cerebrospinal fluid (aCSF): aCSF was prepared in-house, consisting of sodium chloride (6.90 g/L), potassium chloride (0.26 g/L), hydrated magnesium chloride (0.264 g/L), sodium phosphate (0.12 g/L), sodium bicarbonate (2.20 g/L), D-glucose (1.98 g/L), and hydrated calcium chloride (0.37 g/L) in one liter of MilliQ water.

Brain homogenate: the brain of one adult male mouse was extracted in accordance with laboratory animal care guidelines. 5 mL 1x PBS was immediately added to the brain and homogenate was generated by probe-tip sonication for 30 minutes.

Blood plasma: frozen 1 mL aliquots of human blood plasma (pooled, Lee Biosciences) were thawed and diluted with 1x PBS.

Dual-nIR fiber photometry rig and electrical stimulation:

We designed and constructed a mobile dual-nIR fiber photometry rig for use with nIRF fibers in *ex vivo* and *in vivo* applications. A 635 nm excitation laser (35-50 mW at end of conduit fiber) was fiber coupled, collimated, and deflected into a patch fiber by a 900nm long-pass dichroic mirror. The patch fiber allows for individual nIRF fibers to be implanted in tissue and connected when needed via a plastic sleeve. Emission light from nIRF fibers travels through the same patch fiber and passes through the dichroic mirror to an ultrasensitive, thermoregulated nIR camera (Ninox 640 II, Raptor Photonics). The patch fiber was affixed to the camera lens such that the only light entering the lens was from the fiber itself. For each acquisition, Micro-Manager imaging software (v. 1.4.23) acquired 600 frames at 8.33 Hz with 0.5 mA electrical stimulation triggered at frame 200. All nIRF fibers used on this rig are first evaluated for *in vitro* DA response with the spectrometer.

Analysis of fluorescence:

For spectroscopic data, we integrated fluorescence values (arbitrary units) from 1050-1300 nm for all readings. Each fiber's fluorescence in 1x PBS served as the baseline against which subsequent measurements from that fiber were normalized. For nIR camera images, image acquisition was controlled by Micro-Manager software, which summed pixel intensity from a 640 x 512 pixel field of view, an area which encapsulated the totality of the 400 μm -diameter nIRF fiber surface. A line fit between the average of the first 50 frames and average of the last 50 frames of each acquisition was taken as the fluorescence baseline to correct for drift; all fluorescence values are represented normalized relative to that baseline. All analysis was performed in MATLAB using custom scripts.

Results

Optical fibers functionalized with catecholamine nanosensors yield robust responses to dopamine

We developed a protocol for aminosilane-based immobilization of nIRCats on glass optical fibers, loosely based on previous demonstrations of silica silanization (Zhu et al., 2012). 4 mm lengths of 400 μm diameter multimode silica optical fibers were cleaned, then silanized through a one-hour reaction with 5% (3-Aminopropyl)triethoxysilane (APTES) solution in toluene. After overnight curing at 110°C, fibers were passively incubated in nIRCat solution to promote an electrostatic interaction between the DNA adsorbed on the SWNT backbone and the aminosilane bound to the silica of the fiber (Fig. 10A). We first assessed the fluorescent spectra of these nIRCat-functionalized (nIRF) fibers in a 40 mL solution of 1x phosphate buffered saline (PBS) to approximate saline conditions of biological environments. In agreement with the known dopamine response of solution-phase nIRCat (Beyene et al., 2018, 2019), we observed a response profile with characteristic peaks at 1150 and 1200 nm from all fibers. To assess the functionality of immobilized nIRCats, we added aliquots of concentrated dopamine solution directly to the PBS solution to produce sequential solutions of 10 nM, 100 nM, and 1 μM dopamine. As with solution-phase nIRCat, we observed a stepwise increase in fluorescent response above baseline fluorescence, $\Delta F/F_0$, to each subsequent addition of dopamine in 16/21 fibers, though the individual response magnitude varied between replicates (10 nM dopamine = $0.022 \pm 0.056 \Delta F/F_0$, 100 nM dopamine = $0.223 \pm 0.162 \Delta F/F_0$, and 1 μM dopamine = $0.411 \pm 0.230 \Delta F/F_0$ (means \pm SD); $n = 16$; $p < 0.001$ between 10 nM versus 100 nM dopamine and $p = 0.015$ between 100 nM versus 1 μM dopamine, t-test; Fig. 10B,C). The remaining 5 fibers exhibited a decrease in $\Delta F/F_0$ to 1 μM relative to 100 nM dopamine and/or yielded $\Delta F/F_0 < 0.1$ to 1 μM dopamine and thus were deemed non-functional and excluded from further analysis (Fig. 11). Generally, however, our protocol successfully produced fibers sufficiently capable of dopamine within a biologically relevant dynamic range of 10 nM – 1 μM *in vitro*, which we then sought to validate for catecholamine detection from brain tissue.

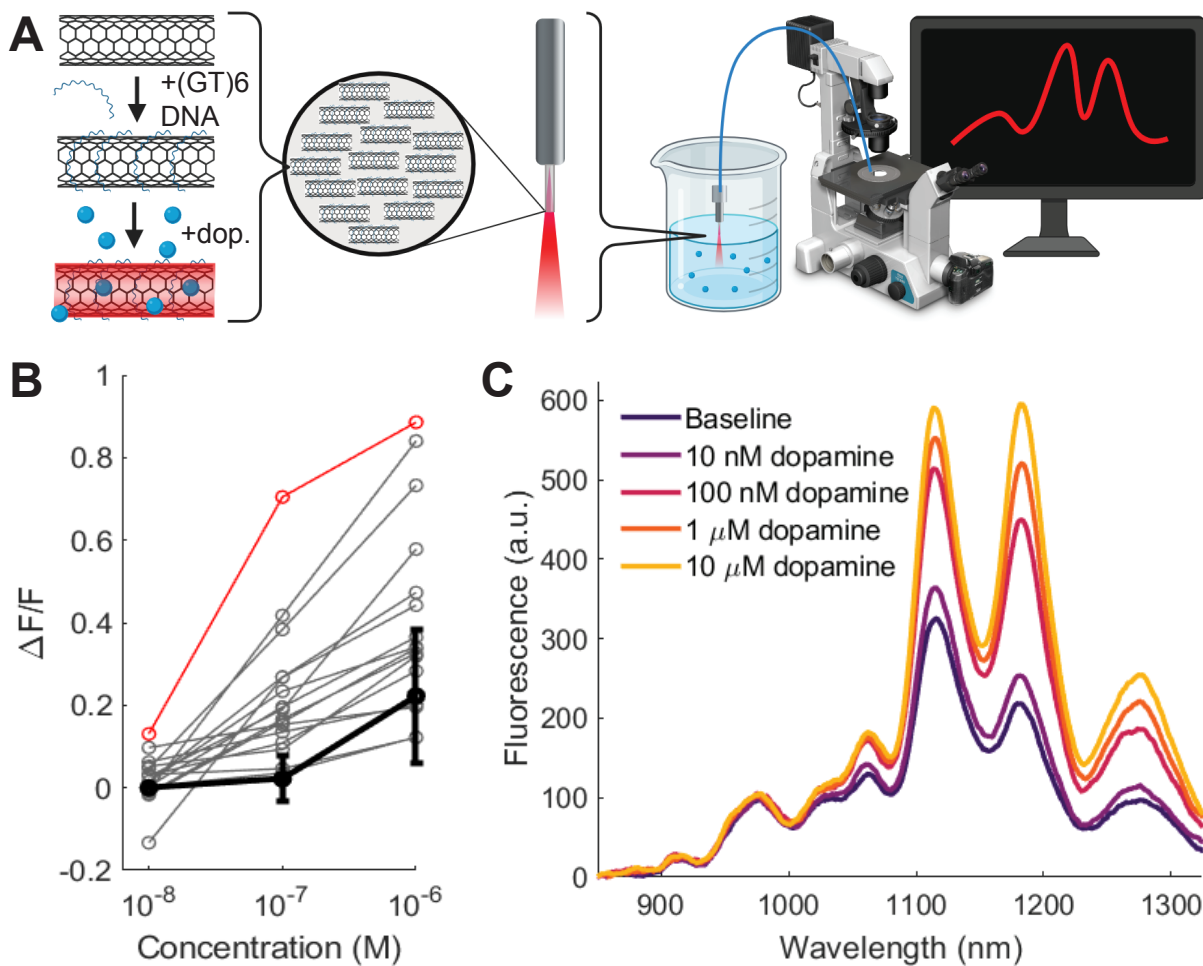


Figure 10: Functionalized fiber manufacture and response to dopamine. A) Schematic of fiber development. B) Integrated fluorescence from 1050-1300nm for increasing concentrations of dopamine for individual fibers (gray lines, $n = 16$) and mean (black line; error bars = SD). C) Representative spectra from one fiber (red in panel B) in 1x PBS and in increasing concentrations of dopamine *in vitro*.

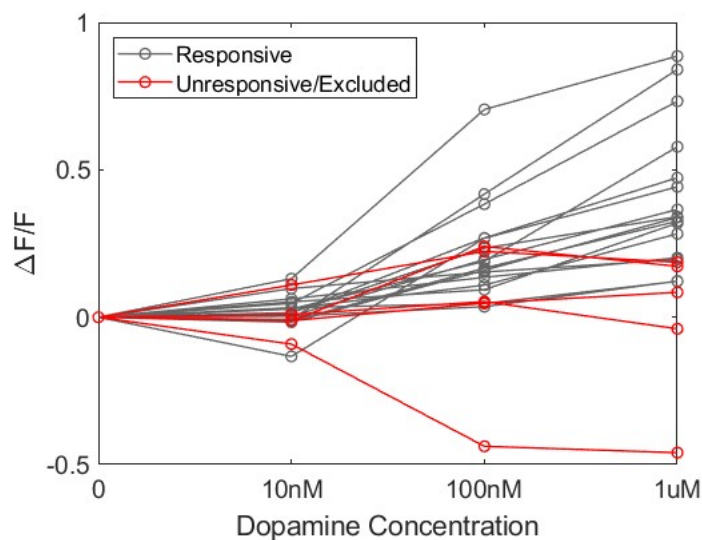


Figure 11: Dopamine response from all prepared fibers. Integrated fluorescence from 1050-1300nm for increasing concentrations of dopamine for individual fibers. Gray = responsive fibers (in Fig. 10A) vs. red = unresponsive fibers excluded from analysis.

Fiber functionality is preserved over months-long timescales and compatible with human biofluids

To test the robustness of our fibers over the timescale of a typical behavioral *in vivo* experiment, we examined the responsiveness of a new batch of nIRF fibers ($n = 6$) after storage in refrigerated 1x PBS. Specifically, we first sought to assess whether nIRCat nanosensors would desorb from our functionalized fibers by storing nIRF fibers in PBS and then using near-infrared spectroscopy to detect any nIRCat nanosensors desorbed into the PBS solution. Following 24 days of storage in PBS, the absorbance of the storage solution at 632 nm was equivalent to a sample of fresh PBS, suggesting minimal desorption of nIRCats from the fiber. We then assessed fiber functionality at this 24-day time point and found that fibers still exhibited a robust response to dopamine, unchanged from our initial measurements ($p = 0.082$ between time points, repeated-measures ANOVA; Fig. 12A). On the date of manufacture, fibers exhibited an average $0.038 \pm 0.051 \Delta F/F_0$ response to 10 nM dopamine, $0.332 \pm 0.193 \Delta F/F_0$ response to 100 nM dopamine, and $0.550 \pm 0.332 \Delta F/F_0$ response to 1 μ M dopamine. At 24 days, fibers yielded an average $0.050 \pm 0.034 \Delta F/F_0$ response to 10 nM dopamine, $0.334 \pm 0.156 \Delta F/F_0$ response to 100 nM dopamine, and $0.790 \pm 0.376 \Delta F/F_0$ response to 1 μ M dopamine. Together, these data demonstrate stability of nIRF fibers in PBS over the course of weeks.

Another consideration in the development of this tool is potential biofouling from biologically relevant molecules that may interfere with the fluorescence of nIRCats (Yang et al., 2020). To assess the impact of exposure to biomolecules, we first incubated another batch of nIRF fibers ($n = 6$) in 10x diluted human blood plasma overnight (>16 hrs) and found no effect on dopamine response the next day (before incubation: 10 nM dopamine = $0.036 \pm 0.050 \Delta F/F_0$, 100 nM dopamine = $0.271 \pm 0.202 \Delta F/F_0$, and 1 μ M dopamine = $0.390 \pm 0.242 \Delta F/F_0$; after incubation: 10 nM dopamine = $0.033 \pm 0.025 \Delta F/F_0$, 100 nM dopamine = $0.198 \pm 0.118 \Delta F/F_0$, and 1 μ M dopamine = $0.381 \pm 0.189 \Delta F/F_0$; $p = 0.623$ between time points, repeated-measures ANOVA; Fig. 12B). These data suggest biomolecules present in blood plasma have minimal effect on nIRF fiber functionality. Blood plasma, however, contains only a small subset of biomolecules present in the living brain. To replicate an environment similar to that relevant to *in vivo* fiber use, we next incubated a new batch of fibers ($n = 4$) in brain homogenate solution for 48 hours and observed a noticeable, but not statistically significant, attenuation of response (before incubation: 10 nM dopamine = $0.080 \pm 0.099 \Delta F/F_0$, 100 nM dopamine = $0.308 \pm 0.156 \Delta F/F_0$, and 1 μ M dopamine = $0.536 \pm 0.306 \Delta F/F_0$; after incubation: 10 nM dopamine = $-0.004 \pm 0.053 \Delta F/F_0$, 100 nM dopamine = $0.098 \pm 0.050 \Delta F/F_0$, and 1 μ M dopamine = $0.278 \pm 0.073 \Delta F/F_0$; $p = 0.222$ between time points, repeated-measures ANOVA; Fig. 12C). We hypothesize that the observed attenuation of our fibers following exposure to brain homogenate could either be due to biofouling compromising the exciton recombination efficiency of nIRCats or endonucleases compromising the integrity of the (GT)₆ functionalization on nIRCat surfaces. Regardless, the attenuated response was not statistically decreased compared to measurements prior to brain homogenate exposure, indicating that nIRF fibers may perform successfully in an *in vivo* biological environment.

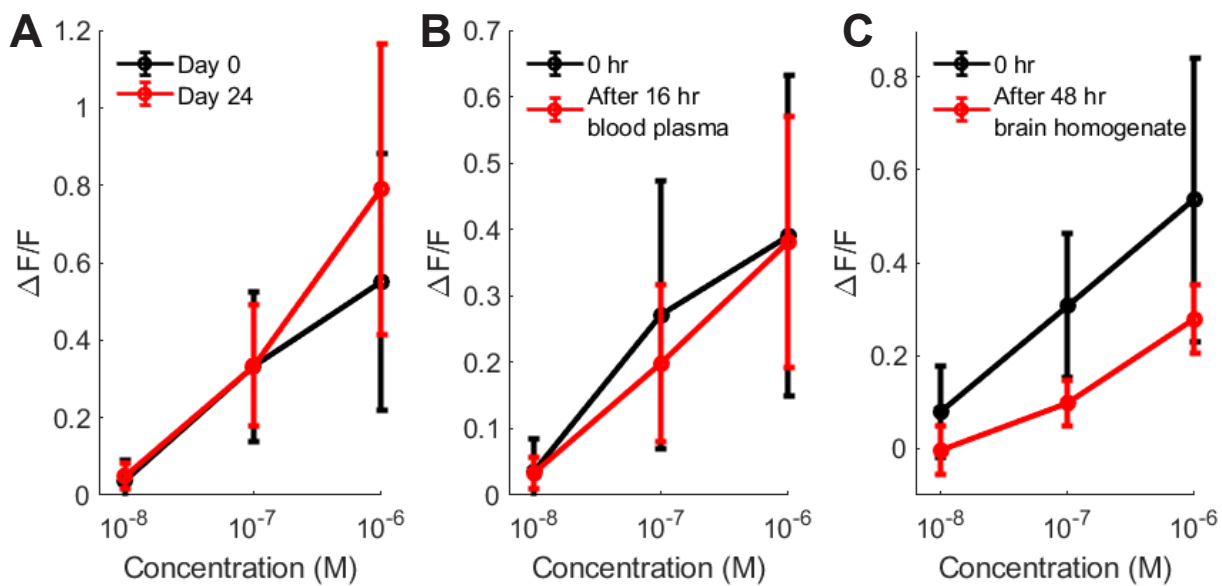


Figure 12: Fiber response to dopamine under different conditions shown in average nIRF fluorescent responses to increasing concentrations of dopamine (error bars = SD; $n = 6$). A) Day of synthesis (black) vs. 24-26 days post-synthesis (red). B) Before plasma incubation (black) vs. after overnight plasma incubation (red). C) Before brain homogenate incubation (black) vs. after 48-hour brain homogenate incubation (red).

We next sought to study nIRF fiber extended storage time and use in a broader range of biological environments. We prepared a new batch of fibers ($n = 4$) for storage at room temperature in dry, clean centrifuge tubes. This batch responded to dopamine similarly to previous batches on the date of manufacture (10 nM dopamine = $0.002 \pm 0.020 \Delta F/F_0$, 100 nM dopamine = $0.414 \pm 0.378 \Delta F/F_0$, and 1 μ M dopamine = $0.687 \pm 0.355 \Delta F/F_0$); these fibers were tested again after long-term storage in PBS for 24 weeks. Remarkably, despite a nearly 50% reduction in baseline fluorescence, 24-week-old nIRF fibers could reliably detect dopamine without a statistically significant attenuation in fluorescent response relative to the initial same-day testing date (10 nM dopamine = $0.024 \pm 0.053 \Delta F/F_0$, 100 nM dopamine = $0.266 \pm 0.174 \Delta F/F_0$, and 1 μ M dopamine = $0.517 \pm 0.235 \Delta F/F_0$; $p = 0.479$ between time points, repeated-measures ANOVA; Fig. 13A,B). These data suggest nIRF fibers are shelf-stable, reusable, and generate repeatable results, ideal for experimental or clinical applications or for use in locations without equipment needed to manufacture nIRF fibers.

We next explored the utility of nIRF fibers in another potential clinical application: biofluid samples commonly used in diagnostic testing. We next tested these same 24-week-old fibers in artificial cerebrospinal fluid (aCSF) and 100x diluted human blood plasma. While heretofore, tests had been performed in 40 mL solution, we modified our protocol to assess nIRF fiber performance in as little as 10 μ L volume to account for the reduced clinical availability of patient biofluids. In all biofluid solutions, though baseline fluorescence was attenuated compared to the baseline in 1x PBS on the manufacturing date, responses to 10 nM dopamine were still comparable to 10 nM dopamine in 1x PBS (40 mL 100x diluted blood plasma: 10 nM dopamine = $0.103 \pm 0.086 \Delta F/F_0$, 100 nM dopamine = $0.307 \pm 0.143 \Delta F/F_0$, and 1 μ M dopamine = $0.467 \pm 0.152 \Delta F/F_0$; 40 mL aCSF: 10 nM dopamine = $0.063 \pm 0.048 \Delta F/F_0$, 100 nM dopamine = $0.190 \pm 0.106 \Delta F/F_0$, and 1 μ M dopamine = $0.289 \pm 0.126 \Delta F/F_0$; 10 μ L aCSF: 10 nM dopamine = $0.114 \pm 0.069 \Delta F/F_0$, 100

nM dopamine = $0.118 \pm 0.043 \Delta F/F_0$, and 1 μM dopamine = $0.143 \pm 0.035 \Delta F/F_0$; 40 mL 1x PBS listed above; $p = 0.872$ between 40 mL 1x PBS versus 40 mL blood plasma, $p = 0.344$ between 40 mL 1x PBS versus 40 mL aCSF, $p = 0.394$ between 40 mL aCSF versus 10 μL aCSF, all repeated-measures ANOVA; Fig. 13A,B, Table 3). These data not only demonstrate the potential clinical utility of nIRF fibers in a variety of biological fluids, but also confirm that baseline fluorescence variations do not impact dopamine detection functionality.

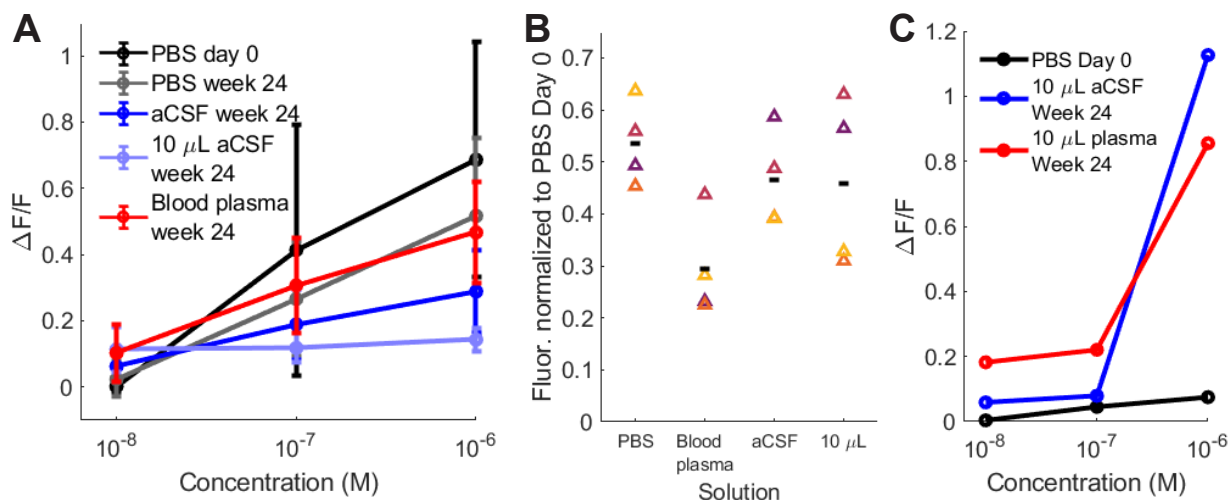


Figure 13: Fiber response to dopamine in biological fluids. A) Average nIRF fiber response in biologically relevant solutions ($n = 4$; error bars = SD) B) Baseline fluorescence after 24 weeks in tested solutions relative to baseline fluorescence in 1x PBS on manufacturing date (colored triangles = individual fibers, black bar = mean) C) Single fiber response profile in clinically relevant solution volumes.

As proof of principle that smaller solution volumes of undiluted blood plasma can be used, we assessed the response of one 24-week-old nIRF fiber in 10 μL aliquots of 10 nM, 100 nM, and 1 μM dopamine. At 24 weeks post-synthesis, in a 10 μL volume, this particular fiber yielded $0.059 \Delta F/F_0$, $0.079 \Delta F/F_0$, and $1.127 \Delta F/F_0$ to 10 nM, 100 nM, and 1 μM dopamine in aCSF, respectively. Surprisingly, we observed an even larger response to dopamine at nanomolar concentrations when this fiber was used to detect dopamine in undiluted human blood plasma, exhibiting $0.182 \Delta F/F_0$, $0.221 \Delta F/F_0$, and $0.856 \Delta F/F_0$ to 10 nM, 100 nM, and 1 μM dopamine, respectively (Fig. 13C). While dopamine is normally present in human blood plasma at sub-nanomolar concentrations, its concentration in cerebrospinal fluid is within the nanomolar range (Gardner & Shoback, 2011; Henjum et al., 2022; Scheinin et al., 1984); moreover, elevated plasma and CSF dopamine levels in the 10 nM range are associated with certain pathologies, including coronary artery disease (Abe et al., 2007) and psychosis (Orhan et al., 2023; Takase et al., 2020). Thus, nIRF fibers' dynamic range may span that of at-risk patient samples. Taken together, these data show that nIRF fibers can detect dopamine in small volumes of human biofluids, supporting the clinical utility of nIRF fibers in indicating potential risk factors for complex human disease.

Table 3. Summarized fiber responses to dopamine ($\Delta F/F$, mean \pm SD)

| Solvent | 40mL 1x PBS | 40mL 1x PBS | 40mL 1x PBS | 40mL 1x PBS | 40mL 1x PBS | 40mL diluted blood plasma | 40mL aCSF | 10 μ L aCSF | 10 μ L undiluted blood plasma |
|---------------------|-------------------|---------------------------------|---------------------------------|--------------------------------|------------------------------|------------------------------------|------------------------------|------------------------------|--|
| Time of measurement | Mfg. date | Post incubation in blood plasma | Post incubation in brain homog. | After 24 days stored in 1x PBS | After 24 weeks stored in air | After 24 weeks stored in air | After 24 weeks stored in air | After 24 weeks stored in air | After 24 weeks stored in air |
| <i>n</i> | 16 | 6 | 4 | 6 | 4 | 4 | 4 | 4 | 1 |
| 10nM dopamine | 0.022 \pm 0.056 | 0.033 \pm 0.025 | -0.004 \pm 0.053 | 0.050 \pm 0.034 | 0.024 \pm 0.053 | 0.103 \pm 0.086 | 0.063 \pm 0.048 | 0.114 \pm 0.069 | 0.182 |
| 100nM dopamine | 0.223 \pm 0.162 | 0.198 \pm 0.118 | 0.098 \pm 0.050 | 0.334 \pm 0.156 | 0.266 \pm 0.174 | 0.307 \pm 0.143 | 0.190 \pm 0.106 | 0.118 \pm 0.043 | 0.221 |
| 1 μ M dopamine | 0.411 \pm 0.230 | 0.381 \pm 0.189 | 0.278 \pm 0.073 | 0.790 \pm 0.376 | 0.517 \pm 0.235 | 0.467 \pm 0.152 | 0.289 \pm 0.126 | 0.143 \pm 0.035 | 0.856 |

Fibers detect electrically evoked endogenous dopamine from living brain tissue

This promising *in vitro* work encouraged us to next test our fibers in *ex vivo* brain tissue. We targeted detection of evoked dopamine release from the dorsal striatum, an area of the brain densely innervated by dopaminergic fibers, as in Beyene et al., 2019. While endogenous dopamine release in the dorsal striatum in response to reward in the intact brain ranges from about 1-20 nM (Natori et al., 2009), electrically evoked dopamine in the same region can extend into the micromolar range (Taylor et al., 2015), well within the detection range of nIRF fibers. We prepared 300 μ m-thick slices of mouse striatum in a bath continually perfused with artificial cerebrospinal fluid, as in previous work with solution-phase nIRCats (Beyene et al., 2019; Yang et al., 2022). Solution-phase nIRCats applied directly to the surface of the slice yielded a rapid (milliseconds) increase in fluorescence upon electrical stimulation of the dorsal striatum, with a slower (seconds) decay correlated with the intensity of stimulation. Given that our fibers present a novel form factor that would require dopamine to diffuse from the tissue surface and through a flowing bath to interact with nIRCats immobilized on the fiber surface, we anticipated the kinetics of our experiment to be slower than that of solution-phase nIRCats on tissue. To measure fluorescence on a compact, mobile system, we constructed a custom dual-nIR fiber photometry rig with a 635nm excitation laser, ultrasensitive thermoregulated nIR camera (Ninox 640, Raptor Photonics) to detect emission light, and flexible patch cord (Fig. 14A). We implanted a platinum iridium stimulating electrode and a nIRF fiber in the same slice, and then affixed the patch cord to the fiber via plastic sleeve. We recorded a small but consistent increase in fluorescence corresponding to stimulation over four consecutive trials (mean peak $\Delta F/F_0 = 0.005$), indicating nIRF fibers, when coupled with a sufficiently sensitive photodetector, can record endogenous dopamine release from *ex vivo* brain tissue (Fig. 14B). As expected, both the rise and decay signal kinetics were slower (on the order of seconds) than similar experiments with solution-phase nIRCats, likely due to the diffusion of dopamine molecules through the bath prior to reaching the nIRF fiber; we anticipate faster kinetics from a fiber implanted in an intact brain. This experiment further serves as a proof of principle that, despite attenuation of signal after exposure to brain tissue, dopamine detection within a biological environment is feasible with nIRF fibers, and our mobile fiber photometry system enables easy access and flexibility from this technology.

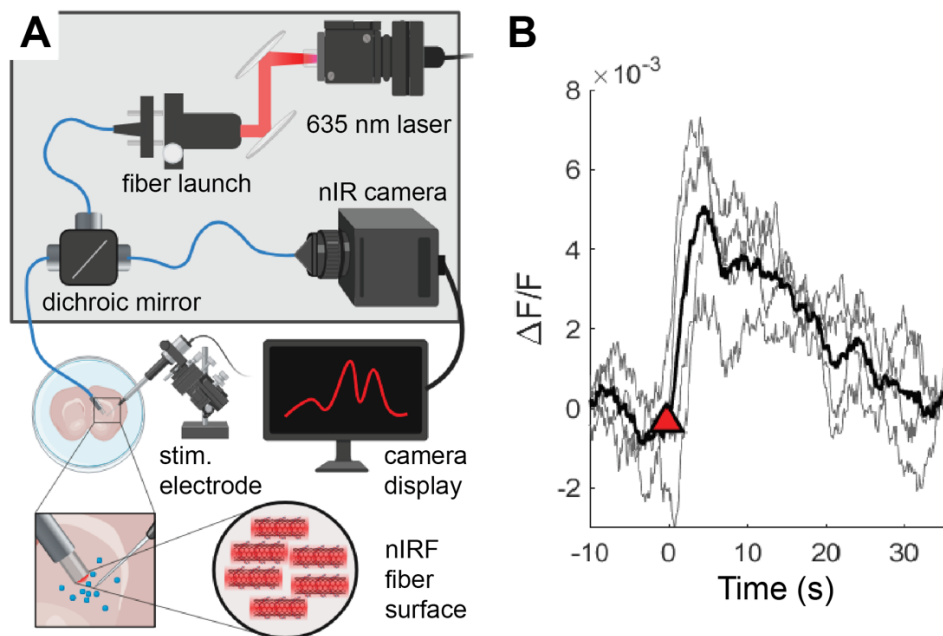


Figure 14: *Ex vivo* fiber response to dopamine. A) Schematic of 12" x 18" breadboard-based fiber photometry rig compatible with other recording platforms. B) Baseline-corrected fluorescent response to electrically evoked DA release in excised brain tissue. Gray traces correspond to individual trials ($n = 4$, one fiber); black = average; red triangle indicates time of stimulation.

Discussion

In summary, we developed a catecholamine-sensitive, near-infrared nanosensor-functionalized optical (nIRF) fibers and a compatible dual-nIR mobile fiber photometry imaging platform to readily detect extracellular dopamine *in vitro* and *ex vivo*. We have demonstrated that this tool can be successfully used to detect signals up to 24 weeks post-production and is robust to biofouling anticipated with chronic implantation in biological tissue. This tool introduces the possibility of real-time extracellular catecholamine imaging, potentially permitting a broader range of time-sensitive studies across multiple species with fewer invasive procedures. Our method offers the additional benefit of compatibility with pharmacological agents that target catecholamine receptors, commonly used research and disease treatment molecular tools that are incompatible for use with optical tools built from catecholamine receptors (e.g., GEDIs) (Dong et al., 2022; Labouesse et al., 2020).

In their current form, nIRF fibers can be used as turnkey, shelf-stable, reversible, reusable probes for detection of dopamine at nanomolar levels in solution. We thus foresee a unique advantage of this tool in the realm of clinical evaluations of catecholamine levels in biofluids such as blood, cerebrospinal fluid, and urine. While blood plasma contains dopamine at sub-nanomolar concentrations (Gardner & Shoback, 2011), norepinephrine is present at 1.5-1.8 nM (Goldstein & Holmes, 2008). CSF contains dopamine at 1.3-21.7 nM (Henjum et al., 2022; Scheinin et al., 1984) and norepinephrine at up to 25 nM (Goldstein et al., 2012; Henjum et al., 2022), and urine contains dopamine at 65-400 $\mu\text{g}/24\text{h}$ (Pagana et al., 2015) and norepinephrine at 15-80 $\mu\text{g}/24\text{h}$

(Hollstein et al., 2020). These concentrations, particularly in CSF and urine, are within the dynamic range detectable by nIRF fibers. There is a growing interest in improved biosensors for clinical catecholamine detection from lower-volume samples (Nawrot et al., 2018; Ravariu, 2023; Senel et al., 2020; Shi et al., 2019; K. Zhang et al., 2018), and we have demonstrated that nIRF fibers can detect dopamine in as little as 10 μ L of sample. Moreover, because our sensor platform does not require the addition of subsequent reagents, nIRF fibers permit reversible catecholamine detection in patient samples, which can then be reused for subsequent assays, reducing the overall volume of sample needed in diagnostic testing. Taken together, these attributes elevate nIRF fibers as a promising first-pass diagnostic tool capable of flagging samples that might require further, more expensive assessment, thus reducing the overall volume of sample needed and saving time and costs. Lastly, the shelf-stability of our fibers makes them attractive for use in settings where their on-site preparation or storage may be impractical or impossible.

One limitation of this tool is the apparent reduction in fluorescence observed after long-term exposure to brain homogenate. Mitigating the effect of biofouling molecules found in an intact brain may require additional investigations of protein corona formation around the SWNT surface, or mitigation of nuclease activity on the nanosensor itself. Our group and others have shown that passivation of SWNTs with polyethylene glycol mitigates SWNT-induced platelet aggregation (Sokolov et al., 2011), permits transmission through the circulatory system *in vivo* (Iverson et al., 2013), improves targeted drug delivery success (Al Faraj et al., 2016), minimizes cytotoxicity and nonspecific cellular interactions (Gao et al., 2017), and reduces expression of inflammatory cytokines, attenuates microglial activation, and further enhances dopamine imaging (Yang et al., 2020). Recent research in our lab has also shown that these beneficial effects are further amplified by passivation with a zwitterion, polysulfobetaine methacrylate. An alternative approach to nIRF fiber synthesis could first encapsulate nIRCats in a hydrogel, which has demonstrated excellent biocompatibility and light-guiding properties (Choi et al., 2013). This strategy has successfully enabled SWNT-based sensors for detection of steroid hormones (Lee et al., 2020), essential vitamins (Bakh et al., 2021), and chemotherapeutic drugs (Son et al., 2023) *in vivo*. Moreover, this strategy has recently proved applicable to large mammal models for multi-week sensing without adverse health effects (Hofferber et al., 2022), suggesting tractability across species. Passivation and/or hydrogel encapsulation of nIRCats on the optical fiber surface may require immobilization techniques other than the silanization approach taken here, but further investigation combining these strategies may present a viable route by which to successfully utilize nIRCats in living brain tissue.

Similarly, it is critical to note that the long-term effects of SWNT exposure are not fully known (Ema et al., 2016; Francis & Devasena, 2018; Mohanta et al., 2019; Ong et al., 2016). While our work has shown no measurable SWNT desorption from functionalized nIRF fibers, solution-phase SWNT can induce adverse biological effects at certain concentrations and exposure durations. For instance, there is some evidence that chemically functionalized multi-walled carbon nanotubes induce a transient immune response in the brain and that SWNTs alter microglial morphology in cell culture (Bardi et al., 2013; Rasras et al., 2019; D. Yang et al., 2020), but it remains unclear how SWNTs affect the brain *in vivo*. As such, future research should take care to more closely investigate the potential toxicity of single-walled carbon nanotubes in brain tissue, and whether their immobilized form function mitigates these toxicities. Given the lack of evidence of SWNT

desorption from the fiber, we anticipate this concern may be mitigated by combination with a functionalized fiber.

To our knowledge, there exist few methods by which to safely and continuously measure catecholamines in the human brain or biofluids without the limitations of microdialysis, FCSV and GEDIs indicated above. The nIRF fiber may be able to mitigate risk of use by reducing size, removing need for electrical stimulation, and reducing need for use of viral transfection or other irreversible treatment (Fig. 15). The small size of the optical fiber may permit relatively easy implantation in live brains, and compatibility with pharmacology means these fibers could be used alongside ongoing clinical trials of new drugs that target dopamine pathways to measure changes in dopamine release without signal interference from the drug's mechanism of action. Furthermore, growing interest in translational fluorescent sensors indicates a future rise in infrastructural support for this technology (Seah et al., 2023). Overall, we foresee this tool as a starting point from which to expand resources available for quickly assessing biofluid catecholamine levels, chronic catecholamine monitoring in genetically intractable or time-sensitive model systems, or and study of the effects of catecholamine pharmacology. These data represent the first step in development of an optical probe for catecholamine detection that may provide a real-time readout of catecholamine release during human surgery or the ability to chronically monitor catecholamine levels in a patient over time, leading to a deeper understanding of the catecholamine dynamics behind the progression and treatment of debilitating human illnesses.

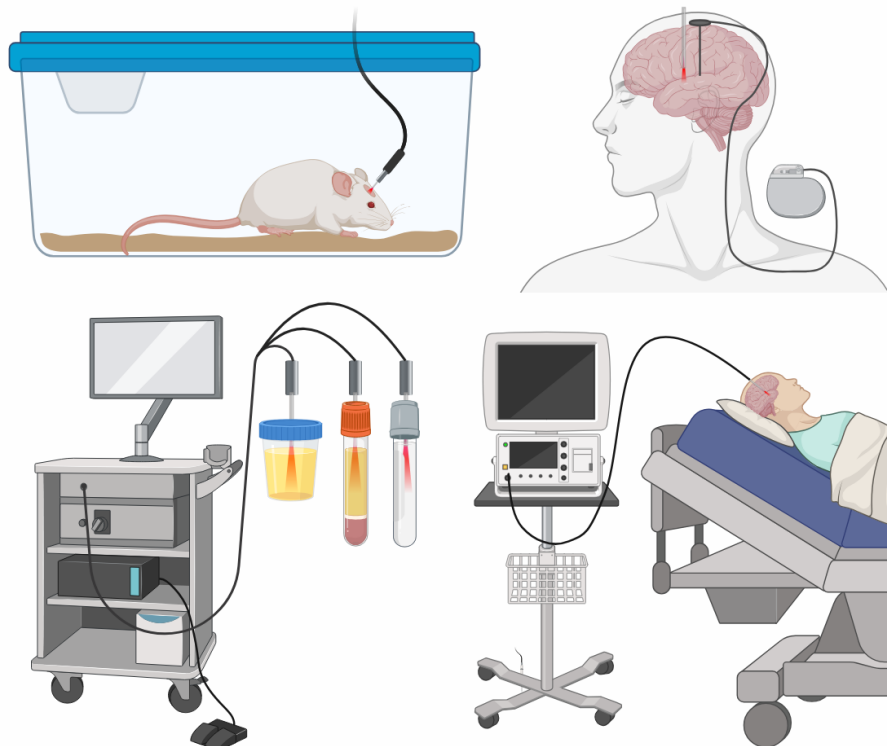


Figure 15: Potential applications of the functionalized fiber. We envision this tool providing utility for (clockwise from top left) behavioral neuroscience experiments in animal models, chronic implantation for monitoring patient catecholamine release with concurrent deep-brain stimulation, acute implantation for monitoring patient catecholamine release during brain surgery, and preliminary analysis of catecholamine levels in clinical samples of biofluids. Figure made in BioRender.

Chapter 4

Teenage Dream: Conclusions and Future Directions

My dissertation research aimed to test the hypothesis that adolescence may be a putative sensitive period for the development of the frontal cortex, with a specific focus on L2/3 of dmPFC. In Chapter 1, I laid out the state of the field, describing what is known about neurophysiological remodeling of the frontal cortex in both humans and rodents over the course of adolescence, and I discussed how these changes are mirrored in behavioral strengths and weaknesses. In Chapter 2, I showed that, though performance of expert-level mice was ultimately comparable, adolescent mice learned this task more quickly than adults. Additionally, while a similar fraction of dmPFC pyramidal neurons encoded task variables between adolescents and adults, more detailed task information was decodable from adolescent neural activity compared to adult activity. Finally, in Chapter 3, I assessed available technologies for studying catecholamine release in biological environments, and I introduced a novel probe for dopamine detection. Overall, this work contributes to a greater understanding of adolescent behavior and frontal cortical development.

A putative sensitive period in adolescence

Most striking from this work is the time course of our experimental findings as it aligns with other changing factors in adolescent dmPFC. While adult mice met criterion performance on our task anywhere from session 3 to session 14 (median = 11.5), adolescent performance clustered between sessions 5-7 in terms of meeting criterion (median = 6) (Chapter 2, Fig. 5C). Comparing the first 7 sessions of adolescents and adults also reveals a faster rate of improvement in adolescent performance than adults. These first 7 sessions correspond to adolescent ages P30-36, a time period of well-documented remodeling in dmPFC. For instance, spine density and turnover decrease beginning in P30s in both L2/3 and L5 of dmPFC, with the highest spine density overlapping with our period of study, from P28-35 (Boivin et al., 2018; Delevich et al., 2020; Drzewiecki et al., 2016; Johnson et al., 2016; Koss et al., 2014; Pöpplau et al., 2023; Zhang et al., 2021; Zuo et al., 2005). Together with peak dendritic complexity at P33-35 (Koss et al., 2014; Pöpplau et al., 2023), these data suggest that this early P30s period experiences an elevated level of cortical plasticity. Moreover, GABAergic synaptic inhibition of L2/3 PYR ramps up substantially in this area between P27-28 and P31-33 and reaches adult levels at P36-38 (Piekarski, Boivin, et al., 2017). This is reflected in increased gamma frequency oscillations in the P28-35 age window (Pöpplau et al., 2023), which have been shown to be generated by PV+ inhibitory interneurons (Bartos et al., 2007; Sohal et al., 2009). We can see further evidence of this rise in inhibition via our calcium imaging neural data presented here, which shows a decrease in activity plateauing around P36 (Chapter 2, Fig. 6A). Together, these factors may be responsible for the more robust decoding of task information we observed in the adolescent, compared to the adult, dmPFC (Chapter 2, Fig. 8C, 9C). The coincidence of peak spine density, peak dendritic complexity, increasing inhibition, and rapid improvement in the go/no-go task, all between the P28-36 window, strengthen evidence in support of a putative sensitive period for frontal cortical development in adolescence.

This argument is built from the groundwork of previous studies demonstrating the role of GABAergic inhibition in the onset of critical periods in sensory cortices. Similarly, in dmPFC, a substantial body of literature details the increase of phasic GABAergic inhibition onto L2/3 and L5 IT-type PYR over the course of adolescence, particularly in early P30s (Delevich et al., 2015, 2019; Piekarski, Boivin, et al., 2017; Vandenberg et al., 2015). As previously discussed (see Chapter 2), the similar processes of inhibitory maturation between the frontal and sensory cortices are a strong motivation for our hypothesis that adolescence is a putative sensitive period. As inhibition is just one of several developing anatomical and physiological factors in the adolescent brain, it is worth noting that other mechanisms may also contribute to the strengthening of our hypothesis.

Additional factors underlying dmPFC plasticity & areas of future research

In addition to increasing phasic inhibitory neurotransmission, I also outlined two other major changes in the adolescent brain in Chapter 1: spine pruning and maturation of the mesocortical dopamine pathway. It is possible that these mechanisms, in addition to inhibitory transmission, position the adolescent brain for a sensitive period in dmPFC. Here I unpack the evidence supporting these changes and elaborate on directions of future research that could contribute to our understanding of this putative sensitive period.

Spine pruning and stabilization

The elevated spine density and dendritic arborization of the P30-35 brain is accompanied by plasticity in long-range connectivity, as evidenced by increased frontal cortex bouton formation in adolescence (Johnson et al., 2016; Mastwal et al., 2014). Together, an increased density of synaptic boutons and dendritic spines may facilitate encoding of information relayed from other brain regions. Importantly, microglia-mediated spine pruning occurs after P35 (Mallya et al., 2019; Pöpplau et al., 2023). Ablation of microglia by colony-stimulating factor 1 receptor inhibitor, PLX3397, from P28-37 caused a lasting increase in gamma power, increase in firing rate of putative L2/3 PYRs, and increase in L2/3 basal spine density in P56-60 mice, thus perpetuating early-adolescent-like dmPFC dynamics into adulthood (Pöpplau et al., 2023). These P56-60 mice also suffered behavioral disadvantages. In a four-choice set-shifting task, mice treated with PLX3397 required more trials to correctly associate one odor out of four with a reward, compared to untreated mice of the same age. When the odor-reward association was switched to a new odor, PLX3397-treated mice again required more trials and made more errors overall, indicating that ablation of microglia and consequent reduction of spine pruning induced behavioral impairments (Pöpplau et al., 2023). Moreover, disruption of spine pruning is a phenotype of certain cognitive conditions associated with impaired learning, such as attention deficit hyperactivity disorder (ADHD) and autism spectrum condition (Forrest et al., 2018; Kim et al., 2017; Silva, 2018; Tang et al., 2014), lending credence to the idea that spine pruning modulates adolescent development.

Our sensitive period hypothesis posits that the adolescent dmPFC is uniquely endowed with plasticity to facilitate learning; some of this plasticity may arise from spine pruning. In contrast to the adolescent brain, the adult brain does not exhibit the same level of plasticity in terms of bouton or spine formation. Computational modeling has suggested that a higher spine density may enable

faster learning (Averbeck, 2022). Our results showing an adolescent advantage in behavior on the go/no-go task, as well as a higher decodability of task information from adolescent neural population activity, may thus be facilitated by the higher density of spines P30-35. In theory, a greater spine density could enable a greater proportion of transient synapse formation during task learning. Some of these synapses may communicate more relevant information than others. The rapid turnover of spines and their associated synapses thus enables a higher sampling rate of environmental information, paring down less critical synapses and retaining those more advantageous to the task at hand. In contrast, the adult brain may not be as equipped to readily update synapses based on environmental feedback (Fig. 16). Thus, spine density and turnover may facilitate informational encoding during a sensitive period.

This reasoning is supported by studies of psychedelic drugs, which have been posited to “re-open” critical periods for social and emotional learning (Calder & Hasler, 2023; Lepow et al., 2021; Lukasiwicz et al., 2021). In mice, social reward learning can be measured through a social reward conditioned place preference paradigm. In this paradigm, mice received 24 hours of social exposure with cage mates on one type of bedding, followed by 24 hours of isolation on another type of bedding. They are then placed into a two-chamber arena with one type of bedding in each chamber. The ratio of time spent in the chamber with socially-conditioned bedding to the time spent in the chamber with isolation-conditioned bedding determines social reward learning. Younger mice exhibit a greater preference for the chamber with socially-conditioned bedding, with a preference peak at P42 that declines to a level of zero preference at age P98 (Nardou et al., 2019). However, P98 mice treated with any one of four psychedelic drugs—lysergic acid diethylamide (LSD), (+/-)-3,4-methylenedioxymethamphetamine (MDMA), ketamine, or ibogaine—exhibit levels of preference comparable to that of P42 mice (Nardou et al., 2019, 2023). This effect was found to be mediated by oxytocin in the nucleus accumbens, where medium spiny neurons exhibited oxytocin receptor-dependent long-term depression at P40, and in animals pretreated with psychedelics, but not saline, at P98 (Nardou et al., 2019; 2023). This cellular-level psychedelic-induced plasticity appears to translate to mPFC as well, where, in recent years, N,N-dimethyltryptamine (DMT), 2,5-dimethoxy-4-iodoamphetamine (DOI), LSD, MDMA, ketamine, and psilocybin have all been shown to induce plasticity on L5 PYR by increasing dendritic arborization, spine growth, synapse formation, and EPSC frequency in rodents (Ly et al., 2018; Moda-Sava et al., 2019; Shao et al., 2021). It remains unclear, however, exactly how this type of plasticity relates to social reward learning, or to what extent psychedelic-induced plasticity may assist in other forms of learning. Thus, to better elucidate the role of dendritic spines in opening (or re-opening) critical periods, future work could examine the use of psychedelics in other animal behavioral paradigms, explore the impact of psychedelic-induced plasticity on different brain regions, or manipulate spine pruning during adolescence in targeted regions of the brain through optogenetic, chemogenetic, or pharmacological means.

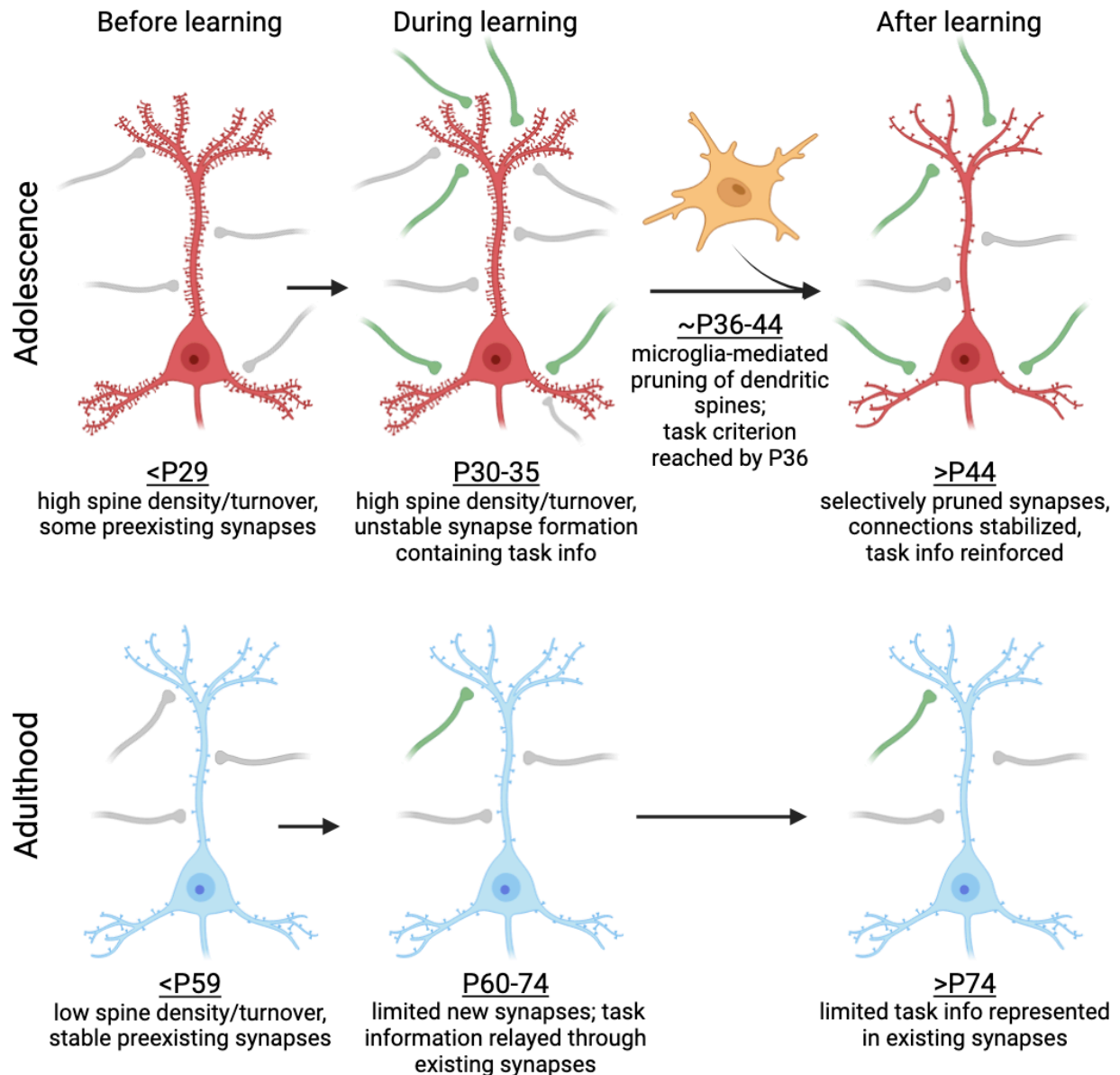


Fig. 16: Schematic of task information representation through synapses on dendritic spines. At P29, L2/3 PYR exhibit many unstable synapses. Through the P30s, new synapses develop, some of which contain task-relevant information. The onset of pruning enables a greater potential for these synapses to become stable. By adulthood (~P45), synapses are stabilized, and there is less potential for new synapses to develop.

Dopamine innervation of deep cortical layers

While our work focused on L2/3 of dmPFC, a parallel body of literature has also examined deep cortical layers, particularly L5. Deep layers have particular relevance when considering changes in dopaminergic neuromodulation over adolescence, as dopaminergic fibers more densely innervate L5 than L2/3 (Kalsbeek et al., 1988; Manitt et al., 2011; Naneix et al., 2012; Willing et al., 2017). Dopaminergic axon growth from the midbrain into dmPFC is directed by guidance cue Netrin-1 and its receptor, deleted in colorectal cancer (DCC), during adolescence (Reynolds, et al.,

2018). Variations in the *Netrin-1* and *DCC* genes have been found in humans and have been implicated in increased risk of psychiatric illness (Vosberg et al., 2020). Adult mice with *Dcc* gene knockdown in dopaminergic VTA neurons exhibit twofold increased dopaminergic varicosities in dmPFC, as well as reduced dendritic spine density on L5 PYR and reduced L5 PYR excitability in this area (Manitt et al., 2011, 2013). Moreover, these mice exhibit a reduced locomotor sensitivity to amphetamine that emerged only in adulthood (Manitt et al., 2013). Importantly, exposure to amphetamine in early adolescence (P22-31) disrupts normal dopaminergic development by increasing the span of dopamine projections in the mPFC but reducing release site density on those projections (Reynolds et al., 2015), which increases the rate of false alarm trials in a go/no-go task similar to ours in adulthood (Reynolds et al., 2019). Thus, dysregulation of dopamine innervation in L5 during adolescence impacts adult learning and health outcomes.

In the PFC, dopamine operates on PYR mainly through D1- and D2-type receptors. D2-type dopamine receptors (D2Rs) are expressed on PYR mainly in deep layers, particularly on putative PT-type PYR (Gee et al., 2012; Santana et al., 2009; Zhang et al., 2021). Activation of D2Rs inhibits excitatory current through NMDA receptors on PYR (Wang et al., 2003), indicating that they may be an important regulator of PYR excitability. Moreover, mice expressing only one copy of the D2R gene experience deficits in spine pruning on L5 PYR in the anterior cingulate region of dmPFC throughout adolescence and into adulthood (Zhang et al., 2021). These PYR also exhibited increased mEPSC, but not mIPSC, frequency after P28, indicating an upset E:I balance, and impaired LTD of NMDA receptors (Zhang et al., 2021). Since LTD has been shown to be another potential mechanism regulating the onset of sensory cortical critical periods (Allen et al., 2003; Selemon, 2013; Yoon et al., 2009), these data together suggest that dopamine in deep cortical layers may play a critical role in shaping frontal cortical function. Furthermore, mice given daily administration of D2R antagonist eticlopride between P21-28, but not in adulthood, spent less time in lit chamber of a 2-chamber light/dark box and in the open spans of an elevated O-maze in adulthood that mice given a saline injection, indicating that D2R inhibition during development can impact adult anxiety behaviors. Taken together, evidence of dopamine-mediated structural developmental in dmPFC during adolescence, the implication of dopamine in adult psychiatric illness, and more recent evidence demonstrating that disruption of appropriate dopaminergic development can impact adult behaviors all make a compelling case for further investigation of the role of dopamine in shaping a putative adolescent sensitive period in dmPFC.

For these reasons, a pressing topic of future research involves development of tools to better study dopamine dynamics in adolescents *in vivo*, particularly in dmPFC. Our work in Chapter 3 is one step in that direction, but there is a still long road to a readily available, turnkey fluorescent probe for dopamine imaging. In the meantime, pharmacological experiments that block or activate dopamine receptors in adolescent dmPFC may be informative for elucidating the role of dopamine in adolescence, and the impact in adulthood of interfering with normal dopamine development. In mice, researchers can take advantage of transgenic lines to evade viral injection and weeks-long wait times for fluorescent protein expression that may otherwise preclude studies in adolescent animals. Our study uses transgenic mice expressing a green genetically encoded calcium indicator in dmPFC PYR; these mice could be interbred with a transgenic line expressed a red-shifted fluorophore in dopaminergic neurons to co-monitor activity of dopamine axons in this region. Similarly, other strains could be crossed to multiplex imaging of different cell types, such as IT and PT-type PYR in L5. These transgenic lines could also be imaged after treatment with dopamine

receptor agonists or antagonists to study the effects of dopamine on cell activity during a task. Given the influence of dopamine on a variety of behavioral and health conditions, there is a plethora of experiments that could break further ground in the realm of adolescence.

The role of parvalbumin-expressing interneurons

As discussed in Chapter 2, evidence from sensory cortices demonstrate the importance of GABAergic inhibition in the onset of sensory critical periods. Mice with reduced GABA synthesis do not exhibit a visual cortex critical period for ocular dominance plasticity, but the critical period can be restored by administration of a GABA_A receptor agonist, specifically through activation of the $\alpha 1$ subunit (Fagiolini et al., 2004; Fagiolini & Hensch, 2000; Hensch et al., 1998). PV INs preferentially target synapses enriched in the $\alpha 1$ subunit (Klausberger et al., 2002), suggesting a role for PV INs, specifically, in critical period regulation. PV INs are densely interconnected and synapse onto the soma of L2/3 PYR across the cortex, where they enforce narrow windows of temporal integration (Packer & Yuste, 2011; Pouille & Scanziani, 2001). Maturation of PV INs inhibition of L2/3 PYR may provide a mechanism by which critical period plasticity develops, as PV INs preferentially suppress spontaneous activity in favor of stimulus-evoked activity, thus promoting a greater sensitivity to environmental cues, particularly rewarding ones (Toyoizumi et al., 2013; Wilmes & Clopath, 2019). Perisomatic innervation of PYR by PV-expressing boutons develops over the critical period in visual cortex but can be delayed by visual deprivation (Chattopadhyaya et al., 2004). PV INs also generate gamma band frequency (40-80 Hz) oscillations in the cortex, which have been shown to peak in primary visual cortex at the onset of the critical period (Bartos et al., 2007; Chen et al., 2015; Lensjø et al., 2017; Quast et al., 2023; Sohal et al., 2009). Thus, to seek evidence of a critical period in other cortical areas, we may look for an increase in GABA-mediated inhibition in L2/3 PYR and PV IN-mediated gamma oscillations, potentially in addition to other changes.

In adolescence, expression of parvalbumin increases in fast-spiking inhibitory interneurons throughout multiple regions of mPFC, increasing to near-adult levels between P35 and P45 (Caballero et al., 2014). From P31-49, PV INs undergo a period of excitatory receptor remodeling exhibited in a markedly reduced NMDA:AMPA ratio due to an increase in AMPA receptors (Wang & Gao, 2009). This NMDA:AMPA balance may help increase and stabilize PV IN activity, thus impacting their increased downstream influence on L2/3 PYR in adolescence. For instance, optogenetic activation of PV INs in mouse prelimbic cortex more strongly inhibited L2/3 PYR linearly with age from juvenility to adulthood (Pöpplau et al., 2023). This transmission may be particularly important in consolidating information from other brain areas, as adult mice exhibit feed-forward inhibition from long-range projections onto L2/3 PYR in dmPFC that is mediated specifically through PV INs (Delevich et al., 2015). Evidence from studies interfering with PV INs activity during adolescence also contribute to our understanding of their importance in frontal cortical development. RNAi-mediated downregulation of PV at P34-38 reduced mIPSCs on L5 PYR at ~P65; these same rats exhibited impaired extinction learning of a fear conditioned response (Caballero et al., 2020). Similarly, chemogenetic inhibition of PV INs from P14-50 resulted in a reduction in mIPSC frequency and amplitude onto L2/3 and impaired performance on a set-shifting task a P90 (Canetta et al., 2022). Together, this work underscores a role for PV INs in mediating developmental changes that impact behavior, but just how PV INs modulate PYR plasticity throughout adolescence remains unclear. It is also not fully known how increasing dopamine

innervation impacts PV IN function in adolescence. Thus, to link together three developing facets of the adolescent dmPFC – PV IN-mediated inhibition onto PYR, spine pruning on PYR, and dopamine’s influence on all classes of neurons – a greater effort is needed to develop tools and behavioral protocols suitable to adolescent experimentation.

Final remarks: the case for adolescence

In this dissertation, I have made a case for a putative adolescent sensitive period, based on our work and a sizable body of previous literature. In Chapter 1, I outlined the structural and functional remodeling of the adolescent dmPFC, with a particular focus on three variables: spine pruning, dopaminergic innervation, and inhibitory neurotransmission; I also highlighted a small sample of the literature on adolescent behavior, focusing on a category of tasks assessing response inhibition. In Chapter 2, I explained how the background literature in sensory cortices demonstrates a crucial role for GABAergic inhibition in the onset of critical periods for neural encoding of external stimuli. I showed how this information may logically extend to other cortices, and in particular, how a documented rise in inhibitory neurotransmission around P30 in mice may signal an analogous type of sensitive period for frontal cortical development. I thus motivated our study to investigate whether adolescents might exhibit a behavioral or neural encoding advantage over adults due to the ongoing development of the adolescent dmPFC around P30. I demonstrated that our study results did, in fact, support our hypothesis of a sensitive period of adolescence, in that adolescent mice learned a go/no-go task faster than adult mice, and the adolescent dmPFC exhibited more robust encoding of task variables. Next, in Chapter 3, I introduced an implantable probe, nIRF fibers, for out-of-the-box dopamine detection as the first step in development of a non-genetically-encoded fluorescent tool for extracellular dopamine imaging *in vivo*. I explored the utility of the current form factor of this probe in *in vitro* and *ex vivo* settings with the intention that eventually, further work will facilitate the transition to *in vivo* animal models, particularly in adolescents. Finally, in this closing chapter, I have demonstrated how many areas remain open for investigation to better unpack the dynamics of the developing adolescent dmPFC and understand how these changes influence behavior.

At this stage, the parameters of an adolescent sensitive period remain unclear. While our group and others have honed the age range to early adolescence, approximately P28-35 in mice, we do not fully understand what governs the boundaries of this period. I have made a case for GABAergic inhibition in regulating its onset, but its offset may be due to other factors—for instance, a certain spine density, or the action of dopamine on PV INs to a certain degree. More work is needed to understand the outlined developmental changes and their regulation, from the level of dopamine molecules and receptors to the level of complex animal behavior. Additionally, it is not clear what types of behaviors may fall under the realm of a frontal cortical sensitive period. As it stands, reports of adolescent behavior on a variety of cognitive tasks are conflicting. One challenge in solidifying the concept of an adolescent sensitive period is to standardize animal behavior protocols across laboratories and come to a consensus regarding the aspect of cognitive control that is addressed by each task. For instance, response inhibition may be assessed by multiple tasks discussed here, including go/no-go, contingency degradation, delay discounting, and the cued response inhibition task, among others. Going forward, it may be beneficial for coalitions of researchers to collaborate more closely on task design.

This work is as important as ever as we start to grapple with the state of adolescent mental health and the implications of adolescent-onset psychiatric illness. Even before the COVID-19 global pandemic, mental health had been worsening among adolescents. The U.S. Center for Disease Control and Prevention reports that the suicide rate among ages 10–24 increased by 62% between 2007 and 2021, from 6.8 deaths to 11.0 per 100,000, making it the second leading cause of death for this age group, only after accidental injury (Curtin & Garnett, 2023). Importantly, this statistic does not take into account the prevalence of suicide attempts or ideation. Similarly, from 2011-2020, emergency rooms witnessed a rise in pediatric mental health-related visits, from 7.7% to 13.1% of all pediatric visits. Significant increases were observed for children (ages 6-11), adolescents (ages 12-17), and young adults (ages 18-24), with the greatest increases in the adolescent group (Bommersbach et al., 2023). Critically, these trends disproportionately impact adolescents of color, who are also less likely to pursue mental health treatment (Douglas et al., 2023; Lipson et al., 2022; Opara et al., 2021). These findings, in addition to their exacerbation by the COVID-19 pandemic, prompted the American Academy of Pediatrics, American Academy of Child and Adolescent Psychiatry, and Children’s Hospital Association to declare a national emergency in child and adolescent mental health in 2021. It is thus imperative that neuroscience turn its attention to adolescent brains, behavior, and experience. In order to address crises of mental health both at the adult and adolescent level, we would do well to investigate the mechanisms at play in the adolescent frontal cortex and how interventions during adolescence, whether behavioral or pharmacological, can shape adult outcomes. We can also recognize and support the unique strengths of the adolescent brain. We ought to remember that while adolescents may be more susceptible to certain detriments, this dissertation has shown, hopefully, that the adolescent brain is also highly capable of learning and encoding information. At this point, we have not yet unpacked its full potential.

References

- Abe, M., Iwaoka, M., Nakamura, T., Kitta, Y., Takano, H., Kodama, Y., Kawabata, K., Obata, J., Mende, A., Kobayashi, T., Fujioka, D., Saito, Y., Hasebe, H., & Kugiyama, K. (2007). Association of high levels of plasma free dopamine with future coronary events in patients with coronary artery disease. *Circulation Journal: Official Journal of the Japanese Circulation Society*, *71*(5), 688–692. <https://doi.org/10.1253/circj.71.688>
- Adleman, N. E., Menon, V., Blasey, C. M., White, C. D., Warsofsky, I. S., Glover, G. H., & Reiss, A. L. (2002). A Developmental fMRI Study of the Stroop Color-Word Task. *NeuroImage*, *16*(1), 61–75. <https://doi.org/10.1006/nimg.2001.1046>
- Adriani, W., & Laviola, G. (2003). Elevated levels of impulsivity and reduced place conditioning with d-amphetamine: Two behavioral features of adolescence in mice. *Behavioral Neuroscience*, *117*(4), 695–703. <https://doi.org/10.1037/0735-7044.117.4.695>
- Al Faraj, A., Shaik, A. S., Ratemi, E., & Halwani, R. (2016). Combination of drug-conjugated SWCNT nanocarriers for efficient therapy of cancer stem cells in a breast cancer animal model. *Journal of Controlled Release*, *225*, 240–251. <https://doi.org/10.1016/j.jconrel.2016.01.053>
- Allen, C. B., Celikel, T., & Feldman, D. E. (2003). Long-term depression induced by sensory deprivation during cortical map plasticity in vivo. *Nature Neuroscience*, *6*(3), 291–299. <https://doi.org/10.1038/nn1012>
- Andersen, S. L., Thompson, A. T., Rutstein, M., Hostetter, J. C., & Teicher, M. H. (2000). Dopamine receptor pruning in prefrontal cortex during the periadolescent period in rats. *Synapse*, *37*(2), 167–169. [https://doi.org/10.1002/1098-2396\(200008\)37:2<167::AID-SYN11>3.0.CO;2-B](https://doi.org/10.1002/1098-2396(200008)37:2<167::AID-SYN11>3.0.CO;2-B)
- Andrzejewski, M. E., Schochet, T. L., Feit, E. C., Harris, R., McKee, B. L., & Kelley, A. E. (2011). A comparison of adult and adolescent rat behavior in operant learning, extinction, and behavioral inhibition paradigms. *Behavioral Neuroscience*, *125*(1), 93–105. <https://doi.org/10.1037/a0022038>
- Arbuthnott, G. W., Fairbrother, I. S., & Butcher, S. P. (1990). Brain microdialysis studies on the control of dopamine release and metabolism in vivo. *Journal of Neuroscience Methods*, *34*(1–3), 73–81. [https://doi.org/10.1016/0165-0270\(90\)90044-g](https://doi.org/10.1016/0165-0270(90)90044-g)
- Aron, A. R. (2007). The Neural Basis of Inhibition in Cognitive Control. *The Neuroscientist*, *13*(3), 214–228. <https://doi.org/10.1177/1073858407299288>
- Asato, M. R., Terwilliger, R., Woo, J., & Luna, B. (2010). White matter development in adolescence: A DTI study. *Cerebral Cortex (New York, N.Y.: 1991)*, *20*(9), 2122–2131. <https://doi.org/10.1093/cercor/bhp282>
- Averbeck, B. B. (2022). Pruning recurrent neural networks replicates adolescent changes in working memory and reinforcement learning. *Proceedings of the National Academy of Sciences of the United States of America*, *119*(22), e2121331119. <https://doi.org/10.1073/pnas.2121331119>
- Bai, J., Blot, K., Tzavara, E., Nosten-Bertrand, M., Giros, B., & Otani, S. (2014). Inhibition of dopamine transporter activity impairs synaptic depression in rat prefrontal cortex through over-stimulation of D1 receptors. *Cerebral Cortex (New York, N.Y.: 1991)*, *24*(4), 945–955. <https://doi.org/10.1093/cercor/bhs376>
- Bakh, N. A., Gong, X., Lee, M. A., Jin, X., Koman, V. B., Park, M., Nguyen, F. T., & Strano, M. S. (2021). Transcutaneous Measurement of Essential Vitamins Using Near-Infrared

- Fluorescent Single-Walled Carbon Nanotube Sensors. *Small (Weinheim an Der Bergstrasse, Germany)*, 17(31), e2100540. <https://doi.org/10.1002/sml.202100540>
- Bang, D., Kishida, K. T., Lohrenz, T., White, J. P., Laxton, A. W., Tatter, S. B., Fleming, S. M., & Montague, P. R. (2020). Sub-second Dopamine and Serotonin Signaling in Human Striatum during Perceptual Decision-Making. *Neuron*, 108(5), 999–1010.e6. <https://doi.org/10.1016/j.neuron.2020.09.015>
- Bardi, G., Nunes, A., Gherardini, L., Bates, K., Al-Jamal, K. T., Gaillard, C., Prato, M., Bianco, A., Pizzorusso, T., & Kostarelou, K. (2013). Functionalized carbon nanotubes in the brain: Cellular internalization and neuroinflammatory responses. *PLoS One*, 8(11), e80964. <https://doi.org/10.1371/journal.pone.0080964>
- Barkat, T. R., Polley, D. B., & Hensch, T. K. (2011). A critical period for auditory thalamocortical connectivity. *Nature Neuroscience*, 14(9), 1189–1194. <https://doi.org/10.1038/nn.2882>
- Barnea-Goraly, N., Lotspeich, L. J., & Reiss, A. L. (2010). Similar white matter aberrations in children with autism and their unaffected siblings: A diffusion tensor imaging study using tract-based spatial statistics. *Archives of General Psychiatry*, 67(10), 1052–1060. <https://doi.org/10.1001/archgenpsychiatry.2010.123>
- Barthas, F., & Kwan, A. C. (2017). Secondary Motor Cortex: Where “Sensory” Meets “Motor” in the Rodent Frontal Cortex. *Trends in Neurosciences*, 40(3), 181–193. <https://doi.org/10.1016/j.tins.2016.11.006>
- Bartos, M., Vida, I., & Jonas, P. (2007). Synaptic mechanisms of synchronized gamma oscillations in inhibitory interneuron networks. *Nature Reviews Neuroscience*, 8(1), 45–56. <https://doi.org/10.1038/nrn2044>
- Bastioli, G., Arnold, J. C., Mancini, M., Mar, A. C., Gamallo-Lana, B., Saadipour, K., Chao, M. V., & Rice, M. E. (2022). Voluntary Exercise Boosts Striatal Dopamine Release: Evidence for the Necessary and Sufficient Role of BDNF. *The Journal of Neuroscience: The Official Journal of the Society for Neuroscience*, 42(23), 4725–4736. <https://doi.org/10.1523/JNEUROSCI.2273-21.2022>
- Basu, S., & Dasgupta, P. S. (2000). Dopamine, a neurotransmitter, influences the immune system. *Journal of Neuroimmunology*, 102(2), 113–124. [https://doi.org/10.1016/s0165-5728\(99\)00176-9](https://doi.org/10.1016/s0165-5728(99)00176-9)
- Bedard, A.-C., Nichols, S., Barbosa, J. A., Schachar, R., Logan, G. D., & Tannock, R. (2002). The Development of Selective Inhibitory Control Across the Life Span. *Developmental Neuropsychology*, 21(1), 93–111. https://doi.org/10.1207/S15326942DN2101_5
- Benes, F. M., Taylor, J. B., & Cunningham, M. C. (2000). Convergence and plasticity of monoaminergic systems in the medial prefrontal cortex during the postnatal period: Implications for the development of psychopathology. *Cerebral Cortex (New York, N.Y.: 1991)*, 10(10), 1014–1027. <https://doi.org/10.1093/cercor/10.10.1014>
- Berke, J. D. (2018). What does dopamine mean? *Nature Neuroscience*, 21(6), Article 6. <https://doi.org/10.1038/s41593-018-0152-y>
- Bernardi, S., Benna, M. K., Rigotti, M., Munuera, J., Fusi, S., & Salzman, C. D. (2020). The Geometry of Abstraction in the Hippocampus and Prefrontal Cortex. *Cell*, 183(4), 954–967.e21. <https://doi.org/10.1016/j.cell.2020.09.031>
- Berridge, C. W. (2008). Noradrenergic modulation of arousal. *Brain Research Reviews*, 58(1), 1–17. <https://doi.org/10.1016/j.brainresrev.2007.10.013>

- Berridge, C. W., Schmeichel, B. E., & España, R. A. (2012). Noradrenergic modulation of wakefulness/arousal. *Sleep Medicine Reviews, 16*(2), 187–197. <https://doi.org/10.1016/j.smr.2011.12.003>
- Beyene, A. G., Alizadehmojarad, A. A., Dorlhiac, G., Goh, N., Streets, A. M., Král, P., Vuković, L., & Landry, M. P. (2018). Ultralarge Modulation of Fluorescence by Neuromodulators in Carbon Nanotubes Functionalized with Self-Assembled Oligonucleotide Rings. *Nano Letters, 18*(11), 6995–7003. <https://doi.org/10.1021/acs.nanolett.8b02937>
- Beyene, A. G., Delevich, K., Del Bonis-O'Donnell, J. T., Piekarski, D. J., Lin, W. C., Thomas, A. W., Yang, S. J., Kosillo, P., Yang, D., Prounis, G. S., Wilbrecht, L., & Landry, M. P. (2019). Imaging striatal dopamine release using a nongenetically encoded near infrared fluorescent catecholamine nanosensor. *Science Advances, 5*(7), eaaw3108. <https://doi.org/10.1126/sciadv.aaw3108>
- Bicks, L. K., Yamamuro, K., Flanigan, M. E., Kim, J. M., Kato, D., Lucas, E. K., Koike, H., Peng, M. S., Brady, D. M., Chandrasekaran, S., Norman, K. J., Smith, M. R., Clem, R. L., Russo, S. J., Akbarian, S., & Morishita, H. (2020). Prefrontal parvalbumin interneurons require juvenile social experience to establish adult social behavior. *Nature Communications, 11*(1), 1003. <https://doi.org/10.1038/s41467-020-14740-z>
- Blakemore, S.-J., & Mills, K. L. (2014). Is Adolescence a Sensitive Period for Sociocultural Processing? *Annual Review of Psychology, 65*(Volume 65, 2014), 187–207. <https://doi.org/10.1146/annurev-psych-010213-115202>
- Boivin, J. R., Piekarski, D. J., Thomas, A. W., & Wilbrecht, L. (2018). Adolescent pruning and stabilization of dendritic spines on cortical layer 5 pyramidal neurons do not depend on gonadal hormones. *Developmental Cognitive Neuroscience, 30*, 100–107. <https://doi.org/10.1016/j.dcn.2018.01.007>
- Bommersbach, T. J., McKean, A. J., Olfson, M., & Rhee, T. G. (2023). National Trends in Mental Health-Related Emergency Department Visits Among Youth, 2011-2020. *JAMA, 329*(17), 1469–1477. <https://doi.org/10.1001/jama.2023.4809>
- Bove, C., Anselmi, L., & Travagli, R. A. (2019). Altered gastric tone and motility response to brain-stem dopamine in a rat model of parkinsonism. *American Journal of Physiology. Gastrointestinal and Liver Physiology, 317*(1), G1–G7. <https://doi.org/10.1152/ajpgi.00076.2019>
- Brecht, M. (2011). Movement, Confusion, and Orienting in Frontal Cortices. *Neuron, 72*(2), 193–196. <https://doi.org/10.1016/j.neuron.2011.10.002>
- Bulumulla, C., Krasley, A. T., Cristofori-Armstrong, B., Valinsky, W. C., Walpita, D., Ackerman, D., Clapham, D. E., & Beyene, A. G. (2022). Visualizing synaptic dopamine efflux with a 2D composite nanofilm. *eLife, 11*, e78773. <https://doi.org/10.7554/eLife.78773>
- Burton, C. L., & Fletcher, P. J. (2012). Age and sex differences in impulsive action in rats: The role of dopamine and glutamate. *Behavioural Brain Research, 230*(1), 21–33. <https://doi.org/10.1016/j.bbr.2012.01.046>
- Caballero, A., Flores-Barrera, E., Cass, D. K., & Tseng, K. Y. (2014). Differential regulation of parvalbumin and calretinin interneurons in the prefrontal cortex during adolescence. *Brain Structure and Function, 219*(1), 395–406. <https://doi.org/10.1007/s00429-013-0508-8>
- Caballero, A., Flores-Barrera, E., Thomases, D. R., & Tseng, K. Y. (2020). Downregulation of parvalbumin expression in the prefrontal cortex during adolescence causes enduring

- prefrontal disinhibition in adulthood. *Neuropsychopharmacology*, 45(9), 1527–1535.
<https://doi.org/10.1038/s41386-020-0709-9>
- Caballero, A., Granberg, R., & Tseng, K. Y. (2016). Mechanisms contributing to prefrontal cortex maturation during adolescence. *Neuroscience and Biobehavioral Reviews*, 70, 4–12. <https://doi.org/10.1016/j.neubiorev.2016.05.013>
- Calder, A. E., & Hasler, G. (2023). Towards an understanding of psychedelic-induced neuroplasticity. *Neuropsychopharmacology*, 48(1), 104–112.
<https://doi.org/10.1038/s41386-022-01389-z>
- Canetta, S. E., Holt, E. S., Benoit, L. J., Teboul, E., Sahyoun, G. M., Ogden, R. T., Harris, A. Z., & Kellendonk, C. (2022). Mature parvalbumin interneuron function in prefrontal cortex requires activity during a postnatal sensitive period. *eLife*, 11, e80324.
<https://doi.org/10.7554/eLife.80324>
- Chattopadhyaya, B., Di Cristo, G., Higashiyama, H., Knott, G. W., Kuhlman, S. J., Welker, E., & Huang, Z. J. (2004). Experience and Activity-Dependent Maturation of Perisomatic GABAergic Innervation in Primary Visual Cortex during a Postnatal Critical Period. *The Journal of Neuroscience*, 24(43), 9598–9611. <https://doi.org/10.1523/JNEUROSCI.1851-04.2004>
- Chau, B. K. H., Jarvis, H., Law, C.-K., & Chong, T. T.-J. (2018). Dopamine and reward: A view from the prefrontal cortex. *Behavioural Pharmacology*, 29(7), 569–583.
<https://doi.org/10.1097/FBP.0000000000000424>
- Chelaru, M. I., Eagleman, S., Andrei, A. R., Milton, R., Kharas, N., & Dragoi, V. (2021). High-order interactions explain the collective behavior of cortical populations in executive but not sensory areas. *Neuron*, 0(0). <https://doi.org/10.1016/j.neuron.2021.09.042>
- Chen, G., Rasch, M. J., Wang, R., & Zhang, X. (2015). Experience-dependent emergence of beta and gamma band oscillations in the primary visual cortex during the critical period. *Scientific Reports*, 5, 17847. <https://doi.org/10.1038/srep17847>
- Chiang, F.-K., Wallis, J. D., & Rich, E. L. (2022). Cognitive strategies shift information from single neurons to populations in prefrontal cortex. *Neuron*, 110(4), 709–721.e4.
<https://doi.org/10.1016/j.neuron.2021.11.021>
- Chikazoe, J. (2010). Localizing performance of go/no-go tasks to prefrontal cortical subregions. *Current Opinion in Psychiatry*, 23(3), 267–272.
<https://doi.org/10.1097/YCO.0b013e3283387a9f>
- Choi, M., Choi, J. W., Kim, S., Nizamoglu, S., Hahn, S. K., & Yun, S. H. (2013). Light-guiding hydrogels for cell-based sensing and optogenetic synthesis in vivo. *Nature Photonics*, 7, 987–994. <https://doi.org/10.1038/nphoton.2013.278>
- Christensen, N. J., & Jensen, E. W. (1994). Effect of psychosocial stress and age on plasma norepinephrine levels: A review. *Psychosomatic Medicine*, 56(1), 77–83.
<https://doi.org/10.1097/00006842-199401000-00010>
- Constantinidis, C., & Luna, B. (2019). Neural Substrates of Inhibitory Control Maturation in Adolescence. *Trends in Neurosciences*, 42(9), 604–616.
<https://doi.org/10.1016/j.tins.2019.07.004>
- Cragg, L. (2016). The development of stimulus and response interference control in midchildhood. *Developmental Psychology*, 52(2), 242–252.
<https://doi.org/10.1037/dev0000074>

- Crone, E. A., & Dahl, R. E. (2012). Understanding adolescence as a period of social-affective engagement and goal flexibility. *Nature Reviews. Neuroscience*, *13*(9), 636–650. <https://doi.org/10.1038/nrn3313>
- Curtin, S., & Garnett, M. (2023). *Suicide and Homicide Death Rates Among Youth and Young Adults Aged 10–24: United States, 2001–2021*. National Center for Health Statistics (U.S.). <https://doi.org/10.15620/cdc:128423>
- Dahl, R. E., Allen, N. B., Wilbrecht, L., & Suleiman, A. B. (2018). Importance of investing in adolescence from a developmental science perspective. *Nature*, *554*(7693), 441–450. <https://doi.org/10.1038/nature25770>
- Dang, W., Jaffe, R. J., Qi, X.-L., & Constantinidis, C. (2021). Emergence of Nonlinear Mixed Selectivity in Prefrontal Cortex after Training. *The Journal of Neuroscience: The Official Journal of the Society for Neuroscience*, *41*(35), 7420–7434. <https://doi.org/10.1523/JNEUROSCI.2814-20.2021>
- De Bellis, M. D., Keshavan, M. S., Beers, S. R., Hall, J., Frustaci, K., Masalehdan, A., Noll, J., & Boring, A. M. (2001). Sex differences in brain maturation during childhood and adolescence. *Cerebral Cortex (New York, N.Y.: 1991)*, *11*(6), 552–557. <https://doi.org/10.1093/cercor/11.6.552>
- DeKeyser, R., Alfi-Shabtay, I., & Ravid, D. (2010). Cross-linguistic evidence for the nature of age effects in second language acquisition. *Applied Psycholinguistics*, *31*(3), 413–438. <https://doi.org/10.1017/S0142716410000056>
- DeKeyser, R. M. (2000). THE ROBUSTNESS OF CRITICAL PERIOD EFFECTS IN SECOND LANGUAGE ACQUISITION. *Studies in Second Language Acquisition*, *22*(4), 499–533. <https://doi.org/10.1017/S0272263100004022>
- Del Campo, N., Chamberlain, S. R., Sahakian, B. J., & Robbins, T. W. (2011). The roles of dopamine and noradrenaline in the pathophysiology and treatment of attention-deficit/hyperactivity disorder. *Biological Psychiatry*, *69*(12), e145-157. <https://doi.org/10.1016/j.biopsych.2011.02.036>
- Delevich, K., Klinger, M., Okada, N. J., & Wilbrecht, L. (2021). Coming of age in the frontal cortex: The role of puberty in cortical maturation. *Seminars in Cell & Developmental Biology*, *118*, 64–72. <https://doi.org/10.1016/j.semcdb.2021.04.021>
- Delevich, K., Okada, N. J., Rahane, A., Zhang, Z., Hall, C. D., & Wilbrecht, L. (2020). Sex and Pubertal Status Influence Dendritic Spine Density on Frontal Corticostriatal Projection Neurons in Mice. *Cerebral Cortex (New York, N.Y.: 1991)*, *30*(6), 3543–3557. <https://doi.org/10.1093/cercor/bhz325>
- Delevich, K., Piekarski, D., & Wilbrecht, L. (2019). Neuroscience: Sex Hormones at Work in the Neocortex. *Current Biology: CB*, *29*(4), R122–R125. <https://doi.org/10.1016/j.cub.2019.01.013>
- Delevich, K., Thomas, A. W., & Wilbrecht, L. (2018). Adolescence and “Late Blooming” Synapses of the Prefrontal Cortex. *Cold Spring Harbor Symposia on Quantitative Biology*, *83*, 37–43. <https://doi.org/10.1101/sqb.2018.83.037507>
- Delevich, K., Tucciarone, J., Huang, Z. J., & Li, B. (2015). The mediodorsal thalamus drives feedforward inhibition in the anterior cingulate cortex via parvalbumin interneurons. *The Journal of Neuroscience: The Official Journal of the Society for Neuroscience*, *35*(14), 5743–5753. <https://doi.org/10.1523/JNEUROSCI.4565-14.2015>

- Devoto, P., Flore, G., Pani, L., & Gessa, G. L. (2001). Evidence for co-release of noradrenaline and dopamine from noradrenergic neurons in the cerebral cortex. *Molecular Psychiatry*, 6(6), Article 6. <https://doi.org/10.1038/sj.mp.4000904>
- Di Domenico, D., & Mapelli, L. (2023). Dopaminergic Modulation of Prefrontal Cortex Inhibition. *Biomedicines*, 11(5), 1276. <https://doi.org/10.3390/biomedicines11051276>
- Dong, C., Zheng, Y., Long-Iyer, K., Wright, E. C., Li, Y., & Tian, L. (2022). Fluorescence Imaging of Neural Activity, Neurochemical Dynamics, and Drug-Specific Receptor Conformation with Genetically Encoded Sensors. *Annual Review of Neuroscience*, 45, 273–294. <https://doi.org/10.1146/annurev-neuro-110520-031137>
- Douglas, C. M., Richardson, L., & Evans, Y. N. (2023). Utilization of Mental Health Services Among Black Adolescents During the COVID-19 Pandemic: A Narrative Review of the Literature. *Current Pediatrics Reports*, 11(1), 7–12. <https://doi.org/10.1007/s40124-023-00282-7>
- Drzewiecki, C. M., Willing, J., & Juraska, J. M. (2016). Synaptic number changes in the medial prefrontal cortex across adolescence in male and female rats: A role for pubertal onset. *Synapse (New York, N.Y.)*, 70(9), 361–368. <https://doi.org/10.1002/syn.21909>
- Ebbesen, C. L., Insanally, M. N., Kopec, C. D., Murakami, M., Saiki, A., & Erlich, J. C. (2018). More than Just a “Motor”: Recent Surprises from the Frontal Cortex. *Journal of Neuroscience*, 38(44), 9402–9413. <https://doi.org/10.1523/JNEUROSCI.1671-18.2018>
- Eckstein, M. K., Master, S. L., Dahl, R. E., Wilbrecht, L., & Collins, A. G. E. (2022). Reinforcement learning and Bayesian inference provide complementary models for the unique advantage of adolescents in stochastic reversal. *Developmental Cognitive Neuroscience*, 55, 101106. <https://doi.org/10.1016/j.dcn.2022.101106>
- Ehringer, H., & Hornykiewicz, O. (1960). [Distribution of noradrenaline and dopamine (3-hydroxytyramine) in the human brain and their behavior in diseases of the extrapyramidal system]. *Klinische Wochenschrift*, 38, 1236–1239. <https://doi.org/10.1007/BF01485901>
- Elizarova, S., Chouaib, A. A., Shaib, A., Hill, B., Mann, F., Brose, N., Kruss, S., & Daniel, J. A. (2022). A fluorescent nanosensor paint detects dopamine release at axonal varicosities with high spatiotemporal resolution. *Proceedings of the National Academy of Sciences of the United States of America*, 119(22), e2202842119. <https://doi.org/10.1073/pnas.2202842119>
- Elrod, R., Peskind, E. R., DiGiacomo, L., Brodtkin, K. I., Veith, R. C., & Raskind, M. A. (1997). Effects of Alzheimer’s disease severity on cerebrospinal fluid norepinephrine concentration. *The American Journal of Psychiatry*, 154(1), 25–30. <https://doi.org/10.1176/ajp.154.1.25>
- Ema, M., Gamo, M., & Honda, K. (2016). A review of toxicity studies of single-walled carbon nanotubes in laboratory animals. *Regulatory Toxicology and Pharmacology: RTP*, 74, 42–63. <https://doi.org/10.1016/j.yrtph.2015.11.015>
- Erzurumlu, R. S., & Gaspar, P. (2012). Development and critical period plasticity of the barrel cortex. *The European Journal of Neuroscience*, 35(10), 1540–1553. <https://doi.org/10.1111/j.1460-9568.2012.08075.x>
- España, R. A., Schmeichel, B. E., & Berridge, C. W. (2016). Norepinephrine at the nexus of arousal, motivation and relapse. *Brain Research*, 1641(Pt B), 207–216. <https://doi.org/10.1016/j.brainres.2016.01.002>
- Espinosa, J. S., & Stryker, M. P. (2012). Development and Plasticity of the Primary Visual Cortex. *Neuron*, 75(2), 230–249. <https://doi.org/10.1016/j.neuron.2012.06.009>

- Evrard, M. R., Li, M., Shen, H., & Smith, S. S. (2021). Preventing adolescent synaptic pruning in mouse prelimbic cortex via local knockdown of $\alpha 4\beta\delta$ GABAA receptors increases anxiety response in adulthood. *Scientific Reports*, *11*(1), 21059. <https://doi.org/10.1038/s41598-021-99965-8>
- Fagiolini, M., Fritschy, J.-M., Löw, K., Möhler, H., Rudolph, U., & Hensch, T. K. (2004). Specific GABAA circuits for visual cortical plasticity. *Science (New York, N.Y.)*, *303*(5664), 1681–1683. <https://doi.org/10.1126/science.1091032>
- Fagiolini, M., & Hensch, T. K. (2000). Inhibitory threshold for critical-period activation in primary visual cortex. *Nature*, *404*(6774), 183–186. <https://doi.org/10.1038/35004582>
- Ferry, B., & McGaugh, J. L. (2000). Role of amygdala norepinephrine in mediating stress hormone regulation of memory storage. *Acta Pharmacologica Sinica*, *21*(6), 481–493.
- Flores-Barrera, E., Thomases, D. R., Heng, L.-J., Cass, D. K., Caballero, A., & Tseng, K. Y. (2014). Late Adolescent Expression of GluN2B Transmission in the Prefrontal Cortex Is Input-Specific and Requires Postsynaptic Protein Kinase A and D1 Dopamine Receptor Signaling. *Biological Psychiatry*, *75*(6), 508–516. <https://doi.org/10.1016/j.biopsych.2013.07.033>
- Floresco, S. B., & Magyar, O. (2006). Mesocortical dopamine modulation of executive functions: Beyond working memory. *Psychopharmacology*, *188*(4), 567–585. <https://doi.org/10.1007/s00213-006-0404-5>
- Forrest, M. P., Parnell, E., & Penzes, P. (2018). Dendritic structural plasticity and neuropsychiatric disease. *Nature Reviews. Neuroscience*, *19*(4), 215–234. <https://doi.org/10.1038/nrn.2018.16>
- Francis, A. P., & Devasena, T. (2018). Toxicity of carbon nanotubes: A review. *Toxicology and Industrial Health*, *34*(3), 200–210. <https://doi.org/10.1177/0748233717747472>
- Friedman, N. P., & Robbins, T. W. (2022). The role of prefrontal cortex in cognitive control and executive function. *Neuropsychopharmacology*, *47*(1), 72–89. <https://doi.org/10.1038/s41386-021-01132-0>
- Galassi, T. V., Antman-Passig, M., Yaari, Z., Jessurun, J., Schwartz, R. E., & Heller, D. A. (2020). Long-term in vivo biocompatibility of single-walled carbon nanotubes. *PloS One*, *15*(5), e0226791. <https://doi.org/10.1371/journal.pone.0226791>
- Gao, Z., Danné, N., Godin, A. G., Lounis, B., & Cognet, L. (2017). Evaluation of Different Single-Walled Carbon Nanotube Surface Coatings for Single-Particle Tracking Applications in Biological Environments. *Nanomaterials*, *7*(11), Article 11. <https://doi.org/10.3390/nano7110393>
- Gardner, D. G., & Shoback, D. (2011). Appendix: Normal Hormone Reference Ranges. In *Greenspan's Basic & Clinical Endocrinology* (9th ed.). The McGraw-Hill Companies. accessmedicine.mhmedical.com/content.aspx?aid=8410499
- Gaskill, P. J., & Khoshbouei, H. (2022). Dopamine and norepinephrine are embracing their immune side and so should we. *Current Opinion in Neurobiology*, *77*, 102626. <https://doi.org/10.1016/j.conb.2022.102626>
- Gee, S., Ellwood, I., Patel, T., Luongo, F., Deisseroth, K., & Sohal, V. S. (2012). Synaptic Activity Unmasks Dopamine D2 Receptor Modulation of a Specific Class of Layer V Pyramidal Neurons in Prefrontal Cortex. *The Journal of Neuroscience*, *32*(14), 4959–4971. <https://doi.org/10.1523/JNEUROSCI.5835-11.2012>

- Goetz, C. G. (2011). The history of Parkinson's disease: Early clinical descriptions and neurological therapies. *Cold Spring Harbor Perspectives in Medicine*, *1*(1), a008862. <https://doi.org/10.1101/cshperspect.a008862>
- Gogtay, N., Giedd, J. N., Lusk, L., Hayashi, K. M., Greenstein, D., Vaituzis, A. C., Nugent, T. F., Herman, D. H., Clasen, L. S., Toga, A. W., Rapoport, J. L., & Thompson, P. M. (2004). Dynamic mapping of human cortical development during childhood through early adulthood. *Proceedings of the National Academy of Sciences of the United States of America*, *101*(21), 8174–8179. <https://doi.org/10.1073/pnas.0402680101>
- Gogtay, N., & Thompson, P. M. (2010). Mapping gray matter development: Implications for typical development and vulnerability to psychopathology. *Brain and Cognition*, *72*(1), 6–15. <https://doi.org/10.1016/j.bandc.2009.08.009>
- Goldman-Rakic, P. S. (1998). The cortical dopamine system: Role in memory and cognition. *Advances in Pharmacology (San Diego, Calif.)*, *42*, 707–711. [https://doi.org/10.1016/s1054-3589\(08\)60846-7](https://doi.org/10.1016/s1054-3589(08)60846-7)
- Goldstein, D. S., & Holmes, C. (2008). Neuronal Source of Plasma Dopamine. *Clinical Chemistry*, *54*(11), 1864–1871. <https://doi.org/10.1373/clinchem.2008.107193>
- Goldstein, D. S., Holmes, C., & Sharabi, Y. (2012). Cerebrospinal fluid biomarkers of central catecholamine deficiency in Parkinson's disease and other synucleinopathies. *Brain: A Journal of Neurology*, *135*(Pt 6), 1900–1913. <https://doi.org/10.1093/brain/aws055>
- Gonzalez-Burgos, G., Miyamae, T., Pafundo, D. E., Yoshino, H., Rotaru, D. C., Hoftman, G., Datta, D., Zhang, Y., Hammond, M., Sampson, A. R., Fish, K. N., Bard Ermentrout, G., & Lewis, D. A. (2015). Functional Maturation of GABA Synapses During Postnatal Development of the Monkey Dorsolateral Prefrontal Cortex. *Cerebral Cortex*, *25*(11), 4076–4093. <https://doi.org/10.1093/cercor/bhu122>
- Grace, A. A. (2016). Dysregulation of the dopamine system in the pathophysiology of schizophrenia and depression. *Nature Reviews. Neuroscience*, *17*(8), 524–532. <https://doi.org/10.1038/nrn.2016.57>
- Grant, R. I., Doncheck, E. M., Vollmer, K. M., Winston, K. T., Romanova, E. V., Siegler, P. N., Holman, H., Bowen, C. W., & Otis, J. M. (2021). Specialized coding patterns among dorsomedial prefrontal neuronal ensembles predict conditioned reward seeking. *eLife*, *10*, e65764. <https://doi.org/10.7554/eLife.65764>
- Greenwood, B. N., Foley, T. E., Le, T. V., Strong, P. V., Loughridge, A. B., Day, H. E. W., & Fleshner, M. (2011). Long-term voluntary wheel running is rewarding and produces plasticity in the mesolimbic reward pathway. *Behavioural Brain Research*, *217*(2), 354–362. <https://doi.org/10.1016/j.bbr.2010.11.005>
- Grella, S. L., Gomes, S. M., Lackie, R. E., Renda, B., & Marrone, D. F. (2021). Norepinephrine as a spatial memory reset signal. *Behavioural Pharmacology*, *32*(7), 531–548. <https://doi.org/10.1097/FBP.0000000000000648>
- Grouzmann, E., & Lamine, F. (2013). Determination of catecholamines in plasma and urine. *Best Practice & Research. Clinical Endocrinology & Metabolism*, *27*(5), 713–723. <https://doi.org/10.1016/j.beem.2013.06.004>
- Harley, C. W. (2004). Norepinephrine and dopamine as learning signals. *Neural Plasticity*, *11*(3–4), 191–204. <https://doi.org/10.1155/np.2004.191>
- Harris, R. C., & Zhang, M.-Z. (2012). Dopamine, the kidney, and hypertension. *Current Hypertension Reports*, *14*(2), 138–143. <https://doi.org/10.1007/s11906-012-0253-z>

- Hartshorne, J. K., Tenenbaum, J. B., & Pinker, S. (2018). A critical period for second language acquisition: Evidence from 2/3 million English speakers. *Cognition*, *177*, 263–277. <https://doi.org/10.1016/j.cognition.2018.04.007>
- Hendler-Neumark, A., & Bisker, G. (2019). Fluorescent Single-Walled Carbon Nanotubes for Protein Detection. *Sensors*, *19*(24), Article 24. <https://doi.org/10.3390/s19245403>
- Henjum, K., Watne, L. O., Godang, K., Halaas, N. B., Eldholm, R. S., Blennow, K., Zetterberg, H., Saltvedt, I., Bollerslev, J., & Knapskog, A. B. (2022). Cerebrospinal fluid catecholamines in Alzheimer’s disease patients with and without biological disease. *Translational Psychiatry*, *12*(1), 151. <https://doi.org/10.1038/s41398-022-01901-5>
- Hensch, T. K. (2005). Critical period plasticity in local cortical circuits. *Nature Reviews Neuroscience*, *6*(11), 877–888. <https://doi.org/10.1038/nrn1787>
- Hensch, T. K., Fagiolini, M., Mataga, N., Stryker, M. P., Baekkeskov, S., & Kash, S. F. (1998). Local GABA circuit control of experience-dependent plasticity in developing visual cortex. *Science (New York, N.Y.)*, *282*(5393), 1504–1508. <https://doi.org/10.1126/science.282.5393.1504>
- Hirst, R. J., Kicks, E. C., Allen, H. A., & Cragg, L. (2019). Cross-modal interference-control is reduced in childhood but maintained in aging: A cohort study of stimulus- and response-interference in cross-modal and unimodal Stroop tasks. *Journal of Experimental Psychology: Human Perception and Performance*, *45*(5), 553–572. <https://doi.org/10.1037/xhp0000608>
- Hofferber, E., Meier, J., Herrera, N., Stapleton, J., Calkins, C., & Iverson, N. (2022). Detection of single walled carbon nanotube based sensors in a large mammal. *Nanomedicine: Nanotechnology, Biology and Medicine*, *40*, 102489. <https://doi.org/10.1016/j.nano.2021.102489>
- Hollstein, T., Basolo, A., Ando, T., Votruba, S. B., Krakoff, J., & Piaggi, P. (2020). Urinary Norepinephrine Is a Metabolic Determinant of 24-Hour Energy Expenditure and Sleeping Metabolic Rate in Adult Humans. *The Journal of Clinical Endocrinology and Metabolism*, *105*(4), 1145–1156. <https://doi.org/10.1210/clinem/dgaa047>
- Hoops, D., & Flores, C. (2017). Making Dopamine Connections in Adolescence. *Trends in Neurosciences*, *40*(12), 709–719. <https://doi.org/10.1016/j.tins.2017.09.004>
- Hoops, D., Reynolds, L. M., Restrepo-Lozano, J.-M., & Flores, C. (2018). Dopamine Development in the Mouse Orbital Prefrontal Cortex Is Protracted and Sensitive to Amphetamine in Adolescence. *eNeuro*, *5*(1), ENEURO.0372-17.2017. <https://doi.org/10.1523/ENEURO.0372-17.2017>
- Huang, Y.-Q., Wu, C., He, X.-F., Wu, D., He, X., Liang, F.-Y., Dai, G.-Y., Pei, Z., Xu, G.-Q., & Lan, Y. (2018). Effects of Voluntary Wheel-Running Types on Hippocampal Neurogenesis and Spatial Cognition in Middle-Aged Mice. *Frontiers in Cellular Neuroscience*, *12*. <https://doi.org/10.3389/fncel.2018.00177>
- Huang, Y.-Y., Simpson, E., Kellendonk, C., & Kandel, E. R. (2004). Genetic evidence for the bidirectional modulation of synaptic plasticity in the prefrontal cortex by D1 receptors. *Proceedings of the National Academy of Sciences of the United States of America*, *101*(9), 3236–3241. <https://doi.org/10.1073/pnas.0308280101>
- Hubbard, K. E., Wells, A., Owens, T. S., Tagen, M., Fraga, C. H., & Stewart, C. F. (2010). Determination of dopamine, serotonin, and their metabolites in pediatric cerebrospinal fluid by isocratic high performance liquid chromatography coupled with electrochemical

- detection. *Biomedical Chromatography: BMC*, 24(6), 626–631.
<https://doi.org/10.1002/bmc.1338>
- Huizinga, M., Dolan, C. V., & van der Molen, M. W. (2006). Age-related change in executive function: Developmental trends and a latent variable analysis. *Neuropsychologia*, 44(11), 2017–2036. <https://doi.org/10.1016/j.neuropsychologia.2006.01.010>
- Huttenlocher, P. R., & Dabholkar, A. S. (1997). Regional differences in synaptogenesis in human cerebral cortex. *The Journal of Comparative Neurology*, 387(2), 167–178.
[https://doi.org/10.1002/\(sici\)1096-9861\(19971020\)387:2<167::aid-cne1>3.0.co;2-z](https://doi.org/10.1002/(sici)1096-9861(19971020)387:2<167::aid-cne1>3.0.co;2-z)
- Iverson, N. M., Barone, P. W., Shandell, M., Trudel, L. J., Sen, S., Sen, F., Ivanov, V., Atolia, E., Farias, E., McNicholas, T. P., Reuel, N., Parry, N. M. A., Wogan, G. N., & Strano, M. S. (2013). In vivo biosensing via tissue-localizable near-infrared-fluorescent single-walled carbon nanotubes. *Nature Nanotechnology*, 8(11), Article 11.
<https://doi.org/10.1038/nnano.2013.222>
- Jain, A., Homayoun, A., Bannister, C. W., & Yum, K. (2015). Single-walled carbon nanotubes as near-infrared optical biosensors for life sciences and biomedicine. *Biotechnology Journal*, 10(3), 447–459. <https://doi.org/10.1002/biot.201400168>
- Jaquins-Gerstl, A., & Michael, A. C. (2015). A review of the effects of FSCV and microdialysis measurements on dopamine release in the surrounding tissue. *The Analyst*, 140(11), 3696–3708. <https://doi.org/10.1039/c4an02065k>
- Johnson, C. M., Loucks, F. A., Peckler, H., Thomas, A. W., Janak, P. H., & Wilbrecht, L. (2016). Long-range orbitofrontal and amygdala axons show divergent patterns of maturation in the frontal cortex across adolescence. *Developmental Cognitive Neuroscience*, 18, 113–120. <https://doi.org/10.1016/j.dcn.2016.01.005>
- Johnson, C., & Wilbrecht, L. (2011). Juvenile mice show greater flexibility in multiple choice reversal learning than adults. *Developmental Cognitive Neuroscience*, 1(4), 540–551.
<https://doi.org/10.1016/j.dcn.2011.05.008>
- Johnson, J. S., & Newport, E. L. (1989). Critical period effects in second language learning: The influence of maturational state on the acquisition of English as a second language. *Cognitive Psychology*, 21(1), 60–99. [https://doi.org/10.1016/0010-0285\(89\)90003-0](https://doi.org/10.1016/0010-0285(89)90003-0)
- Jose, P. A., Eisner, G. M., & Felder, R. A. (2003). Regulation of blood pressure by dopamine receptors. *Nephron. Physiology*, 95(2), p19-27. <https://doi.org/10.1159/000073676>
- Juwariah, T., Suhariadi, F., Soedirham, O., Priyanto, A., Setiyorini, E., Siskaningrum, A., Adhianata, H., & Fernandes, A. da C. (2022). Childhood adversities and mental health problems: A systematic review. *Journal of Public Health Research*, 11(3), 22799036221106613. <https://doi.org/10.1177/22799036221106613>
- Kalsbeek, A., Voorn, P., Buijs, R. M., Pool, C. W., & Uylings, H. B. (1988). Development of the dopaminergic innervation in the prefrontal cortex of the rat. *The Journal of Comparative Neurology*, 269(1), 58–72. <https://doi.org/10.1002/cne.902690105>
- Kang, W.-Y., Yang, Q., Jiang, X.-F., Chen, W., Zhang, L.-Y., Wang, X.-Y., Zhang, L.-N., Quinn, T. J., Liu, J., & Chen, S.-D. (2014). Salivary DJ-1 could be an indicator of Parkinson’s disease progression. *Frontiers in Aging Neuroscience*, 6, 102.
<https://doi.org/10.3389/fnagi.2014.00102>
- Kessler, R. C., McLaughlin, K. A., Green, J. G., Gruber, M. J., Sampson, N. A., Zaslavsky, A. M., Aguilar-Gaxiola, S., Alhamzawi, A. O., Alonso, J., Angermeyer, M., Benjet, C., Bromet, E., Chatterji, S., de Girolamo, G., Demyttenaere, K., Fayyad, J., Florescu, S., Gal, G., Gureje, O., ... Williams, D. R. (2010). Childhood adversities and adult

- psychopathology in the WHO World Mental Health Surveys. *The British Journal of Psychiatry*, 197(5), 378–385. <https://doi.org/10.1192/bjp.bp.110.080499>
- Kilpatrick, M., Church, E., Danish, S., Stiefel, M., Jaggi, J., Halpern, C., Kerr, M., Maloney, E., Robinson, M., Lucki, I., Krizman-Grenda, E., & Baltuch, G. (2010). Intracerebral microdialysis during deep brain stimulation surgery. *Journal of Neuroscience Methods*, 190(1), 106–111. <https://doi.org/10.1016/j.jneumeth.2010.04.013>
- Kim, H.-J., Cho, M.-H., Shim, W. H., Kim, J. K., Jeon, E.-Y., Kim, D.-H., & Yoon, S.-Y. (2017). Deficient autophagy in microglia impairs synaptic pruning and causes social behavioral defects. *Molecular Psychiatry*, 22(11), 1576–1584. <https://doi.org/10.1038/mp.2016.103>
- Kishida, K. T., Saez, I., Lohrenz, T., Witcher, M. R., Laxton, A. W., Tatter, S. B., White, J. P., Ellis, T. L., Phillips, P. E. M., & Montague, P. R. (2016). Subsecond dopamine fluctuations in human striatum encode superposed error signals about actual and counterfactual reward. *Proceedings of the National Academy of Sciences*, 113(1), 200–205. <https://doi.org/10.1073/pnas.1513619112>
- Klausberger, T., Roberts, J. D. B., & Somogyi, P. (2002). Cell type- and input-specific differences in the number and subtypes of synaptic GABA(A) receptors in the hippocampus. *The Journal of Neuroscience: The Official Journal of the Society for Neuroscience*, 22(7), 2513–2521. <https://doi.org/10.1523/JNEUROSCI.22-07-02513.2002>
- Kolb, B., Mychasiuk, R., Muhammad, A., Li, Y., Frost, D. O., & Gibb, R. (2012). Experience and the developing prefrontal cortex. *Proceedings of the National Academy of Sciences*, 109(supplement_2), 17186–17193. <https://doi.org/10.1073/pnas.1121251109>
- Koob, G. F. (1999). Corticotropin-releasing factor, norepinephrine, and stress. *Biological Psychiatry*, 46(9), 1167–1180. [https://doi.org/10.1016/s0006-3223\(99\)00164-x](https://doi.org/10.1016/s0006-3223(99)00164-x)
- Koss, W. A., Belden, C. E., Hristov, A. D., & Juraska, J. M. (2014). Dendritic remodeling in the adolescent medial prefrontal cortex and the basolateral amygdala of male and female rats. *Synapse*, 68(2), 61–72. <https://doi.org/10.1002/syn.21716>
- Kruss, S., Hilmer, A. J., Zhang, J., Reuel, N. F., Mu, B., & Strano, M. S. (2013). Carbon nanotubes as optical biomedical sensors. *Advanced Drug Delivery Reviews*, 65(15), 1933–1950. <https://doi.org/10.1016/j.addr.2013.07.015>
- Labouesse, M. A., Cola, R. B., & Patriarchi, T. (2020). GPCR-Based Dopamine Sensors—A Detailed Guide to Inform Sensor Choice for In Vivo Imaging. *International Journal of Molecular Sciences*, 21(21), 8048. <https://doi.org/10.3390/ijms21218048>
- Lamanna, J., Isotti, F., Ferro, M., Spadini, S., Racchetti, G., Musazzi, L., & Malgaroli, A. (2022). Occlusion of dopamine-dependent synaptic plasticity in the prefrontal cortex mediates the expression of depressive-like behavior and is modulated by ketamine. *Scientific Reports*, 12(1), 11055. <https://doi.org/10.1038/s41598-022-14694-w>
- Lambert, G., Johansson, M., Agren, H., & Friberg, P. (2000). Reduced brain norepinephrine and dopamine release in treatment-refractory depressive illness: Evidence in support of the catecholamine hypothesis of mood disorders. *Archives of General Psychiatry*, 57(8), 787–793. <https://doi.org/10.1001/archpsyc.57.8.787>
- Larsen, B., Cui, Z., Adebimpe, A., Pines, A., Alexander-Bloch, A., Bertolero, M., Calkins, M. E., Gur, R. E., Gur, R. C., Mahadevan, A. S., Moore, T. M., Roalf, D. R., Seidnitz, J., Sydnor, V. J., Wolf, D. H., & Satterthwaite, T. D. (2022). A developmental reduction of

- the excitation:inhibition ratio in association cortex during adolescence. *Science Advances*, 8(5), eabj8750. <https://doi.org/10.1126/sciadv.abj8750>
- Larsen, B., & Luna, B. (2015). In vivo evidence of neurophysiological maturation of the human adolescent striatum. *Developmental Cognitive Neuroscience*, 12, 74–85. <https://doi.org/10.1016/j.dcn.2014.12.003>
- Larsen, B., & Luna, B. (2018). Adolescence as a neurobiological critical period for the development of higher-order cognition. *Neuroscience & Biobehavioral Reviews*, 94, 179–195. <https://doi.org/10.1016/j.neubiorev.2018.09.005>
- Laubach, M., Amarante, L. M., Swanson, K., & White, S. R. (2018). What, If Anything, Is Rodent Prefrontal Cortex? *eNeuro*, 5(5), ENEURO.0315-18.2018. <https://doi.org/10.1523/ENEURO.0315-18.2018>
- Lebel, C., Walker, L., Leemans, A., Phillips, L., & Beaulieu, C. (2008). Microstructural maturation of the human brain from childhood to adulthood. *NeuroImage*, 40(3), 1044–1055. <https://doi.org/10.1016/j.neuroimage.2007.12.053>
- Lee, M. A., Wang, S., Jin, X., Bakh, N. A., Nguyen, F. T., Dong, J., Silmore, K. S., Gong, X., Pham, C., Jones, K. K., Muthupalani, S., Bisker, G., Son, M., & Strano, M. S. (2020). Implantable Nanosensors for Human Steroid Hormone Sensing In Vivo Using a Self-Templating Corona Phase Molecular Recognition. *Advanced Healthcare Materials*, 9(21), e2000429. <https://doi.org/10.1002/adhm.202000429>
- Lensjø, K. K., Lepperød, M. E., Dick, G., Hafting, T., & Fyhn, M. (2017). Removal of Perineuronal Nets Unlocks Juvenile Plasticity Through Network Mechanisms of Decreased Inhibition and Increased Gamma Activity. *The Journal of Neuroscience: The Official Journal of the Society for Neuroscience*, 37(5), 1269–1283. <https://doi.org/10.1523/JNEUROSCI.2504-16.2016>
- Lepow, L., Morishita, H., & Yehuda, R. (2021). Critical Period Plasticity as a Framework for Psychedelic-Assisted Psychotherapy. *Frontiers in Neuroscience*, 15. <https://doi.org/10.3389/fnins.2021.710004>
- Levelt, C. N., & Hübener, M. (2012). Critical-period plasticity in the visual cortex. *Annual Review of Neuroscience*, 35(Volume 35, 2012), 309–330. <https://doi.org/10.1146/annurev-neuro-061010-113813>
- Lewis, F. C., Reeve, R. A., Kelly, S. P., & Johnson, K. A. (2017). Evidence of substantial development of inhibitory control and sustained attention between 6 and 8 years of age on an unpredictable Go/No-Go task. *Journal of Experimental Child Psychology*, 157, 66–80. <https://doi.org/10.1016/j.jecp.2016.12.008>
- Li, D. C., Hinton, E. A., Guo, J., Knight, K. A., Sequeira, M. K., Wynne, M. E., Dighe, N. M., & Gourley, S. L. (2024). Social experience in adolescence shapes prefrontal cortex structure and function in adulthood. *Molecular Psychiatry*, 1–12. <https://doi.org/10.1038/s41380-024-02540-6>
- Li, X., Sun, H., Zhu, Y., Wang, F., Wang, X., Han, L., Cui, D., Luo, D., Zhai, Y., Zhuo, L., Xu, X., Yang, J., & Li, Y. (2022). Dysregulation of prefrontal parvalbumin interneurons leads to adult aggression induced by social isolation stress during adolescence. *Frontiers in Molecular Neuroscience*, 15, 1010152. <https://doi.org/10.3389/fnmol.2022.1010152>
- Li, Z., de Barros, A. L. B., Soares, D. C. F., Moss, S. N., & Alisaraie, L. (2017). Functionalized single-walled carbon nanotubes: Cellular uptake, biodistribution and applications in drug delivery. *International Journal of Pharmaceutics*, 524(1), 41–54. <https://doi.org/10.1016/j.ijpharm.2017.03.017>

- Lipner, E., O'Brien, K. J., Pike, M. R., Ered, A., & Ellman, L. M. (2023). Environmental Risk Factors and Cognitive Outcomes in Psychosis: Pre-, Perinatal, and Early Life Adversity. *Current Topics in Behavioral Neurosciences*, 63, 205–240. https://doi.org/10.1007/7854_2022_378
- Lipson, S. K., Zhou, S., Abelson, S., Heinze, J., Jirsa, M., Morigney, J., Patterson, A., Singh, M., & Eisenberg, D. (2022). Trends in college student mental health and help-seeking by race/ethnicity: Findings from the national healthy minds study, 2013-2021. *Journal of Affective Disorders*, 306, 138–147. <https://doi.org/10.1016/j.jad.2022.03.038>
- Liston, C., Watts, R., Tottenham, N., Davidson, M. C., Niogi, S., Ulug, A. M., & Casey, B. J. (2006). Frontostriatal microstructure modulates efficient recruitment of cognitive control. *Cerebral Cortex (New York, N.Y.: 1991)*, 16(4), 553–560. <https://doi.org/10.1093/cercor/bhj003>
- Liu, J., Liu, D., Pu, X., Zou, K., Xie, T., Li, Y., & Yao, H. (2023). The Secondary Motor Cortex-striatum Circuit Contributes to Suppressing Inappropriate Responses in Perceptual Decision Behavior. *Neuroscience Bulletin*, 39(10), 1544–1560. <https://doi.org/10.1007/s12264-023-01073-2>
- Liu, L., Li, Q., Li, N., Ling, J., Liu, R., Wang, Y., Sun, L., Chen, X. H., & Bi, K. (2011). Simultaneous determination of catecholamines and their metabolites related to Alzheimer's disease in human urine. *Journal of Separation Science*, 34(10), 1198–1204. <https://doi.org/10.1002/jssc.201000799>
- Liu, Y.-F., Chen, H., Wu, C.-L., Kuo, Y.-M., Yu, L., Huang, A.-M., Wu, F.-S., Chuang, J.-I., & Jen, C. J. (2009). Differential effects of treadmill running and wheel running on spatial or aversive learning and memory: Roles of amygdalar brain-derived neurotrophic factor and synaptotagmin I. *The Journal of Physiology*, 587(Pt 13), 3221–3231. <https://doi.org/10.1113/jphysiol.2009.173088>
- Lo, S. Q., Sng, J. C. G., & Augustine, G. J. (2017). Defining a critical period for inhibitory circuits within the somatosensory cortex. *Scientific Reports*, 7(1), 7271. <https://doi.org/10.1038/s41598-017-07400-8>
- Lohani, S., Martig, A. K., Deisseroth, K., Witten, I. B., & Moghaddam, B. (2019). Dopamine Modulation of Prefrontal Cortex Activity Is Manifold and Operates at Multiple Temporal and Spatial Scales. *Cell Reports*, 27(1), 99-114.e6. <https://doi.org/10.1016/j.celrep.2019.03.012>
- Lubec, J., Kalaba, P., Hussein, A. M., Feyissa, D. D., Kotob, M. H., Mahmmoud, R. R., Wieder, O., Garon, A., Sagheddu, C., Ilic, M., Dragačević, V., Cybulska-Klosowicz, A., Zehl, M., Wackerlig, J., Sartori, S. B., Ebner, K., Kouhnavardi, S., Roller, A., Gajic, N., ... Lubec, G. (2021). Reinstatement of synaptic plasticity in the aging brain through specific dopamine transporter inhibition. *Molecular Psychiatry*, 26(12), 7076–7090. <https://doi.org/10.1038/s41380-021-01214-x>
- Luciana, M., & Collins, P. F. (2022). Is Adolescence a Sensitive Period for the Development of Incentive-Reward Motivation? *Current Topics in Behavioral Neurosciences*, 53, 79–99. https://doi.org/10.1007/7854_2021_275
- Lucio Boschen, S., Trevathan, J., Hara, S. A., Asp, A., & Lujan, J. L. (2021). Defining a Path Toward the Use of Fast-Scan Cyclic Voltammetry in Human Studies. *Frontiers in Neuroscience*, 15. <https://doi.org/10.3389/fnins.2021.728092>

- Lukasiewicz, K., Baker, J. J., Zuo, Y., & Lu, J. (2021). Serotonergic Psychedelics in Neural Plasticity. *Frontiers in Molecular Neuroscience*, *14*.
<https://doi.org/10.3389/fnmol.2021.748359>
- Luna, B., Garver, K. E., Urban, T. A., Lazar, N. A., & Sweeney, J. A. (2004). Maturation of cognitive processes from late childhood to adulthood. *Child Development*, *75*(5), 1357–1372. <https://doi.org/10.1111/j.1467-8624.2004.00745.x>
- Luna, B., Marek, S., Larsen, B., Tervo-Clemmens, B., & Chahal, R. (2015). An Integrative Model of the Maturation of Cognitive Control. *Annual Review of Neuroscience*, *38*(Volume 38, 2015), 151–170. <https://doi.org/10.1146/annurev-neuro-071714-034054>
- Ly, C., Greb, A. C., Cameron, L. P., Wong, J. M., Barragan, E. V., Wilson, P. C., Burbach, K. F., Zarandi, S. S., Sood, A., Paddy, M. R., Duim, W. C., Dennis, M. Y., McAllister, A. K., Ori-McKenney, K. M., Gray, J. A., & Olson, D. E. (2018). Psychedelics Promote Structural and Functional Neural Plasticity. *Cell Reports*, *23*(11), 3170–3182.
<https://doi.org/10.1016/j.celrep.2018.05.022>
- Maggi, S., Peyrache, A., & Humphries, M. D. (2018). An ensemble code in medial prefrontal cortex links prior events to outcomes during learning. *Nature Communications*, *9*(1), 2204. <https://doi.org/10.1038/s41467-018-04638-2>
- Malave, L., van Dijk, M. T., & Anacker, C. (2022). Early life adversity shapes neural circuit function during sensitive postnatal developmental periods. *Translational Psychiatry*, *12*(1), 306. <https://doi.org/10.1038/s41398-022-02092-9>
- Mallya, A. P., Wang, H.-D., Lee, H. N. R., & Deutch, A. Y. (2019). Microglial Pruning of Synapses in the Prefrontal Cortex During Adolescence. *Cerebral Cortex (New York, N.Y.: 1991)*, *29*(4), 1634–1643. <https://doi.org/10.1093/cercor/bhy061>
- Manitt, C., Eng, C., Pokinko, M., Ryan, R. T., Torres-Berrío, A., Lopez, J. P., Yogendran, S. V., Daubaras, M. J. J., Grant, A., Schmidt, E. R. E., Tronche, F., Krimpenfort, P., Cooper, H. M., Pasterkamp, R. J., Kolb, B., Turecki, G., Wong, T. P., Nestler, E. J., Giros, B., & Flores, C. (2013). Dcc orchestrates the development of the prefrontal cortex during adolescence and is altered in psychiatric patients. *Translational Psychiatry*, *3*, e338.
<https://doi.org/10.1038/tp.2013.105>
- Manitt, C., Mimee, A., Eng, C., Pokinko, M., Stroh, T., Cooper, H. M., Kolb, B., & Flores, C. (2011a). The Netrin Receptor DCC Is Required in the Pubertal Organization of Mesocortical Dopamine Circuitry. *Journal of Neuroscience*, *31*(23), 8381–8394.
<https://doi.org/10.1523/JNEUROSCI.0606-11.2011>
- Marder, E. (2011). Variability, compensation, and modulation in neurons and circuits. *Proceedings of the National Academy of Sciences*, *108*(supplement_3), 15542–15548.
<https://doi.org/10.1073/pnas.1010674108>
- Markham, J. A., Morris, J. R., & Juraska, J. M. (2007). Neuron number decreases in the rat ventral, but not dorsal, medial prefrontal cortex between adolescence and adulthood. *Neuroscience*, *144*(3), 961–968. <https://doi.org/10.1016/j.neuroscience.2006.10.015>
- Marsh, R., Zhu, H., Schultz, R. T., Quackenbush, G., Royal, J., Skudlarski, P., & Peterson, B. S. (2006). A developmental fMRI study of self-regulatory control. *Human Brain Mapping*, *27*(11), 848–863. <https://doi.org/10.1002/hbm.20225>
- Martorana, A., & Koch, G. (2014). Is dopamine involved in Alzheimer's disease? *Frontiers in Aging Neuroscience*, *6*, 252. <https://doi.org/10.3389/fnagi.2014.00252>
- Mastwal, S., Ye, Y., Ren, M., Jimenez, D. V., Martinowich, K., Gerfen, C. R., & Wang, K. H. (2014). Phasic dopamine neuron activity elicits unique mesofrontal plasticity in

- adolescence. *The Journal of Neuroscience: The Official Journal of the Society for Neuroscience*, 34(29), 9484–9496. <https://doi.org/10.1523/JNEUROSCI.1114-14.2014>
- Matser, Y. A. H., Verly, I. R. N., van der Ham, M., de Sain-van der Velden, M. G. M., Verhoeven-Duif, N. M., Ash, S., Cangemi, G., Barco, S., Popovic, M. B., van Kuilenburg, A. B. P., Tytgat, G. A. M., & SIOPEX Catecholamine Working Group. (2023). Optimising urinary catecholamine metabolite diagnostics for neuroblastoma. *Pediatric Blood & Cancer*, 70(6), e30289. <https://doi.org/10.1002/pbc.30289>
- Matthyse, S. (1973). Antipsychotic drug actions: A clue to the neuropathology of schizophrenia? *Federation Proceedings*, 32(2), 200–205.
- McCutcheon, J. E., & Marinelli, M. (2009). Age matters. *The European Journal of Neuroscience*, 29(5), 997–1014. <https://doi.org/10.1111/j.1460-9568.2009.06648.x>
- Meunier, C. N. J., Chameau, P., & Fossier, P. M. (2017). Modulation of Synaptic Plasticity in the Cortex Needs to Understand All the Players. *Frontiers in Synaptic Neuroscience*, 9. <https://doi.org/10.3389/fnsyn.2017.00002>
- Mignini, F., Streccioni, V., & Amenta, F. (2003). Autonomic innervation of immune organs and neuroimmune modulation. *Autonomic & Autacoid Pharmacology*, 23(1), 1–25. <https://doi.org/10.1046/j.1474-8673.2003.00280.x>
- Moda-Sava, R. N., Murdock, M. H., Parekh, P. K., Fetcho, R. N., Huang, B. S., Huynh, T. N., Witzum, J., Shaver, D. C., Rosenthal, D. L., Alway, E. J., Lopez, K., Meng, Y., Nellissen, L., Grosenick, L., Milner, T. A., Deisseroth, K., Bito, H., Kasai, H., & Liston, C. (2019). Sustained rescue of prefrontal circuit dysfunction by antidepressant-induced spine formation. *Science (New York, N.Y.)*, 364(6436), eaat8078. <https://doi.org/10.1126/science.aat8078>
- Mohanta, D., Patnaik, S., Sood, S., & Das, N. (2019). Carbon nanotubes: Evaluation of toxicity at biointerfaces. *Journal of Pharmaceutical Analysis*, 9(5), 293–300. <https://doi.org/10.1016/j.jpha.2019.04.003>
- Moreno-Castilla, P., Pérez-Ortega, R., Violante-Soria, V., Balderas, I., & Bermúdez-Rattoni, F. (2017). Hippocampal release of dopamine and norepinephrine encodes novel contextual information. *Hippocampus*, 27(5), 547–557. <https://doi.org/10.1002/hipo.22711>
- Muller, T. H., Butler, J. L., Veselic, S., Miranda, B., Wallis, J. D., Dayan, P., Behrens, T. E. J., Kurth-Nelson, Z., & Kennerley, S. W. (2024). Distributional reinforcement learning in prefrontal cortex. *Nature Neuroscience*, 27(3), 403–408. <https://doi.org/10.1038/s41593-023-01535-w>
- Murray, A. M., Weihmueller, F. B., Marshall, J. F., Hurtig, H. I., Gottleib, G. L., & Joyce, J. N. (1995). Damage to dopamine systems differs between Parkinson’s disease and Alzheimer’s disease with parkinsonism. *Annals of Neurology*, 37(3), 300–312. <https://doi.org/10.1002/ana.410370306>
- Nabel, E. M., Garkun, Y., Koike, H., Sadahiro, M., Liang, A., Norman, K. J., Taccheri, G., Demars, M. P., Im, S., Caro, K., Lopez, S., Bateh, J., Hof, P. R., Clem, R. L., & Morishita, H. (2020). Adolescent frontal top-down neurons receive heightened local drive to establish adult attentional behavior in mice. *Nature Communications*, 11(1), 3983. <https://doi.org/10.1038/s41467-020-17787-0>
- Naneix, F., Marchand, A. R., Di Scala, G., Pape, J.-R., & Coutureau, E. (2012). Parallel maturation of goal-directed behavior and dopaminergic systems during adolescence. *The Journal of Neuroscience: The Official Journal of the Society for Neuroscience*, 32(46), 16223–16232. <https://doi.org/10.1523/JNEUROSCI.3080-12.2012>

- Nardou, R., Lewis, E. M., Rothhaas, R., Xu, R., Yang, A., Boyden, E., & Dölen, G. (2019). Oxytocin-dependent reopening of a social reward learning critical period with MDMA. *Nature*, *569*(7754), 116–120. <https://doi.org/10.1038/s41586-019-1075-9>
- Nardou, R., Sawyer, E., Song, Y. J., Wilkinson, M., Padovan-Hernandez, Y., de Deus, J. L., Wright, N., Lama, C., Faltin, S., Goff, L. A., Stein-O'Brien, G. L., & Dölen, G. (2023). Psychedelics reopen the social reward learning critical period. *Nature*, *618*(7966), 790–798. <https://doi.org/10.1038/s41586-023-06204-3>
- Natori, S., Yoshimi, K., Takahashi, T., Kagohashi, M., Oyama, G., Shimo, Y., Hattori, N., & Kitazawa, S. (2009). Subsecond reward-related dopamine release in the mouse dorsal striatum. *Neuroscience Research*, *63*(4), 267–272. <https://doi.org/10.1016/j.neures.2008.12.011>
- Nawrot, W., Drzozga, K., Baluta, S., Cabaj, J., & Malecha, K. (2018). A Fluorescent Biosensors for Detection Vital Body Fluids' Agents. *Sensors*, *18*(8), Article 8. <https://doi.org/10.3390/s18082357>
- Newport, E. L. (1990). Maturation constraints on language learning. *Cognitive Science*, *14*(1), 11–28. [https://doi.org/10.1016/0364-0213\(90\)90024-Q](https://doi.org/10.1016/0364-0213(90)90024-Q)
- Oh, W. C., Rodríguez, G., Asede, D., Jung, K., Hwang, I.-W., Ogelman, R., Bolton, M. M., & Kwon, H.-B. (2021). Dysregulation of the mesoprefrontal dopamine circuit mediates an early-life stress-induced synaptic imbalance in the prefrontal cortex. *Cell Reports*, *35*(5), 109074. <https://doi.org/10.1016/j.celrep.2021.109074>
- O'Leary, D. D., Ruff, N. L., & Dyck, R. H. (1994). Development, critical period plasticity, and adult reorganizations of mammalian somatosensory systems. *Current Opinion in Neurobiology*, *4*(4), 535–544. [https://doi.org/10.1016/0959-4388\(94\)90054-x](https://doi.org/10.1016/0959-4388(94)90054-x)
- Ong, L.-C., Chung, F. F.-L., Tan, Y.-F., & Leong, C.-O. (2016). Toxicity of single-walled carbon nanotubes. *Archives of Toxicology*, *90*(1), 103–118. <https://doi.org/10.1007/s00204-014-1376-6>
- Opara, I., Weissinger, G. M., Lardier, D. T., Lanier, Y., Carter, S., & Brawner, B. M. (2021). Mental Health Burden among Black Adolescents: The Need for Better Assessment, Diagnosis and Treatment Engagement. *Social Work in Mental Health*, *19*(2), 88–104. <https://doi.org/10.1080/15332985.2021.1879345>
- Ordaz, S. J., Foran, W., Velanova, K., & Luna, B. (2013). Longitudinal Growth Curves of Brain Function Underlying Inhibitory Control through Adolescence. *Journal of Neuroscience*, *33*(46), 18109–18124. <https://doi.org/10.1523/JNEUROSCI.1741-13.2013>
- Orhan, F., Goiny, M., Becklén, M., Mathé, L., Piehl, F., Schwieler, L., Fatouros-Bergman, H., Farde, L., Cervenka, S., Sellgren, C. M., Engberg, G., & Erhardt, S. (2023). CSF dopamine is elevated in first-episode psychosis and associates to symptom severity and cognitive performance. *Schizophrenia Research*, *257*, 34–40. <https://doi.org/10.1016/j.schres.2023.05.012>
- Otani, S., Bai, J., & Blot, K. (2015). Dopaminergic modulation of synaptic plasticity in rat prefrontal neurons. *Neuroscience Bulletin*, *31*(2), 183–190. <https://doi.org/10.1007/s12264-014-1507-3>
- Ott, T., & Nieder, A. (2019). Dopamine and Cognitive Control in Prefrontal Cortex. *Trends in Cognitive Sciences*, *23*(3), 213–234. <https://doi.org/10.1016/j.tics.2018.12.006>
- Ottenheimer, D. J., Hjort, M. M., Bowen, A. J., Steinmetz, N. A., & Stuber, G. D. (2023). A stable, distributed code for cue value in mouse cortex during reward learning. *eLife*, *12*, RP84604. <https://doi.org/10.7554/eLife.84604>

- Pachitariu, M., Stringer, C., Dipoppa, M., Schröder, S., Rossi, L. F., Dagleish, H., Carandini, M., & Harris, K. D. (2017). *Suite2p: Beyond 10,000 neurons with standard two-photon microscopy* (p. 061507). bioRxiv. <https://doi.org/10.1101/061507>
- Packer, A. M., & Yuste, R. (2011). Dense, unspecific connectivity of neocortical parvalbumin-positive interneurons: A canonical microcircuit for inhibition? *The Journal of Neuroscience: The Official Journal of the Society for Neuroscience*, *31*(37), 13260–13271. <https://doi.org/10.1523/JNEUROSCI.3131-11.2011>
- Pagana, K. D., Pagana, T. J., & Pagana, T. N. (2015). *Mosby's diagnostic and laboratory test reference* (Twelfth edition). Elsevier. <https://www.clinicalkey.com/nursing/dura/browse/bookChapter/3-s2.0-C20120030694>
- Pancholi, R., Ryan, L., & Peron, S. (2023). Learning in a sensory cortical microstimulation task is associated with elevated representational stability. *Nature Communications*, *14*(1), 3860. <https://doi.org/10.1038/s41467-023-39542-x>
- Parthasarathy, A., Herikstad, R., Bong, J. H., Medina, F. S., Libedinsky, C., & Yen, S.-C. (2017). Mixed selectivity morphs population codes in prefrontal cortex. *Nature Neuroscience*, *20*(12), 1770–1779. <https://doi.org/10.1038/s41593-017-0003-2>
- Paslawski, W., Khosousi, S., Hertz, E., Markaki, I., Boxer, A., & Svenningsson, P. (2023). Large-scale proximity extension assay reveals CSF midkine and DOPA decarboxylase as supportive diagnostic biomarkers for Parkinson's disease. *Translational Neurodegeneration*, *12*(1), 42. <https://doi.org/10.1186/s40035-023-00374-w>
- Patriarchi, T., Cho, J. R., Merten, K., Howe, M. W., Marley, A., Xiong, W.-H., Folk, R. W., Broussard, G. J., Liang, R., Jang, M. J., Zhong, H., Dombek, D., von Zastrow, M., Nimmerjahn, A., Gradinaru, V., Williams, J. T., & Tian, L. (2018). Ultrafast neuronal imaging of dopamine dynamics with designed genetically encoded sensors. *Science (New York, N.Y.)*, *360*(6396), eaat4422. <https://doi.org/10.1126/science.aat4422>
- Pattwell, S. S., Bath, K. G., Casey, B. J., Ninan, I., & Lee, F. S. (2011). Selective early-acquired fear memories undergo temporary suppression during adolescence. *Proceedings of the National Academy of Sciences*, *108*(3), 1182–1187. <https://doi.org/10.1073/pnas.1012975108>
- Paus, T., Keshavan, M., & Giedd, J. N. (2008). Why do many psychiatric disorders emerge during adolescence? *Nature Reviews. Neuroscience*, *9*(12), 947–957. <https://doi.org/10.1038/nrn2513>
- Pavāl, D. (2017). A Dopamine Hypothesis of Autism Spectrum Disorder. *Developmental Neuroscience*, *39*(5), 355–360. <https://doi.org/10.1159/000478725>
- Penfield, W., & Roberts, L. (2014). *Speech and Brain Mechanisms*. Princeton University Press.
- Perrin, J. S., Hervé, P.-Y., Leonard, G., Perron, M., Pike, G. B., Pitiot, A., Richer, L., Veillette, S., Pausova, Z., & Paus, T. (2008). Growth of white matter in the adolescent brain: Role of testosterone and androgen receptor. *The Journal of Neuroscience: The Official Journal of the Society for Neuroscience*, *28*(38), 9519–9524. <https://doi.org/10.1523/JNEUROSCI.1212-08.2008>
- Perrin, J. S., Leonard, G., Perron, M., Pike, G. B., Pitiot, A., Richer, L., Veillette, S., Pausova, Z., & Paus, T. (2009). Sex differences in the growth of white matter during adolescence. *NeuroImage*, *45*(4), 1055–1066. <https://doi.org/10.1016/j.neuroimage.2009.01.023>
- Petanjek, Z., Judaš, M., Šimic, G., Rasin, M. R., Uylings, H. B. M., Rakic, P., & Kostovic, I. (2011). Extraordinary neoteny of synaptic spines in the human prefrontal cortex.

- Proceedings of the National Academy of Sciences of the United States of America*, 108(32), 13281–13286. <https://doi.org/10.1073/pnas.1105108108>
- Peters, A. J., Marica, A.-M., Fabre, J. M. J., Harris, K. D., & Carandini, M. (2022). Visuomotor learning promotes visually evoked activity in the medial prefrontal cortex. *Cell Reports*, 41(3), 111487. <https://doi.org/10.1016/j.celrep.2022.111487>
- Peters, K. Z., & Naneix, F. (2022). The role of dopamine and endocannabinoid systems in prefrontal cortex development: Adolescence as a critical period. *Frontiers in Neural Circuits*, 16, 939235. <https://doi.org/10.3389/fncir.2022.939235>
- Piekarski, D. J., Boivin, J. R., & Wilbrecht, L. (2017). Ovarian Hormones Organize the Maturation of Inhibitory Neurotransmission in the Frontal Cortex at Puberty Onset in Female Mice. *Current Biology: CB*, 27(12), 1735-1745.e3. <https://doi.org/10.1016/j.cub.2017.05.027>
- Piekarski, D. J., Johnson, C., Boivin, J. R., Thomas, A. W., Lin, W. C., Delevich, K., Galarce, E., & Wilbrecht, L. (2017). Does puberty mark a transition in sensitive periods for plasticity in the associative neocortex? *Brain Research*, 1654(Pt B), 123–144. <https://doi.org/10.1016/j.brainres.2016.08.042>
- Pignatelli, M., & Bonci, A. (2015). Role of Dopamine Neurons in Reward and Aversion: A Synaptic Plasticity Perspective. *Neuron*, 86(5), 1145–1157. <https://doi.org/10.1016/j.neuron.2015.04.015>
- Pinkston, J. W., & Lamb, R. J. (2011). Delay discounting in C57BL/6J and DBA/2J mice: Adolescent-limited and life-persistent patterns of impulsivity. *Behavioral Neuroscience*, 125(2), 194–201. <https://doi.org/10.1037/a0022919>
- Pnevmatikakis, E. A., & Giovannucci, A. (2017). NoRMCorre: An online algorithm for piecewise rigid motion correction of calcium imaging data. *Journal of Neuroscience Methods*, 291, 83–94. <https://doi.org/10.1016/j.jneumeth.2017.07.031>
- Pollmann, A., Fritz, J., Barker, E., & Fuhrmann, D. (2023). Networks of Adversity in Childhood and Adolescence and Their Relationship to Adult Mental Health. *Research on Child and Adolescent Psychopathology*, 51(12), 1769–1784. <https://doi.org/10.1007/s10802-022-00976-4>
- Pöplau, J. A., Schwarze, T., Dorofeikova, M., Pochinok, I., Günther, A., Marquardt, A., & Hanganu-Opatz, I. L. (2023). Reorganization of adolescent prefrontal cortex circuitry is required for mouse cognitive maturation. *Neuron*, S089662732300805X. <https://doi.org/10.1016/j.neuron.2023.10.024>
- Post, M. R., & Sulzer, D. (2021). The chemical tools for imaging dopamine release. *Cell Chemical Biology*, 28(6), 748–764. <https://doi.org/10.1016/j.chembiol.2021.04.005>
- Pouille, F., & Scanziani, M. (2001). Enforcement of Temporal Fidelity in Pyramidal Cells by Somatic Feed-Forward Inhibition. *Science*, 293(5532), 1159–1163. <https://doi.org/10.1126/science.1060342>
- Price, R. B., Tervo-Clemmens, B. C., Panny, B., Degutis, M., Griffio, A., & Woody, M. (2021). Biobehavioral correlates of an fMRI index of striatal tissue iron in depressed patients. *Translational Psychiatry*, 11(1), 1–8. <https://doi.org/10.1038/s41398-021-01553-x>
- Puig, M. V., Antzoulatos, E. G., & Miller, E. K. (2014). Prefrontal Dopamine in Associative Learning and Memory. *Neuroscience*, 282, 217–229. <https://doi.org/10.1016/j.neuroscience.2014.09.026>
- Quast, K. B., Reh, R. K., Caiati, M. D., Kopell, N., McCarthy, M. M., & Hensch, T. K. (2023). Rapid synaptic and gamma rhythm signature of mouse critical period plasticity.

- Proceedings of the National Academy of Sciences*, 120(2), e2123182120.
<https://doi.org/10.1073/pnas.2123182120>
- RANDRUP, A., I, M., R, F., J, G., L, M., B, K., & J, S. K. (1975). MANIA, DEPRESSION, AND BRAIN DOPAMINE. *MANIA, DEPRESSION, AND BRAIN DOPAMINE*.
- Ranjbar-Slamloo, Y., & Fazlali, Z. (2019). Dopamine and Noradrenaline in the Brain; Overlapping or Dissociate Functions? *Frontiers in Molecular Neuroscience*, 12, 334.
<https://doi.org/10.3389/fnmol.2019.00334>
- Rasras, S., Kalantari, H., Rezaei, M., Dehghani, M. A., Zeidooni, L., Alikarami, K., Dehghani, F., & Alboghobeish, S. (2019). Single-walled and multiwalled carbon nanotubes induce oxidative stress in isolated rat brain mitochondria. *Toxicology and Industrial Health*, 35(7), 497–506. <https://doi.org/10.1177/0748233719856983>
- Ravariu, C. (2023). From Enzymatic Dopamine Biosensors to OECT Biosensors of Dopamine. *Biosensors*, 13(8), Article 8. <https://doi.org/10.3390/bios13080806>
- Ravindranath, O., Calabro, F. J., Foran, W., & Luna, B. (2022). Pubertal development underlies optimization of inhibitory control through specialization of ventrolateral prefrontal cortex. *Developmental Cognitive Neuroscience*, 58, 101162.
<https://doi.org/10.1016/j.dcn.2022.101162>
- Ray, P., & Steckl, A. J. (2019). Label-Free Optical Detection of Multiple Biomarkers in Sweat, Plasma, Urine, and Saliva. *ACS Sensors*, 4(5), 1346–1357.
<https://doi.org/10.1021/acssensors.9b00301>
- Reinert, S., Hübener, M., Bonhoeffer, T., & Goltstein, P. M. (2021). Mouse prefrontal cortex represents learned rules for categorization. *Nature*, 593(7859), Article 7859.
<https://doi.org/10.1038/s41586-021-03452-z>
- Reneman, L., van der Pluijm, M., Schranter, A., & van de Giessen, E. (2021). Imaging of the dopamine system with focus on pharmacological MRI and neuromelanin imaging. *European Journal of Radiology*, 140, 109752.
<https://doi.org/10.1016/j.ejrad.2021.109752>
- Reynolds, L. M., & Flores, C. (2021). Mesocorticolimbic Dopamine Pathways Across Adolescence: Diversity in Development. *Frontiers in Neural Circuits*, 15, 735625.
<https://doi.org/10.3389/fncir.2021.735625>
- Reynolds, L. M., Makowski, C. S., Yogendran, S. V., Kiessling, S., Cermakian, N., & Flores, C. (2015). Amphetamine in Adolescence Disrupts the Development of Medial Prefrontal Cortex Dopamine Connectivity in a dcc-Dependent Manner. *Neuropsychopharmacology*, 40(5), 1101–1112. <https://doi.org/10.1038/npp.2014.287>
- Reynolds, L. M., Pokinko, M., Torres Berrío, A., Cuesta, S., Lambert, L. C., Del Cid Pellitero, E., Wodzinski, M., Manitt, C., Krimpenfort, P., Kolb, B., & Flores, C. (2018). DCC receptors drive prefrontal cortex maturation by determining dopamine axon targeting in adolescence. *Biological Psychiatry*, 83(2), 181–192.
<https://doi.org/10.1016/j.biopsych.2017.06.009>
- Reynolds, L. M., Yetnikoff, L., Pokinko, M., Wodzinski, M., Epelbaum, J. G., Lambert, L. C., Cossette, M.-P., Arvanitogiannis, A., & Flores, C. (2019). Early Adolescence is a Critical Period for the Maturation of Inhibitory Behavior. *Cerebral Cortex (New York, N.Y.: 1991)*, 29(9), 3676–3686. <https://doi.org/10.1093/cercor/bhy247>
- Rigotti, M., Barak, O., Warden, M. R., Wang, X.-J., Daw, N. D., Miller, E. K., & Fusi, S. (2013). The importance of mixed selectivity in complex cognitive tasks. *Nature*, 497(7451), Article 7451. <https://doi.org/10.1038/nature12160>

- Rommelfanger, K. S., & Weinshenker, D. (2007). Norepinephrine: The redheaded stepchild of Parkinson's disease. *Biochemical Pharmacology*, *74*(2), 177–190. <https://doi.org/10.1016/j.bcp.2007.01.036>
- Rubí, B., & Maechler, P. (2010). Minireview: New roles for peripheral dopamine on metabolic control and tumor growth: let's seek the balance. *Endocrinology*, *151*(12), 5570–5581. <https://doi.org/10.1210/en.2010-0745>
- Salkoff, D. B., Zaghera, E., McCarthy, E., & McCormick, D. A. (2020). Movement and Performance Explain Widespread Cortical Activity in a Visual Detection Task. *Cerebral Cortex (New York, NY)*, *30*(1), 421–437. <https://doi.org/10.1093/cercor/bhz206>
- Sánchez-Soto, M., Bonifazi, A., Cai, N. S., Ellenberger, M. P., Newman, A. H., Ferré, S., & Yano, H. (2016). Evidence for Noncanonical Neurotransmitter Activation: Norepinephrine as a Dopamine D2-Like Receptor Agonist. *Molecular Pharmacology*, *89*(4), 457–466. <https://doi.org/10.1124/mol.115.101808>
- Santana, N., Mengod, G., & Artigas, F. (2009). Quantitative analysis of the expression of dopamine D1 and D2 receptors in pyramidal and GABAergic neurons of the rat prefrontal cortex. *Cerebral Cortex (New York, N.Y.: 1991)*, *19*(4), 849–860. <https://doi.org/10.1093/cercor/bhn134>
- Santonocito, R., Tuccitto, N., Pappalardo, A., & Trusso Sfrassetto, G. (2022). Smartphone-Based Dopamine Detection by Fluorescent Supramolecular Sensor. *Molecules*, *27*(21), Article 21. <https://doi.org/10.3390/molecules27217503>
- Savransky, A., Chiappelli, J., Du, X., Carino, K., Kvarata, M., Bruce, H., Kochunov, P., Goldwasser, E., Tan, Y., Hare, S., & Hong, L. E. (2021). Association of working memory and elevated overnight urinary norepinephrine in patients with schizophrenia. *Journal of Psychiatric Research*, *137*, 89–95. <https://doi.org/10.1016/j.jpsychires.2021.02.005>
- Scheinin, M., Seppala, T., Koulu, M., & Linnoila, M. (1984). Determination of conjugated dopamine in cerebrospinal fluid from humans and non-human primates with high performance liquid chromatography using electrochemical detection. *Acta Pharmacologica Et Toxicologica*, *55*(2), 88–94. <https://doi.org/10.1111/j.1600-0773.1984.tb01967.x>
- Schultz, W. (1998). Predictive Reward Signal of Dopamine Neurons. *Journal of Neurophysiology*, *80*(1), 1–27. <https://doi.org/10.1152/jn.1998.80.1.1>
- Seah, D., Cheng, Z., & Vendrell, M. (2023). Fluorescent Probes for Imaging in Humans: Where Are We Now? *ACS Nano*, *17*(20), 19478–19490. <https://doi.org/10.1021/acsnano.3c03564>
- Selemon, L. D. (2013). A role for synaptic plasticity in the adolescent development of executive function. *Translational Psychiatry*, *3*(3), e238–e238. <https://doi.org/10.1038/tp.2013.7>
- Senel, M., Dervisevic, E., Alhassen, S., Dervisevic, M., Alachkar, A., Cadarso, V. J., & Voelcker, N. H. (2020). Microfluidic Electrochemical Sensor for Cerebrospinal Fluid and Blood Dopamine Detection in a Mouse Model of Parkinson's Disease. *Analytical Chemistry*, *92*(18), 12347–12355. <https://doi.org/10.1021/acs.analchem.0c02032>
- Shao, L.-X., Liao, C., Gregg, I., Davoudian, P. A., Savalia, N. K., Delagarza, K., & Kwan, A. C. (2021). Psilocybin induces rapid and persistent growth of dendritic spines in frontal cortex in vivo. *Neuron*, *109*(16), 2535–2544.e4. <https://doi.org/10.1016/j.neuron.2021.06.008>

- Sheynikhovich, D., Otani, S., Bai, J., & Arleo, A. (2022). Long-term memory, synaptic plasticity and dopamine in rodent medial prefrontal cortex: Role in executive functions. *Frontiers in Behavioral Neuroscience*, *16*, 1068271. <https://doi.org/10.3389/fnbeh.2022.1068271>
- Shi, Y., Pang, Y., Huang, N., Sun, C., Pan, Y., Cheng, Y., Long, Y., & Zheng, H. (2019). Competitive method for fluorescent dopamine detection in cerebrospinal fluid based on the peroxidase-like activity of ficin. *Spectrochimica Acta Part A: Molecular and Biomolecular Spectroscopy*, *209*, 8–13. <https://doi.org/10.1016/j.saa.2018.10.033>
- Siegenthaler, J. R., Gushiken, B. C., Hill, D. F., Cowen, S. L., & Heien, M. L. (2020). Moving Fast-Scan Cyclic Voltammetry toward FDA Compliance with Capacitive Decoupling Patient Protection. *ACS Sensors*, *5*(7), 1890–1899. <https://doi.org/10.1021/acssensors.9b02249>
- Silva, P. N. de. (2018). Do patterns of synaptic pruning underlie psychoses, autism and ADHD? *BJPsych Advances*, *24*(3), 212–217. <https://doi.org/10.1192/bja.2017.27>
- Simmonds, D. J., Pekar, J. J., & Mostofsky, S. H. (2008). Meta-analysis of Go/No-go tasks demonstrating that fMRI activation associated with response inhibition is task-dependent. *Neuropsychologia*, *46*(1), 224–232. <https://doi.org/10.1016/j.neuropsychologia.2007.07.015>
- Simon, N. W., Gregory, T. A., Wood, J., & Moghaddam, B. (2013). Differences in response initiation and behavioral flexibility between adolescent and adult rats. *Behavioral Neuroscience*, *127*(1), 23–32. <https://doi.org/10.1037/a0031328>
- Siniscalchi, M. J., Phoumthipphavong, V., Ali, F., Lozano, M., & Kwan, A. C. (2016). Fast and slow transitions in frontal ensemble activity during flexible sensorimotor behavior. *Nature Neuroscience*, *19*(9), 1234–1242. <https://doi.org/10.1038/nn.4342>
- Siniscalchi, M. J., Wang, H., & Kwan, A. C. (2019). Enhanced Population Coding for Rewarded Choices in the Medial Frontal Cortex of the Mouse. *Cerebral Cortex*, *29*(10), 4090–4106. <https://doi.org/10.1093/cercor/bhy292>
- Smith, A. M., Mancini, M. C., & Nie, S. (2009). Bioimaging: Second window for in vivo imaging. *Nature Nanotechnology*, *4*(11), 710–711. <https://doi.org/10.1038/nnano.2009.326>
- Sohal, V. S., Zhang, F., Yizhar, O., & Deisseroth, K. (2009). Parvalbumin neurons and gamma rhythms enhance cortical circuit performance. *Nature*, *459*(7247), 698–702. <https://doi.org/10.1038/nature07991>
- Sokolov, A. V., Aseychev, A. V., Kostevich, V. A., Gusev, A. A., Gusev, S. A., & Vlasova, I. I. (2011). Functionalization of single-walled carbon nanotubes regulates their effect on hemostasis. *Journal of Physics: Conference Series*, *291*, 012054. <https://doi.org/10.1088/1742-6596/291/1/012054>
- Somerville, L. H., Hare, T., & Casey, B. J. (2011). Frontostriatal maturation predicts cognitive control failure to appetitive cues in adolescents. *Journal of Cognitive Neuroscience*, *23*(9), 2123–2134. <https://doi.org/10.1162/jocn.2010.21572>
- Son, M., Mehra, P., Nguyen, F. T., Jin, X., Koman, V. B., Gong, X., Lee, M. A., Bakh, N. A., & Strano, M. S. (2023). Molecular Recognition and In Vivo Detection of Temozolomide and 5-Aminoimidazole-4-carboxamide for Glioblastoma Using Near-Infrared Fluorescent Carbon Nanotube Sensors. *ACS Nano*, *17*(1), 240–250. <https://doi.org/10.1021/acsnano.2c07264>

- Southwell, D. G., Froemke, R. C., Alvarez-Buylla, A., Stryker, M. P., & Gandhi, S. P. (2010). Cortical Plasticity Induced by Inhibitory Neuron Transplantation. *Science (New York, N.Y.)*, 327(5969), 1145–1148. <https://doi.org/10.1126/science.1183962>
- Sowell, E. R., Peterson, B. S., Thompson, P. M., Welcome, S. E., Henkenius, A. L., & Toga, A. W. (2003). Mapping cortical change across the human life span. *Nature Neuroscience*, 6(3), 309–315. <https://doi.org/10.1038/nn1008>
- Sturman, D. A., Mandell, D. R., & Moghaddam, B. (2010). Adolescents exhibit behavioral differences from adults during instrumental learning and extinction. *Behavioral Neuroscience*, 124(1), 16–25. <https://doi.org/10.1037/a0018463>
- Sun, F., Zeng, J., Jing, M., Zhou, J., Feng, J., Owen, S. F., Luo, Y., Li, F., Wang, H., Yamaguchi, T., Yong, Z., Gao, Y., Peng, W., Wang, L., Zhang, S., Du, J., Lin, D., Xu, M., Kreitzer, A. C., ... Li, Y. (2018). A Genetically Encoded Fluorescent Sensor Enables Rapid and Specific Detection of Dopamine in Flies, Fish, and Mice. *Cell*, 174(2), 481–496.e19. <https://doi.org/10.1016/j.cell.2018.06.042>
- Takase, M., Kimura, H., Kanahara, N., Nakata, Y., & Iyo, M. (2020). Plasma monoamines change under dopamine supersensitivity psychosis in patients with schizophrenia: A comparison with first-episode psychosis. *Journal of Psychopharmacology (Oxford, England)*, 34(5), 540–547. <https://doi.org/10.1177/0269881119900982>
- Takesian, A. E., Bogart, L. J., Lichtman, J. W., & Hensch, T. K. (2018). Inhibitory circuit gating of auditory critical-period plasticity. *Nature Neuroscience*, 21(2), 218–227. <https://doi.org/10.1038/s41593-017-0064-2>
- Tang, Y., Stryker, M. P., Alvarez-Buylla, A., & Espinosa, J. S. (2014). Cortical plasticity induced by transplantation of embryonic somatostatin or parvalbumin interneurons. *Proceedings of the National Academy of Sciences of the United States of America*, 111(51), 18339–18344. <https://doi.org/10.1073/pnas.1421844112>
- Tank, A. W., & Lee Wong, D. (2015). Peripheral and central effects of circulating catecholamines. *Comprehensive Physiology*, 5(1), 1–15. <https://doi.org/10.1002/cphy.c140007>
- Tarazi, F. I., & Baldessarini, R. J. (2000). Comparative postnatal development of dopamine D(1), D(2) and D(4) receptors in rat forebrain. *International Journal of Developmental Neuroscience: The Official Journal of the International Society for Developmental Neuroscience*, 18(1), 29–37. [https://doi.org/10.1016/s0736-5748\(99\)00108-2](https://doi.org/10.1016/s0736-5748(99)00108-2)
- Taylor, I. M., Nesbitt, K. M., Walters, S. H., Varner, E. L., Shu, Z., Bartlow, K. M., Jaquins-Gerstl, A. S., & Michael, A. C. (2015). Kinetic diversity of dopamine transmission in the dorsal striatum. *Journal of Neurochemistry*, 133(4), 522–531. <https://doi.org/10.1111/jnc.13059>
- Toyoizumi, T., Miyamoto, H., Yazaki-Sugiyama, Y., Atapour, N., Hensch, T. K., & Miller, K. D. (2013). A Theory of the Transition to Critical Period Plasticity: Inhibition Selectively Suppresses Spontaneous Activity. *Neuron*, 80(1), 51–63. <https://doi.org/10.1016/j.neuron.2013.07.022>
- Tseng, K. Y., & O'Donnell, P. (2005). Post-pubertal Emergence of Prefrontal Cortical Up States Induced by D1–NMDA Co-activation. *Cerebral Cortex*, 15(1), 49–57. <https://doi.org/10.1093/cercor/bhh107>
- Tseng, K.-Y., & O'Donnell, P. (2007). Dopamine modulation of prefrontal cortical interneurons changes during adolescence. *Cerebral Cortex (New York, N.Y.: 1991)*, 17(5), 1235–1240. <https://doi.org/10.1093/cercor/bhl034>

- Ungerstedt, U. (1971). Adipsia and aphagia after 6-hydroxydopamine induced degeneration of the nigro-striatal dopamine system. *Acta Physiologica Scandinavica. Supplementum*, 367, 95–122. <https://doi.org/10.1111/j.1365-201x.1971.tb11001.x>
- Unsworth, N., & Robison, M. K. (2017). A locus coeruleus-norepinephrine account of individual differences in working memory capacity and attention control. *Psychonomic Bulletin & Review*, 24(4), 1282–1311. <https://doi.org/10.3758/s13423-016-1220-5>
- van de Laar, M. C., van den Wildenberg, W. P. M., van Boxtel, G. J. M., & van der Molen, M. W. (2014). Development of response activation and inhibition in a selective stop-signal task. *Biological Psychology*, 102, 54–67. <https://doi.org/10.1016/j.biopsycho.2014.06.003>
- van der Schaaf, M. E., Warmerdam, E., Crone, E. A., & Cools, R. (2011). Distinct linear and non-linear trajectories of reward and punishment reversal learning during development: Relevance for dopamine's role in adolescent decision making. *Developmental Cognitive Neuroscience*, 1(4), 578–590. <https://doi.org/10.1016/j.dcn.2011.06.007>
- Vandenberg, A., Piekarski, D. J., Caporale, N., Munoz-Cuevas, F. J., & Wilbrecht, L. (2015). Adolescent maturation of inhibitory inputs onto cingulate cortex neurons is cell-type specific and TrkB dependent. *Frontiers in Neural Circuits*, 9, 5. <https://doi.org/10.3389/fncir.2015.00005>
- Vander Weele, C. M., Siciliano, C. A., Matthews, G. A., Namburi, P., Izadmehr, E. M., Espinel, I. C., Nieh, E. H., Schut, E. H. S., Padilla-Coreano, N., Burgos-Robles, A., Chang, C.-J., Kimchi, E. Y., Beyeler, A., Wichmann, R., Wildes, C. P., & Tye, K. M. (2018). Dopamine enhances signal-to-noise ratio in cortical-brainstem encoding of aversive stimuli. *Nature*, 563(7731), 397–401. <https://doi.org/10.1038/s41586-018-0682-1>
- Vassilev, P., Pantoja-Urban, A. H., Giroux, M., Nouel, D., Hernandez, G., Orsini, T., & Flores, C. (2021). Unique effects of social defeat stress in adolescent male mice on the Netrin-1/DCC pathway, prefrontal cortex dopamine and cognition (Social stress in adolescent vs. Adult male mice). *eNeuro*, 8(2), ENEURO.0045-21.2021. <https://doi.org/10.1523/ENEURO.0045-21.2021>
- Verly, I. R. N., Leen, R., Meinsma, J. R., Hooijer, G. K. J., Savci-Heijink, C. D., van Nes, J., Broekmans, M., Wanders, R. J. A., van Kuilenburg, A. B. P., & Tytgat, G. a. M. (2019). Catecholamine excretion profiles identify clinical subgroups of neuroblastoma patients. *European Journal of Cancer (Oxford, England: 1990)*, 111, 21–29. <https://doi.org/10.1016/j.ejca.2019.01.014>
- Vermeiren, Y., Hirschberg, Y., Mertens, I., & De Deyn, P. P. (2020). Biofluid Markers for Prodromal Parkinson's Disease: Evidence From a Catecholaminergic Perspective. *Frontiers in Neurology*, 11, 595. <https://doi.org/10.3389/fneur.2020.00595>
- Vosberg, D. E., Leyton, M., & Flores, C. (2020). The Netrin-1/DCC guidance system: Dopamine pathway maturation and psychiatric disorders emerging in adolescence. *Molecular Psychiatry*, 25(2), 297–307. <https://doi.org/10.1038/s41380-019-0561-7>
- Wahlstrom, D., Collins, P., White, T., & Luciana, M. (2010). Developmental changes in dopamine neurotransmission in adolescence: Behavioral implications and issues in assessment. *Brain and Cognition*, 72(1), 146–159. <https://doi.org/10.1016/j.bandc.2009.10.013>
- Wang, G., Zhou, H.-H., Luo, L., Qin, L.-Q., Yin, J., Yu, Z., Zhang, L., & Wan, Z. (2021). Voluntary wheel running is capable of improving cognitive function only in the young but not the middle-aged male APPSwe/PS1De9 mice. *Neurochemistry International*, 145, 105010. <https://doi.org/10.1016/j.neuint.2021.105010>

- Wang, H., Ortega, H. K., Atilgan, H., Murphy, C. E., & Kwan, A. C. (2022). Pupil Correlates of Decision Variables in Mice Playing a Competitive Mixed-Strategy Game. *eNeuro*, *9*(2), ENEURO.0457-21.2022. <https://doi.org/10.1523/ENEURO.0457-21.2022>
- Wang, H.-X., & Gao, W.-J. (2009). Cell type-specific development of NMDA receptors in the interneurons of rat prefrontal cortex. *Neuropsychopharmacology: Official Publication of the American College of Neuropsychopharmacology*, *34*(8), 2028–2040. <https://doi.org/10.1038/npp.2009.20>
- Wang, J., Dai, J., Xu, Y., Dai, X., Zhang, Y., Shi, W., Sellergren, B., & Pan, G. (2019). Molecularly Imprinted Fluorescent Test Strip for Direct, Rapid, and Visual Dopamine Detection in Tiny Amount of Biofluid. *Small (Weinheim an Der Bergstrasse, Germany)*, *15*(1), e1803913. <https://doi.org/10.1002/sml.201803913>
- Wang, X., Zhong, P., Gu, Z., & Yan, Z. (2003). Regulation of NMDA Receptors by Dopamine D4 Signaling in Prefrontal Cortex. *The Journal of Neuroscience*, *23*(30), 9852–9861. <https://doi.org/10.1523/JNEUROSCI.23-30-09852.2003>
- Wang, Z., Lou, S., Ma, X., Guo, H., Liu, Y., Chen, W., Lin, D., & Yang, Y. (2023). Neural ensembles in the murine medial prefrontal cortex process distinct information during visual perceptual learning. *BMC Biology*, *21*, 44. <https://doi.org/10.1186/s12915-023-01529-x>
- Waters, R. C., & Gould, E. (2022). Early Life Adversity and Neuropsychiatric Disease: Differential Outcomes and Translational Relevance of Rodent Models. *Frontiers in Systems Neuroscience*, *16*, 860847. <https://doi.org/10.3389/fnsys.2022.860847>
- Weickert, C. S., Webster, M. J., Gondipalli, P., Rothmond, D., Fatula, R. J., Herman, M. M., Kleinman, J. E., & Akil, M. (2007). Postnatal alterations in dopaminergic markers in the human prefrontal cortex. *Neuroscience*, *144*(3), 1109–1119. <https://doi.org/10.1016/j.neuroscience.2006.10.009>
- Westbrook, S. R., Hankosky, E. R., Dwyer, M. R., & Gulley, J. M. (2018). Age and sex differences in behavioral flexibility, sensitivity to reward value, and risky decision-making. *Behavioral Neuroscience*, *132*(2), 75–87. <https://doi.org/10.1037/bne0000235>
- Wilbrecht, L., & Davidow, J. Y. (2024). Goal-directed learning in adolescence: Neurocognitive development and contextual influences. *Nature Reviews Neuroscience*, 1–19. <https://doi.org/10.1038/s41583-023-00783-w>
- Williams, B. R., Ponesse, J. S., Schachar, R. J., Logan, G. D., & Tannock, R. (1999). Development of inhibitory control across the life span. *Developmental Psychology*, *35*(1), 205–213. <https://doi.org/10.1037//0012-1649.35.1.205>
- Willing, J., Cortes, L. R., Brodsky, J. M., Kim, T., & Juraska, J. M. (2017). Innervation of the medial prefrontal cortex by tyrosine hydroxylase immunoreactive fibers during adolescence in male and female rats. *Developmental Psychobiology*, *59*(5), 583–589. <https://doi.org/10.1002/dev.21525>
- Willing, J., & Juraska, J. M. (2015). The timing of neuronal loss across adolescence in the medial prefrontal cortex of male and female rats. *Neuroscience*, *301*, 268–275. <https://doi.org/10.1016/j.neuroscience.2015.05.073>
- Wilmes, K. A., & Clopath, C. (2019). Inhibitory microcircuits for top-down plasticity of sensory representations. *Nature Communications*, *10*(1), 5055. <https://doi.org/10.1038/s41467-019-12972-2>

- Winter, S., Dieckmann, M., & Schwabe, K. (2009). Dopamine in the prefrontal cortex regulates rats behavioral flexibility to changing reward value. *Behavioural Brain Research*, *198*(1), 206–213. <https://doi.org/10.1016/j.bbr.2008.10.040>
- Wójcik, M. J., Stroud, J. P., Wasmuht, D., Kusunoki, M., Kadohisa, M., Myers, N. E., Hunt, L. T., Duncan, J., & Stokes, M. G. (2023). *Learning shapes neural geometry in the prefrontal cortex* (p. 2023.04.24.538054). bioRxiv. <https://doi.org/10.1101/2023.04.24.538054>
- Wool, L. E., Lak, A., Carandini, M., & Harris, K. D. (2023). *Mouse frontal cortex nonlinearly encodes sensory, choice and outcome signals* (p. 2023.05.11.539851). bioRxiv. <https://doi.org/10.1101/2023.05.11.539851>
- Xing, B., Li, Y.-C., & Gao, W.-J. (2016). Norepinephrine versus dopamine and their interaction in modulating synaptic function in the prefrontal cortex. *Brain Research*, *1641*(Pt B), 217–233. <https://doi.org/10.1016/j.brainres.2016.01.005>
- Yang, D., Yang, S. J., Del Bonis-O'Donnell, J. T., Pinals, R. L., & Landry, M. P. (2020). Mitigation of Carbon Nanotube Neurosensor Induced Transcriptomic and Morphological Changes in Mouse Microglia with Surface Passivation. *ACS Nano*, *14*(10), 13794–13805. <https://doi.org/10.1021/acsnano.0c06154>
- Yang, J.-H., & Kwan, A. C. (2021). Secondary motor cortex: Broadcasting and biasing animal's decisions through long-range circuits. *International Review of Neurobiology*, *158*, 443–470. <https://doi.org/10.1016/bs.irn.2020.11.008>
- Yang, S. J., O'Donnell, J. T. del B., Giordani, F., Wang, J., Lui, A., Piekarski, D., Irrinki, A., Schaffer, D. V., & Landry, M. P. (2022). *Synaptic scale dopamine disruption in Huntington's Disease model mice imaged with near infrared catecholamine nanosensors* (p. 2022.09.19.508617). bioRxiv. <https://doi.org/10.1101/2022.09.19.508617>
- Yoon, B.-J., Smith, G. B., Heynen, A. J., Neve, R. L., & Bear, M. F. (2009). Essential role for a long-term depression mechanism in ocular dominance plasticity. *Proceedings of the National Academy of Sciences of the United States of America*, *106*(24), 9860–9865. <https://doi.org/10.1073/pnas.0901305106>
- Zatka-Haas, P., Steinmetz, N. A., Carandini, M., & Harris, K. D. (2021). Sensory coding and the causal impact of mouse cortex in a visual decision. *eLife*, *10*, e63163. <https://doi.org/10.7554/eLife.63163>
- Zhang, F., Yuan, S., Shao, F., & Wang, W. (2016). Adolescent Social Defeat Induced Alterations in Social Behavior and Cognitive Flexibility in Adult Mice: Effects of Developmental Stage and Social Condition. *Frontiers in Behavioral Neuroscience*, *10*. <https://doi.org/10.3389/fnbeh.2016.00149>
- Zhang, K., Liu, Y., Wang, Y., Zhang, R., Liu, J., Wei, J., Qian, H., Qian, K., Chen, R., & Liu, B. (2018). Quantitative SERS Detection of Dopamine in Cerebrospinal Fluid by Dual-Recognition-Induced Hot Spot Generation. *ACS Applied Materials & Interfaces*, *10*(18), 15388–15394. <https://doi.org/10.1021/acsnano.8b01063>
- Zhang, Y.-Q., Lin, W.-P., Huang, L.-P., Zhao, B., Zhang, C.-C., & Yin, D.-M. (2021). Dopamine D2 receptor regulates cortical synaptic pruning in rodents. *Nature Communications*, *12*(1), 6444. <https://doi.org/10.1038/s41467-021-26769-9>
- Zhou, X., Zhu, D., Qi, X.-L., Li, S., King, S. G., Salinas, E., Stanford, T. R., & Constantinidis, C. (2016). Neural correlates of working memory development in adolescent primates. *Nature Communications*, *7*, 13423. <https://doi.org/10.1038/ncomms13423>

- Zhu, M., Lerum, M. Z., & Chen, W. (2012). How to prepare reproducible, homogeneous, and hydrolytically stable aminosilane-derived layers on silica. *Langmuir: The ACS Journal of Surfaces and Colloids*, 28(1), 416–423. <https://doi.org/10.1021/la203638g>
- Zuo, Y., Lin, A., Chang, P., & Gan, W.-B. (2005). Development of long-term dendritic spine stability in diverse regions of cerebral cortex. *Neuron*, 46(2), 181–189. <https://doi.org/10.1016/j.neuron.2005.04.001>